Republic of Iraq
Ministry of Higher Education
and Scientific Research
University of Babylon
College of Materials Engineering
Department of Metallurgical Engineering

Improvement of Mechanical and Electrochemical Properties of Biomedical Ti6Al4V alloy by Ta and Zr addition

A this is submitted to Council of the College of Materials Engineering , University of Babylon in Partial Fulfillment of the Requirements for the Master Degree in Materials Engineering / Metallurgical

By
Aounsalwjood Amer Mahmood Mohammed

Supervised by

Prof.Dr.
Haydar H.Jamal Al Deen

Prof.Dr.
Abdulraheem kadhim AbidAli

2021 A.D 1442 A.H

بسم الله الرحمن الرحيم

﴿إِنَمَا يَخْشَى اللهَ مِن عِبَادِهِ الْعُلَمَاءُ إِنَّ اللهَ عَزِيزٌ غَفُورٌ﴾

صدق الله العلي العظيم

سورة فاطر: الآية (28)

Supervisor Certificate

We certify that this thesis entitled (**Improvement of Mechanical and Electrochemical Properties of Biomedical Ti6Al4V alloy by Ta and Zr addition**) is Prepared by (**Anasalwjood Amer Mahmood)** under my supervision at the Department of Metallurgical Engineering / College of materials Engineering/ University of Babylon in partial fulfillment of the requirements for the degree of Master of Science in Material's Engineering/Metallurgical.

Signature:
Dr. Haydar H.Jamal Al Deen
Date: / / 2021

Signature:
Dr. Abdulraheem kadhim AbidAli
Date: / / 2021

Dedication

The One whose throne is in the sky…To the One whom we praise and

thank… **Allah** .

To **my dears Dad** and **Mum;**
The reason of what I have become today. Thanks for your great support and conditions care through my life.

To **my dear husband**, you were my support and did not abandon me, you were with me step by step, I thank you for enduring my very difficult circumstances and without getting bored, you are a blessing and I thank God for that;

Faris Wahib

To my **dear daughter** forgive me I didn't care about you because of studying and you very need attention;

Fatima (Fayrouz)

To **my dear sister** and **her children** because you always you are a source of support, happiness and encouragement.

Mays Alreem , Rida and **Mustafaa.**

To **my aunt** , because she always prays to me .

To **Zainab** , because she helped me.

To **my colleagues** , thank you for everything.

With Respect

Anasalwjood Amer Mahmood

2021

Acknowledgments

Great thanks to allah Almighty my Creator and inspirational for being merciful to me and gave me health, strength and protection.

I cannot express enough thanks and gratitude to my supervisor, **Dr. Haydar H.Jamal Al Deen & Dr. Abdulraheem kadhim AbidAli** support, helped, encouraged, and gave me all the acknowledgement I need to finish my research. It was a great privilege and honor to work and study under Their guidance

My thank to everyone work in metallic and non-matallic laboratories in Materials Engineering college/ University of Babylon.

Iam extremly grateful to my family and my husband for their love, prayers, caring and continuing support made this work possible. I am also extremely thankful to my friends for their kind support.

Anasalwjood Amer Mahmood

2021

Summary

Ti6Al4V alloy has widespread potential in biomedical applications due to their high degree of biocompatibility, favorable mechanical properties, high corrosion resistance and high the possibility of osseointegration,Ti6Al4V alloy contains the elements (Al and V) which are characterized by being toxic elements harmful in the human body, but with existing Ti increase biocompatibility for alloy .

In this study, all alloys have been prepared by powder metallurgy technique, then the alloying elements (Tantalum, Zirconium) have been added in different compositions (0.5,1, 1.5 and 2 wt%) to the master alloy (90wt%Ti-6wt%Al-4wt%V) in order to study the effect of these elements on microstructure characterization (XRD, SEM, EDS and Light optical microscope), electrochemical (Open circuit and Polarization teats), toxicity (Static immersion test) and mechanical and physical properties (Density and Porosity , Contact angle , Hardness and Dry wear tests) of this alloy. The compact pressure was determined as 600MP and the green alloys sintered at $550^{o}C$ for 1h then at $1000^{o}C$ for 2 h in inert gas (Argon), then leave the samples to cooled in the furnace to room temperature .

Results appear , the XRD results that all alloys (with and without additives) consist of two phases (α-Ti) &(β-Ti) at room temperature and the addition of Ta and Zr in these percentages have an effect on increases present β phase.

The physical properties , the porosity percentage decreases gradually with the increasing (Ta, Zr), the contact angle result refer decreases gradually with the increasing (Ta, Zr) compare to contact angle for base alloy in Hank's and saliva solutions .

The mechanical properties , the hardness values with addition of Ta, Zr leads to higher values of hardness compared with the master alloy . The dry

wear resistance increases with the addition of Ta, Zr elements, but dry wear resistance of master alloys with Zr additives is higher as a compared to master alloys and master alloys with Ta additives.

The electrochemical properties , the results of corrosion of Ti-6Al-4V alloy showed significant improvement after the addition of each Ta, Zr in artificial saliva and Hank's solutions. It was shown that higher improvement with the addition of the 2wt%Zr where the percentage of improvement was (91%) in Hank's solution. While the higher improvement percentage in artificial saliva was (77%) for 2wt%Zr. The corrosion current density for used alloys in Hank's solution is lower than that for artificial saliva solution.

The static immersion tests for all alloys for 21 days in artificial saliva and Hank's solutions illustrate that very low concentrations of metals ions release are observed. The amount of released ions when additive 2%Zr is lesser than base alloy and base alloy with addition Ta in all solutions.

List of Contents

List of Tables

List of Figures

List of Latin Symbols

Symbol	Meaning	Units
E	Elastic modulus	GPa
N	Spindle speed	Rpm
T	Temperature	C°
W	Weight	G

List of Greek Symbols

Symbol	Meaning	Units
A	Alpha phase	-
B	Beta phase	-
P		g/cm^3 + Kg/m^3

List of Subscripts

Symbol	Meaning	Units
D_o	Density of oil	g/cm^3
D_w	Density of water	g/cm^3
$E_{coor.}$	Corrosion potential	mV
$I_{coor.}$	Corrosion current density	$\mu A/ cm^2$
Ms	Temperature martensite starts	^{o}C
Mf	Temperature martensite finished	^{o}C
Tβ	β Transformation temperature	^{o}C
Wt	Weight percentage	%

List of Abbreviations

Symbol	Meaning
ASTM	American society for testing and materials
AFM	Atomic force microscopy
ATT	Allotropic transformation temperature
BCC	Body center cubic
HB	Brinell hardness
BPD	Binary phase diagram
CP-Ti	Commercially pure titanium
EW	Equivalent weight
EDS	Energy-dispersive spectrometry
HCP	Hexagonal close packed
ISO	International organization for standardization
JIS	Japanese industrial standard
LOM	Light optical microscope
mV	Millivolt
MA	Mechanical alloying
mpy	Mils per year
OCP	Open-circuit potential

P/M	Powder metallurgy
Scanning electron microscopy	SEM
Saturated calomel electrode	SCE
X-ray diffraction	XRD

Chapter One

Introduction

Chapter One
Introduction

1.1 General view

A speciality of medicine is developing, every day, more and more. This is the increasingly growing development of orthopedics, which brings together the parallel development of biomaterials. According to, the term "biomaterial" was defined at the Conference of the National Institute for the Development of Consensus in Health, in 1982, as: "any substance (other than a non-drug), or combination of substances, synthetic or natural in origin, that can be used for a while, completely or partially, as part of a system that treats, augments or replaces any tissue, organ or function of the body" [1].

There is an incentive for the development of biomaterials due to the need to reduce surgeries to treatment damaged implants[2]. The national market for orthopaedic implants has been increasing, estimated at US $ 64 million-year. In 1999, it was $ 4.4 billion in the world. In Brazil, it is estimated that, on average, 24,000 total hip prosthetic implants are performed per year.

Figure (1.1) shows the developments of implant materials in the last century [3]. It is expectation that (70%-80%) from implants are produced from metallic materials [4].

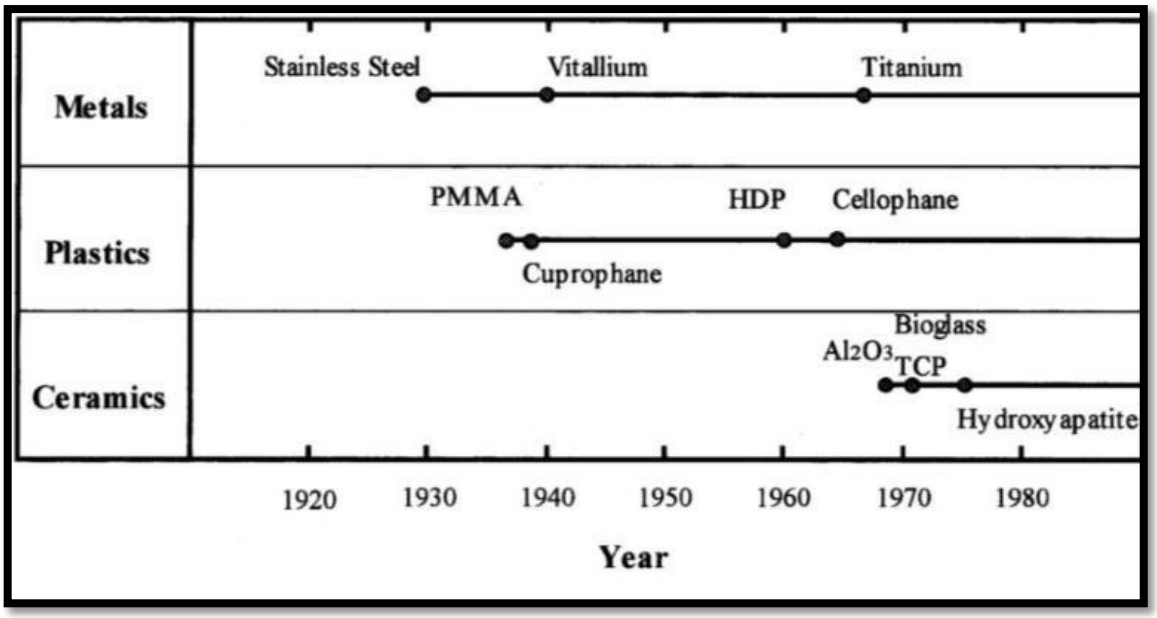

Figure (1-1) Shows the developments of implant materials in the last century [5].

Metals are previously considered as unfavourite materials for biomaterials because of the environmental and human damage are caused by weighty metals, because an improvement in the safety of metals for medical use is central, requiring efforts have been made to obtain better mechanical durability and corrosion resistance [6]

Some of metals and their alloys are commonly utilized as biomedical materials because of higher mechanical properties, a number of implants are utilized as passives ,exchange for stiff tissues substitute. For example, knee joints and total hips, for fracture healing help as screws and bone plate and dental implants [7]

The most metals as Nickel (Ni), Chromium (Cr), Titanium (Ti), Tungsten (W), Iron (Fe) , Cobalt (Co), Tantalum (Ta), Niobium (Nb), and Molybdenum (Mo) are utilized to produce alloys for industrial implants are able to endure by the human body [7]

Metals show excellent resistance to fracture and strength, which are essential to the medical application which requires load bearing among broad diversity of metallic materials, some of them do not cause serious

toxic reactions in the human body, including Ti alloys, stainless steels, Co alloys, and noble metals [8].

Every part of metallic implants is ''non-magnetic''these are basic for the ,implants to be good-compatible with magnetic resonance imaging (MRI) techniques and to be marked in (X-ray) imaging .

Several metals have been used for bone fixating and dental reparation for more than 2000 years ago and have a long history as biomaterials. The properties of metals conclude from their metal bonds and their advantages as biomaterials are as follows:-

1. High fracture toughness.
2. Biocompatibility .
3. Suitable elasticity and rigidity.
4. Non toxicity.
5. Non-magnetic
6. Light weight
7. High strength
8. High electro conductivity [9].

The mainly utilized of metals in joint substitutions are : (Co-Cr , titanium-based alloy and stainless steels), these major types have favour in joint substitutions [5].

1.2 Technical Aspects of Implants in General

In the development of implants, doctors and scientists, in general, have encountered problems. Bones have, among their mechanical properties, considered very important, called the modulus of elasticity, or young's modulus, whose symbol is E Its corresponding value is between (10 and 30)GPa, which gives them adequate resistance [10] In addition , they are incredibly light . In case of damage, they need to be replaced by artificial materials (biomaterials), which are equally light and resistant and also, which are biocompatible with osteoblasts [10] . The term

’’biocompatibility’’ was redefined in 1987 as: ’’the ability a specified amaterial to perform specificapplication with tissue appropriate response in the surrounding area’’ [11].

The biocompatibility of artificial materials is defined within the following premises: elasticity modules E with values close to the bone E, adequate porosities, so that they can establish good junctions with natural bone cells , which are set by embracing the prosthesis by expanding the ramifications of these cells and using them without risk of infections [11].

Titanium and its alloys stand out because of their excellent properties, which are: low modulus of elasticity, low density, high mechanical and corrosion resistance, and superior biocompatibilities when compared to austenitic stainless steel and Co-Cr alloys [10].

Considering that the E (elastic modulus) value of Ti (102 GPa) is a higher value than the E of human cortical bone (10 to 30 GPa), there is a difference in stiffness between them and therefore, the load will not be transferred appropriately to the latter, generating stresses that can shear the bone implant interface and cause the consequent loosening of the implant [12].

Therefore, the preferred titanium alloys for orthopedic applications should have a low elastic modulus, excellent mechanical strength, corrosion resistance, formability, adequate porosity, and less potentially toxic elements. [13- 14].

There has been a reduction in the shear force and modulus of metallic materials’ elasticity by making them porous. This reduces the damage to the tissues adjacent to the implant, promotes bone-implant interconnection, increasing bone fixation, and prolonging its duration [15]. Thus, it is seen the importance and needs to continue technical research work in orthopedics.

1.3 Implant Properties

The main requirements for a modern-day implant can broadly be categorized into three equally important features [16]:

- The body of human must be compatible with the material used in the prosthesis. While it is understandable that there is bound to be some amount of tissue reaction attributed to the introduction of a foreign material, the resulting changes in physical, mechanical, and chemical properties inside the localized environment should not lead to local deleterious changes and harmful systemic effects.
- The implant must have the desired balance of physical and mechanical properties necessary to perform as expected. The specific optimization of properties like ductility, elasticity, yield stress, time-dependent deformation, ultimate strength, strength of fatigue, hardness, and resistance of wear which depend on the type and functionality of the specific implant part.
- The device must be relatively easy to fabricate, being reproducible, consistent, and conforming to all technical and biological requirements. Some of the constraints may contain the techniques to produce excellent surface finish or texture, the capability of the material to achieve adequate sterilization, and the cost of production.

1.4 Titanium as a Biomaterial

Ti is a new structural material with excellent comprehensive properties, described in Table (1-1) below [17].

Table (1-1): Properties of Ti [17].

Property	Typical value
Density (g/)	4.5
Melting Point (°C)	1668
Elastic modulus (GPa)	116
Tensile Strengths (MPa)	550

Therefore, titanium alloys have been increasingly widely used in aviation, aerospace, chemical, shipbuilding, medical fields, and other industrial departments. Titanium with a low density of 4.5 g/cm^3 is only 60% of iron's density [17].

A considerable change has occurred in the use of titanium and the number of new alloys and product forms selected from the medical implants designer. Since the early 1990s, the ''Metallurgical Materials'' subcommittee has developed several new ASTM standards for titanium based alloy biomaterials. These consensus standards are listed in table (1-2) [18].

Table (1-2): ASTM standard for titanium alloys [18].

Common Name	ASTM/ISO	Microstructure	UNS Number
Ti-5Al-2.5Fe Alloy	ISO 5832-10	α + ß	unsigned
Ti-6Al-7Nb Alloy	ASTM F 1295, ISO 5832-11	α + ß	R56700
Ti-6Al-4V Alloy	ASTM F 1472, ISO 5832-3	α + ß	R56400
Ti-13Nb-13Zr Alloy	ASTM F 1713	Metastable ß	R58130
Ti-12Mo-6Zr-2Fe	Alloy ASTM F 1813	Metastable ß	R58120
Ti-15Mo Alloy	ASTM F 2066	Metastable ß	R58150
Ti-3Al-2.5V Alloy	ASTM F 2146	α + ß	R56320
Ti-35Nb-7Zr-5Ta Alloy	Sub. F04.12.23	Metastable ß	R58350

1.5 Problems of Titanium and its Alloys

The titanium alloys used in implants present three significant problems [19]:

1. High cost because of the amount of processing energy and melting and casting difficulties.
2. Higher elastic modulus compared to bone.
3. Although Ti inert behavior is a suitable property, its bone attachment is difficult because it does not react with the human tissues.
4. The elastic moduli and strength of titanium and its alloys are much higher than those of human bones, resulting in stress shielding and implants failure. Researchers have tried to develop new types of titanium alloys, to reduce the implants modulus to the level approaching human bones. On the other hand, the mechanical properties of titanium can be adjusted by pore, and the stress shielding effect will be reduced. Porous titanium with porosity in a wide range can be prepared with powder metallurgy methods [20].

1.6 The Ti6Al4V Alloy

The alloy have the advantage of combining important and prominent properties such as high strength, low density, high corrosion resistance, inactivity of the living body environment and enhanced compatibility, low elastic modulus and high ability to adhere to bone or other tissues, because of these characteristics, this alloy is the first choice to many applications , the alloy Ti6Al4V is the best in its properties compared to traditional stainless steels and alloys based on cobalt [21] Ti6Al4V is the ideal choice for life medicine . The Ti6Al4V alloy is used to replace the damaged hard tissue parts of bones and for joints, bone

screws, plates, and hip and knee implants. Because it have good mechanical properties [22-23].

1.7 The Aim of This Work

This work aims to study the modification of Ti6Al4V alloy which produced by powder metallurgy because Ti6Al4V alloy contains the elements (Al and V) which are characterized by being toxic elements harmful in the human body by the addition of tantalum and zirconium elements in different percentages (0.5, 1, 1.5, and 2 wt.%) for base alloy to get rid of effect (Al and V) . To investigate the effect of Zr and Ta, several tests should be accomplished: -

1. Electrochemical test (open circuit, polarization and ion release).
2. Mechanical and physics tests (compression , hardness ,dry wear , density ,porosity and contact angle).
3. Microstructure characterization (XRD, LOM , SEM , and EDX).

Chapter Two

Theoretical Part

&

Literature Review

Chapter Two

Theoretical Part and Literature Review

2.1 Introduction

In this chapter, shown the theoretical issues related to the phase diagram and the types of alloys according to the microstructure. Alpha alloys, beta alloys, and (alpha + beta) alloys, and the method of preparing the powder metallurgy to the alloy. Also , includes learn about the types of corrosion, and the property of hardness and compression.

2.2 Metallurgy of Titanium Base Alloy

Pure titanium, in addition the majority of titanium alloys, crystallizes at low temperature in a modified ideally hexagonal close-packed (hcp) structure, called α-titanium. At high temperature, however , the body- centered cubic (bcc) structure is stable and is referred to as β-titanium at 882±2°C. The complete transformation from one into another crystal structure is called the allotropic transformation; the respective transformation temperature is called the transus temperature. The presence of the two various crystal structure and the corresponding allotropic transformation temperature is of central importance since they are the basis for the large variety of properties achieved by the alloys of titanium [24-25].The atomic unit cells of the referred structure are shown in figure (2-1) .

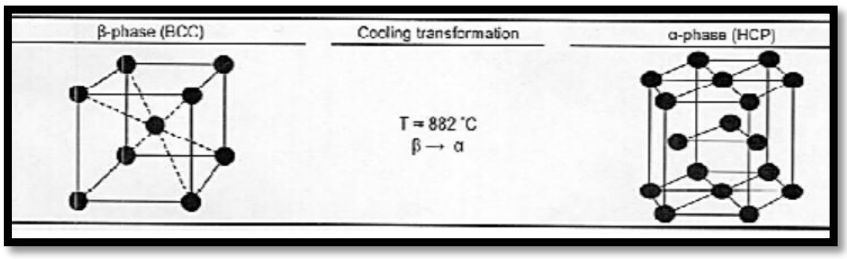

Figure (2-1): Crystallographic cell and allotropic transformation of pure titanium [25].

2.2.1 Phase Diagram (Ti -Al)

Ti-Al binary phase diagram (BPD) is the most important phase diagram of Ti alloys, Al is as essential for alloying titanium as carbon is for iron.

Al is the most abundant metal in the earth's crust (8.8%), and it has found large applications due to its low density (2.71 g/cm^3) and high corrosion resistance [26].

Ti is the seventh most abundant metal in the earth's crust (0.63%) and the fourth most widely used material in industry after iron, Al and Mg . It is used in many applications such as building ships and aircraft and is used in medical engineering in particular because of the properties of Ti and its alloys such as high compatibility, non-toxicity and high corrosion resistance [27] .

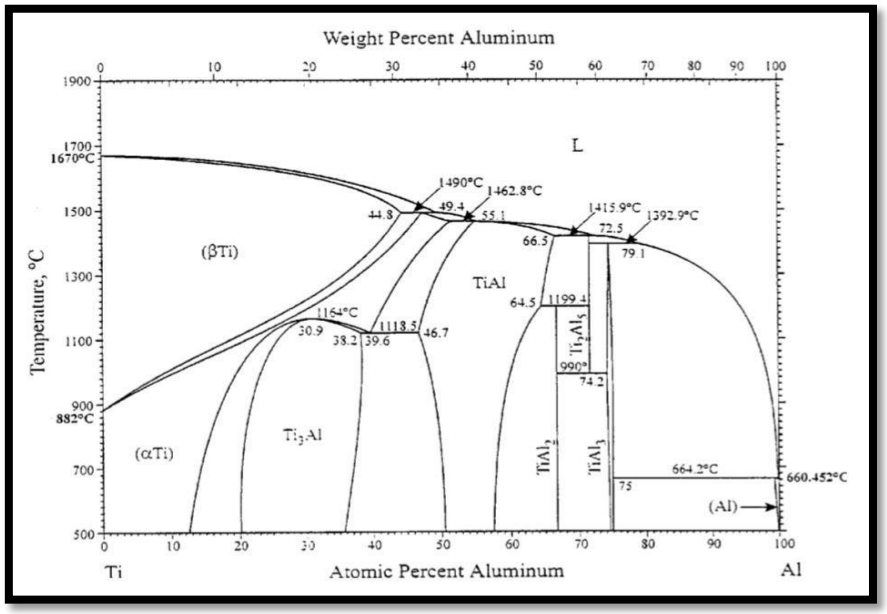

Figure (2-2) :Ti- Al binary phase diagram [28].

In Figure (2-2) , the phase diagram (Ti-Al), it is clear that there is an alpha phase and a beta phase, as well as that addition of aluminum, which is characterized by its role in stabilizing the alpha phase by raising the temperature of the phase transition alpha / beta , Al causes ductility and strength , as well enhance the Ti_3Al phase, and thus it is not expected

that it will remain phase beta titanium, where clear from the phase diagram that other phases are Ti_3Al phase and TiAl phase Also shown as that the field (Ti_3Al + alpha) narrows with increasing temperature at 1179 ^{o} C. The presence of Al does not cause a change in the microstructure, and Al as it is clear in the Figure (2-2) has a very high solubility in titanium where shown the equilibrium phases occurring in (Ti-Al) systems are Ti_3Al compounded with hexagonal close-packed superlattice structures and TiAl and $TiAl_3$ intermetallic compounds with tetragonal structures [29-30]. Further, $TiAl_2$ and Ti_2Al_5 phases are found on the aluminum-rich side of the diagram [29]. As can be seen, phases (Ti_3Al and TiAl) exist over a large range in the Ti-rich side [29].

2.2.2 Phase Diagram of (Ti- V)

Titanium has emerged as a very attractive metal for numerous applications. It has the highest strength to density ratio in comparison to other widely used metals such as iron , nickel and aluminum based alloys. Titanium has exceptional corrosion resistance in many environments, often exceeding the corrosion resistance of stainless steels [30], and provide moderate resistance to oxidation, alloying with vanadium enhances their ductility, strength, oxidation, and corrosion resistance [31].

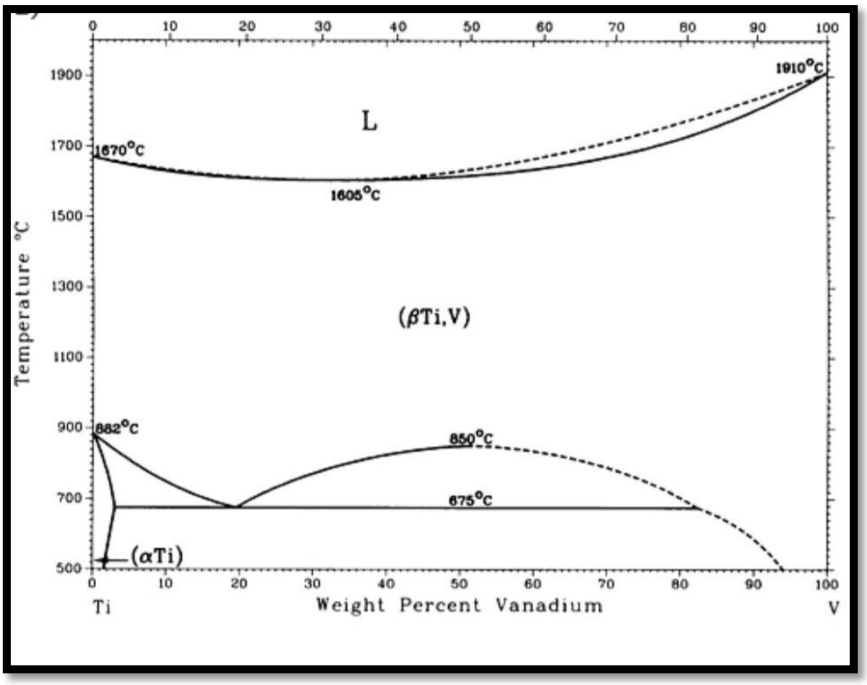

Fig. (2-3): Binary phase diagrams for Ti-V [32].

The addition of V leads to a significant change in the microstructure, as vanadium is a β stabilizer and allows α and β to coexist at room temperature [33] .

The equilibrium phases of the Ti-V system consisting of (1) the close-packed hexagonal (α) solid solution restricted to temperatures below the α/β transformation for pure Ti below 882 °C Ti-rich alloys , and (2) the body-centered cubic (β) solid solution with a complete range of solid solubility above 882 °C. The solubility of V in (α-Ti) is large compared to the solubility of Mo, Nb, W, or Ta, which form analogous phase diagrams [34]. Because of present of the element vanadium which caused the temperature to decrease converted to , alpha phase shift to beta to 675°C being a beta-phase stabilizing element, where from a temperature of 675°C and below there is only an alpha phase and above 675°C there is beta phase , whenever the temperature increases, the beta phase increases when it reaches 850°C there is beta phase just.

2.2.3 Ternary Phase Diagram of Ti6Al4V

The purpose of this study is to obtain a thermodynamic description for the Al-Ti-V ternary system, thus providing a scientific basis for Ti–Al–V calculation and a guide for materials design . Where γ-based TiAl alloys are attractive materials for high-temperature applications because of low density, high-temperature strength, and oxidation resistance [35]. However, the poor ductility at room temperature (RT) has hindered the application of TiAl alloys. The addition of ternary alloying elements such as V could improve the RT ductility and yield strength of TiAl alloys [36], resulting in the for- motion of β-phase with bcc_A2 structure that facilitates ductility and deformation [37] or a duplex phase structure of α2 with hcp_A3 structure and γ with L1o structure [38].

Phase equilibrium in the Ti–Al–V system at 1200 $\overset{o}{C}$ in Fig (2-4) an isothermal section of Ti–Al–V at 1200 $\overset{o}{C}$. The isothermal section is characterized by five single-phase regions (i.e., α phase with hcp_A3 structure, β phase with bcc_A2 structure, γ phase with L1o structure, δ phase with D82 structure, and ε phase with D022 structure) and three three-phase regions (α+γ+ε, α+δ+ε, and α+β+δ). The single α phase at 1200 °C is highly extended, while the other single-phase regions remain almost unchanged, resulting in the emergence of new three-phase regions

.

Table (2-1) Phase designations in the Ti–Al–V system along with crystal structure data [39].

Phase (designation)	Strukturbericht designation
β, (βTi), bcc_A2	A2
α, (αTi), hcp_A3	A3
γ, γTiAl, TiAl	L1o
δ,V5Al8	D82
ε, TiAl3	D022

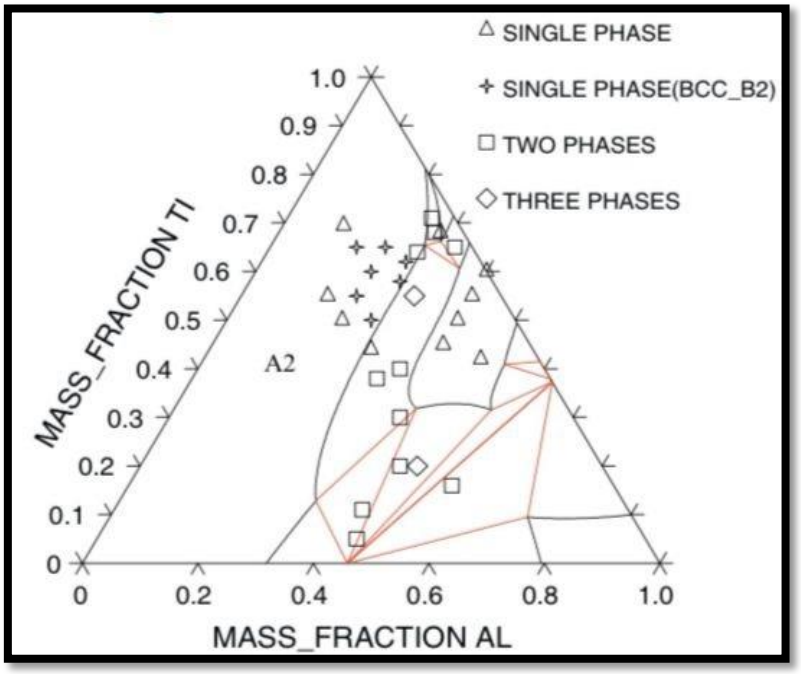

Fig (2-4) The isothermal section of Ti–Al–V ternary system at 1200C° versus expert- mental data [40].

2.3 Effects of Alloying Elements on Titanium Alloys

Ti alloying element fall into three classes: α- stabilizers, β-stabilizers, and neutral. The alloying elements (Al, O, N, etc.) that tend to stabilize α phase are called α stabilizers and the addition of these elements leads to an increase in the allotropic transformation temperature (ATT), however, elements that stabilize β phase are known as β stabilizers (Nb, Ta, Mo, Mg, V, W, Fe, Ni, Cr, Co, Mn, Cu, etc.) and the addition of these elements decrease the β transus temperature, when a eutectoid transformation happen, this β –stabilizer is described eutectoid β stabilizer, otherwise, it is called an isomorphs β- stabilizer. If no significant change in the ATT is observed, in that case, the alloying elements are defined as neutral elements (Zr and Sn), addition of α and β stabilizers to Ti gives rise to a field in the corresponding phase diagram where both α and β phases may coexist [41]. Figure (2-5) shows a

schematic representation of the phase diagram types between Ti and its alloying elements.

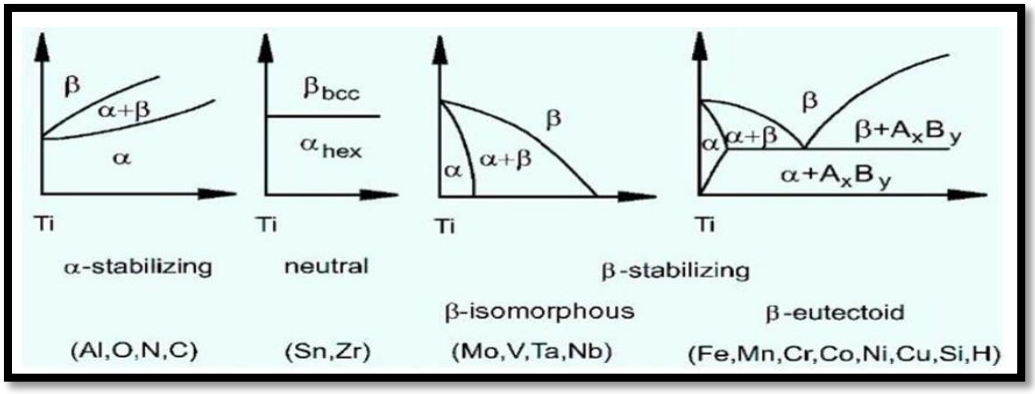

Figure (2-5): Schematic representation of kinds of phase diagram between titanium and its alloying elements [41].

2.3.1 Alpha Titanium Alloys (α-Ti Alloys)

The α type titanium alloys are mainly fabricated from commercially pure titanium, and alloyed with a stabilizing elements singly or in combination , resulting in microstructure of a phase at room temperature. The α type titanium alloy is characterized by the lack of a heat treatment response since it consist entirely of α phase or only a small amount of the metastable β phase remaining (2-5wt%) after cooling from high temperatures . The alloys show acceptable strength , good toughness , high resistance of creep , good weldability due to their heat treatment insensitivities, poor forge ability particularly at temperature below the beta transus, and because the absence of a ductile –brittle transition , they are suitable for cryogenic application [42] .

2.3.2 Alpha beta - Titanium Alloys (α+ β Ti Alloys)

At room temperature, Ti (α+ β) alloy contains α and β phases. The formation of β phases happens due to the presence of V element that acts as β phase stabilizer in Ti6Al4V alloy , the V element is as β stabilizer at room temperature .Ti (α+ β) alloys are high in strength and corrosion resistance. With the presence of β phase in Ti alloys (bcc crystal

structure), Ti alloys become easy to fabricate through hot forming treatment [43].

2.3.3 Beta Titanium Alloys (β -Ti Alloys)

β titanium alloys can be further classified into three groups stable β metastable β, and beta –rich (α+ β) alloys A schematic phase diagram for isomorphous titanium alloys is shown in Figure (2-6). The stability of the beta phase is determined by the cumulative wt.% of β stabilizers. Alloys containing between 10 wt.% and 15 wt.% of β stabilizing elements , result in the beta phase being retained at room temperature in a metastable condition . These alloys are an attractive alternative to (α+ β) Ti alloys because of their high strength, deep hardening , and wide proessing window. Another advantage of these alloys is their excellent forge ability. However because of the large amount of heavy element required to stabilize the beta phase, beta alloys are 10% heavier than (α+ β) alloys [44].

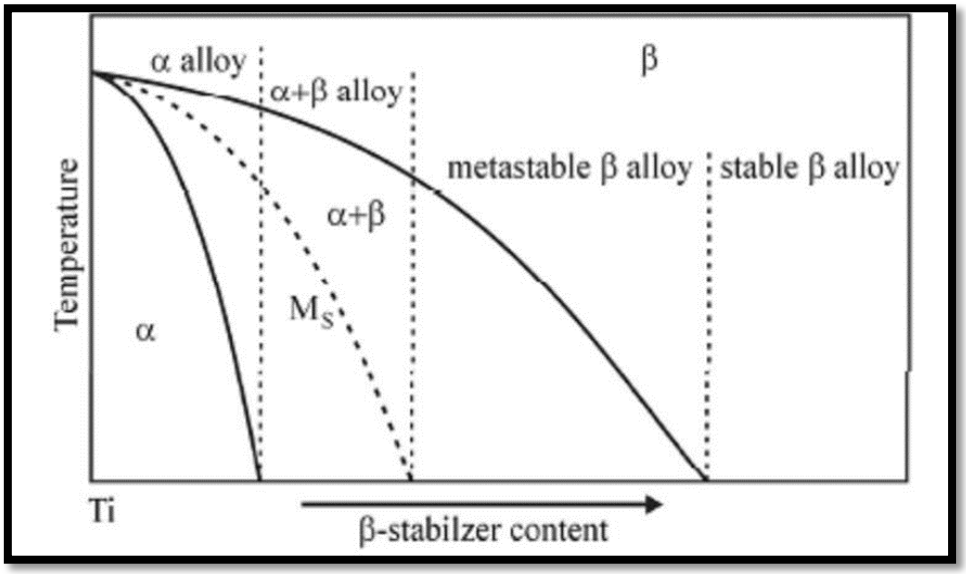

Figure (2-6): Represents the classification of titanium α,β and α+β, as well as Ms is temperature at which martensite begins to form when cooling from the β phase field to room temperature and Mf is the temperature at which reaction is complete [44].

2.4 Biocompatibility

The biomaterials applied as implants in the human body are to be nontoxic. The achievement of the biocompatibility for implants is essentially dependent on the response of the human body to the implants. The host reaction due to by the implants degradation in the body control the biocompatibility of implants [45] . Ti has a low modulus of elasticity (i.e. young's modulus) which matched closely to the bone. As a result, loads from skeletal could be more evenly distributed between bone and implant, and led to a lower incidence of bone degradation which lead to of stress shielding for the area around the for bone orthopedic implant [46-47-48].

2.5 Titanium Alloys Processing

The properties of Ti alloys are affected obviously by the manufacturing operation . Fabrication technique can be classified as casting and powder metallurgy.

2.5.1 Casting

Processes of casting are among the oldest methods for industrialization metal goods. In more early casting processes (much of them are still used today), the mold or form used must be destroyed in order to remove the product after solidification. The need for a permanent mold, which could be used to product components in endless quantities, was the obvious alternative [49] .

Casting techniques are employed when:

1. The finished shape is so large or complicated that any other method would be impractical,
2. A particular alloy is so low in ductility that forming by either hot or cold working would be difficult.

3. In compared with other manufacturing processes, the final step in the refining of even ductile metals may involve a casting process [50].

2.5.2 Powder Metallurgy of Ti Base Alloy

Powder metallurgy (PM) is a celebrated technology to produce parts of small size and sophisticated shapes. This might be one of the most important applications for this technology, where more recently, the vast majority of manufacturing of industrial parts is based on the PM manufacturing methods, where an easy manufacturing route by compressing the powder in dies followed by sintering step is produced. This manufacturing path might be called the mass production PM method, where cost is the main parameter to take into account, and properties, always under the engineering requirements are in the second level of request [51-52] .

The main steps to manufacture parts by powder metallurgy process are shown in figure (2-6). The steps include: blending and mixing of powders, cold compaction, and sintering [53].

Powder metallurgy is an important commercial technology and this because of the following considerations:-

1. PM parts can be accumulated and produced to required shape or near required shape, which eliminate or decrease the requirement for subsequent machining [54].
2. PM process is low in wasting materials - about 97% of the starting powders are converted to product [55-56]. This compares satisfactorily to processes of casting in which sprues , runner, and risers [55].
3. In PM parts, a production of porous metal parts such as filters, gears, and oil-impregnated bearings can be made with a particular level of porosity [57].

4. Some metals that are hard to manufacture by other methods they can be shaped by powder metallurgy such as W filaments for incandescent lamp bulbs [56].
5. PM distinguishes how producing such as certain alloy combinations made by PM cannot be shaped in other methods [55].
6. PM is the most favorable casting processes in dimensional control, tolerances of + 0.13 mm is held regularly [55].
7. PM production methods can be mechanical for economical production [57].

There are limitations associated with PM processing [58]:-

1. Owing to the fairly high compacting pressures required to press the powder, the wear on the dies is high.
2. Due to high rate of wear of dies, high costs for dies and presses the method is rendered uneconomical particularly for small runs.
3. Since the compacted parts must be ejected from the die without fracture, therefore, the shapes that may be made by this method are limited.
4. The equipment required is very costly.
5. A completely dense product is not possible without heating the product after pressing operation.
6. In the low melting powders such as Zn , Sn , and Cd, occasionally some thermal difficulties appear.
7. The physical properties obtained by this process are lower than those obtained by other processes.
8. Many metal powder are explosive at room temperature.

2.6 Corrosion Behavior

Corrosion is a subversive attack on metallic materials when in contact with a chemical environment. Human body fluid pH in different tissues varies in the range from one to nine. That may be considered an extremely corrosive environment for metallic materials because of the presence of a particular amount of NaCl and a series of acids. The presence of a high chloride concentration is also considered to accelerate corrosion of metallic implants, leading to metal ion release. Additionally, most metallic implants are undergone a static loading or a low-frequency cyclic loading. The corrosion damage of the metallic biomaterials is found in many forms like crevice, pitting, fretting, galvanic, wear, intergranular, and fatigue corrosion. The attack rate of general corrosion is very low due to the spontaneous formation of passive surface layers on most metallic implants utilized at present [59] .

2.6.1 Types of Corrosion

Pitting Corrosion Localized corrosion attack made on the resistant surface produces pitting corrosion. It commonly occurs on base metals protected by a naturally forming thin film of an oxide (for instance, the firmly adherent TiO_2 over the Ti surface) when the film's potential exceeds the oxide's breakdown potential in an aggressive environment. In the presence of given ions such as chlorides and sulfides, the film locally breaks down, and rapid dissolution of underlying metal occurs in the form of pits [60] .

Crevice Corrosion Occurs from the geometry of the implant/prostheses assembly. Corrosion of an alloy is more significant in the aperture's small sheltered volume created by contact with another material. The other metal could be part of the same or different alloy's fastener, a sheltered crown, cement packing, or implant prostheses joint [60] .

2.7 Hardness

Hardness mean in the metals industry, it may be thought of as resistance to plastic deformation . Hardness may also be referred to as mean contact pressure. The hardness test is, the most valuable and most widely used mechanical test for evaluating the properties of metals . The principal purpose of the hardness test is to determine the suitability of a material for a given application, or the particular treatment to which the material has been subjected. The ease the hardness test can be made it the most common method of inspection for metals and alloys Principally, the importance of hardness testing has to do with the relationship between hardness and other properties of material. For example, both the hardness test and the tensile test measure the resistance of a metal to plastic flow, and results of these tests may closely parallel each other. The hardness test is preferred because it is simple, easy and relatively nondestructive. Hardness has no quantitative value, except in terms of a given load applied in a specified manner for a specified duration and a specified penetrator shape [61].

2.7.1 Brinell Hardness

Hardness is the property for a material (metal) and which shown of its ability to resist abrasion, it is the resistance of a material to permanent deformation of the surface. The hardness of a surface of the material is of course a direct result of inter-atomic forces on the surface of the material. Brinell hardness is a combined effect of compressive, elastic and plastic properties relative to the mode of penetration, shape of penetrator, etc. Brinell hardness as shown in Fig (2-7) ,calculated by pressing a hardened ball into test specimen under standardized load as shown in Fig (2-8). Brinell hardness tests are used to determine hardness of metallic materials, to check quality level of products, for uniformity of samples of

metals, results of heat treatment. Ball used in Brinell hardness testing should be polished and free from surface defects [62-63-64].

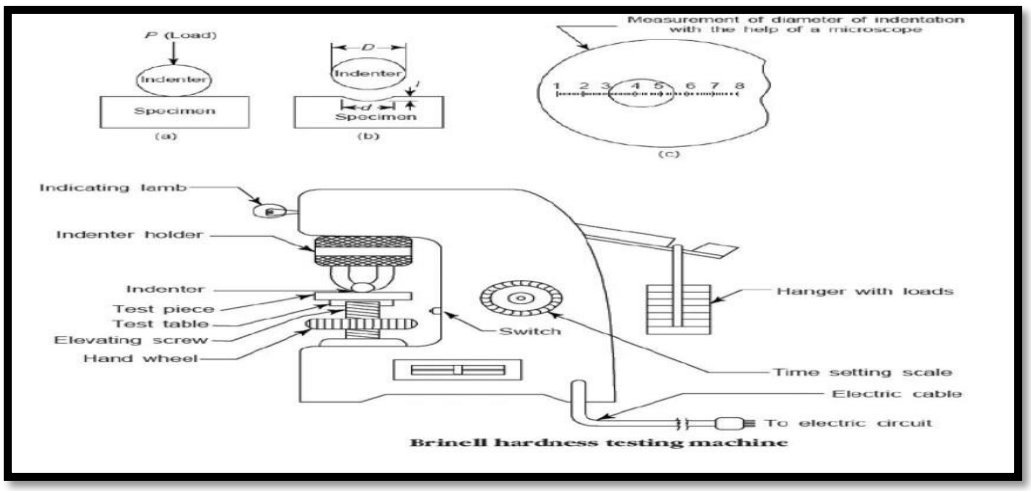

Fig (2-7) Brinell hardness test [62-63-64].

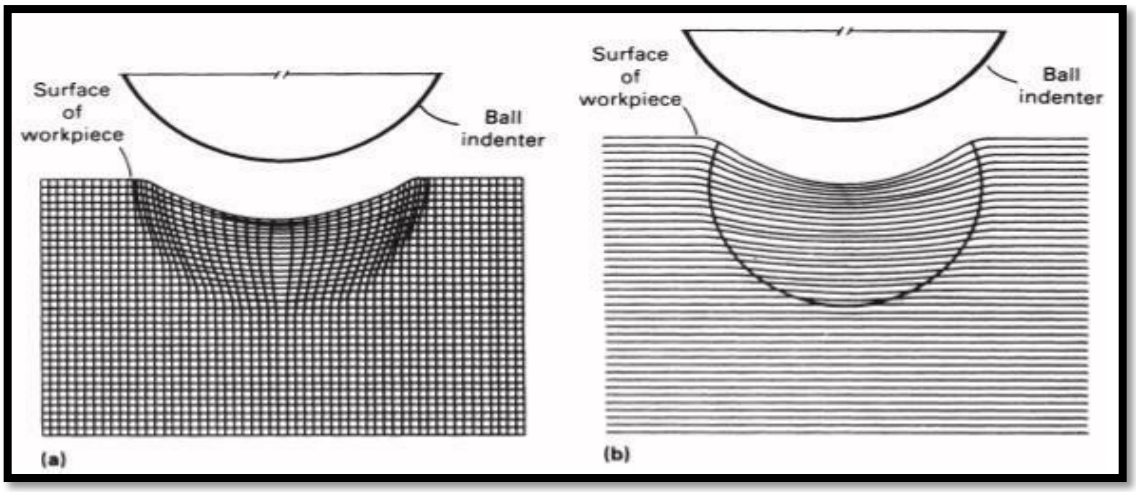

Fig (2-8) Deformed grid pattern on a meridional plane in a brinell hardness test. (a) Modeling clay. (b) Low-carbon steel. [64].

2.8 Application of Ti6Al4V in Medical Field

One of the most promising medical engineering materials, Ti and its alloys Due to its excellent properties, interest is growing in the application of Ti alloys to mechanical and tribological components in the field of biomedicine [65].

There are many reasons for choosing titanium and its alloys in these vital applications in the manufacture of prosthetics and dental applications :-

- Its small density and best mechanical strength is the reason for its high specific strength
- Titanium alloys with superior resistance to corrosion in body fluids
- Less modulus elasticity about (50%-60%) of that competing cobalt-based super alloys. [66]

The majority of metallic materials that are attractive to biomedical applications are Ti and its alloys . In medicine, it is widely used for the manufacture of orthopedic devices and under load dentistry, where it is used in implant devices that replace hard tissues . Examples of such applications are artificial knee joints, artificial hip joints, fracture fixation screws, bone plates, pacemakers, artificial heart valves, and artificial hearts [67]

Replacing worn or damaged joints to restore lost human bone structure and function is one of its primary applications [68].

2.8.1 Dentistry Applications

Dental implants from titanium have become the most widely accepted and successful used type of implant due to their tendency to osseointegration wherefore bone-forming cells adhere with implants, where titanium and its alloys are used in dental devices such as implants, crowns, bridges, and components of dental implants (the screw and abutment) [69] . Ti implant is a structural and functional bridge that forms between the body bone and the newly implanted foreign body. Orthodontic braces made of titanium are gaining in popularity because they are stronger, safer and lighter than their steel counterparts . The biocompatibility of medical titanium makes its use more than other

competing alloys as show in Figure (2-9) implant of titanium in dental application.

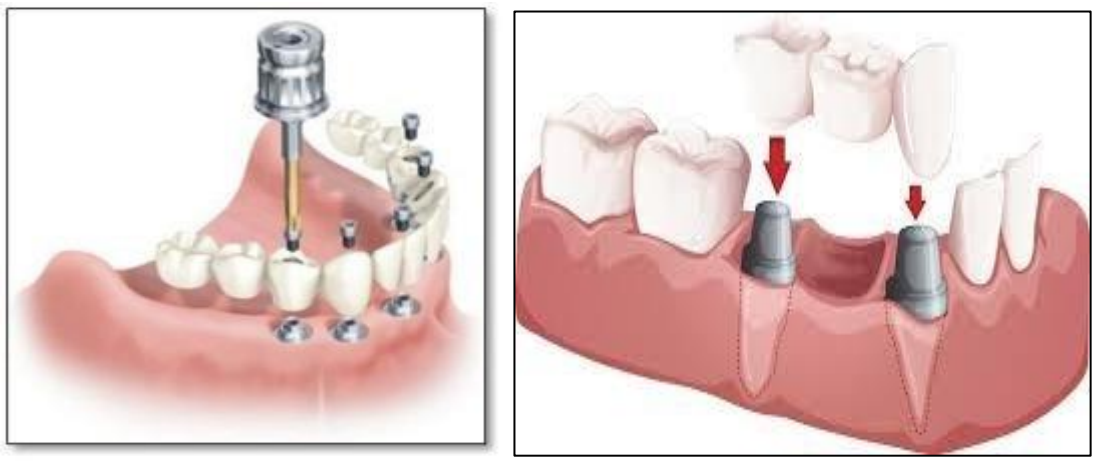

Figure (2-9) Implant of titanium in dental application [70].

2.8.2 Joint Replacement

Replacing worn or damaged joints to restore the lost structure and functions of human bone is one important application of Ti6Al4V alloy. The reason for this is that Ti and its alloys are considered a desirable class of implant materials for orthopedic applications due to the ability of these alloys to combine good mechanical properties and biocompatibility [71-72], and Ti alloys are also used for this purpose due to their durability, biocompatibility, and several decades from experience, Ti being less hard than other metals, and therefore better suited for skeletal reconstruction [73].

2.8.2.1 Hip Replacement

Ti6Al4V alloys are of great interest in the medical field in many medical applications especially hip replacement [74]. Where the most widely used Ti alloy in this application is titanium alloyed with Al and V. This is because typically, (α+ β) alloys can achieve optimum properties necessary for demanding loading bearing applications by balancing the amounts of alpha and beta stabilizers [75-76]. Hip ball and sockets as shows in Figure (2-10) which are made as a replacement for the joint and

made of Ti metal as it has the ability to remain in the patient's body for more than 20 years, in addition to the titanium's that had sufficient ability to osseointegration , which allows the use of titanium alloys in bone implant applications [77-78].

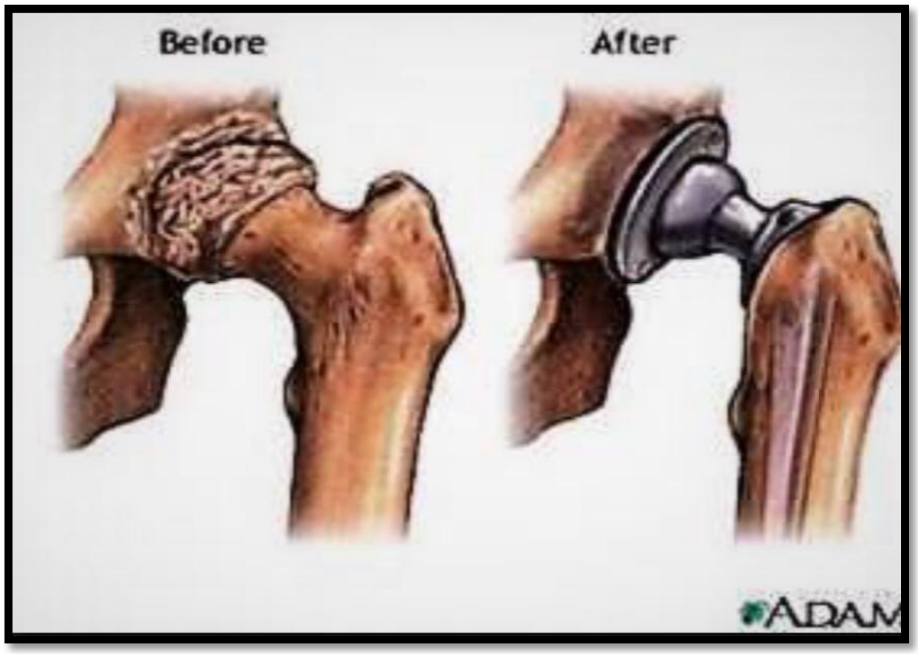

Fig (2-10) Hip replacement [79].

2.8.2.2 Knee Replacement

Titanium is considered biocompatible because of its non-toxic feature and the human body does not reject it and for these reasons it is used in various medical applications such as knee replacement Ti and its alloys are characterized by having a low modulus of elasticity, which matches closely with the bone. Because of this feature, it is possible to distribute the loads from the skeleton equally between the implants and the bone, and this leads to a reduction in the rate of bone erosion and this is due to the protection from stress [80-81] as shown in Figure (2-11).

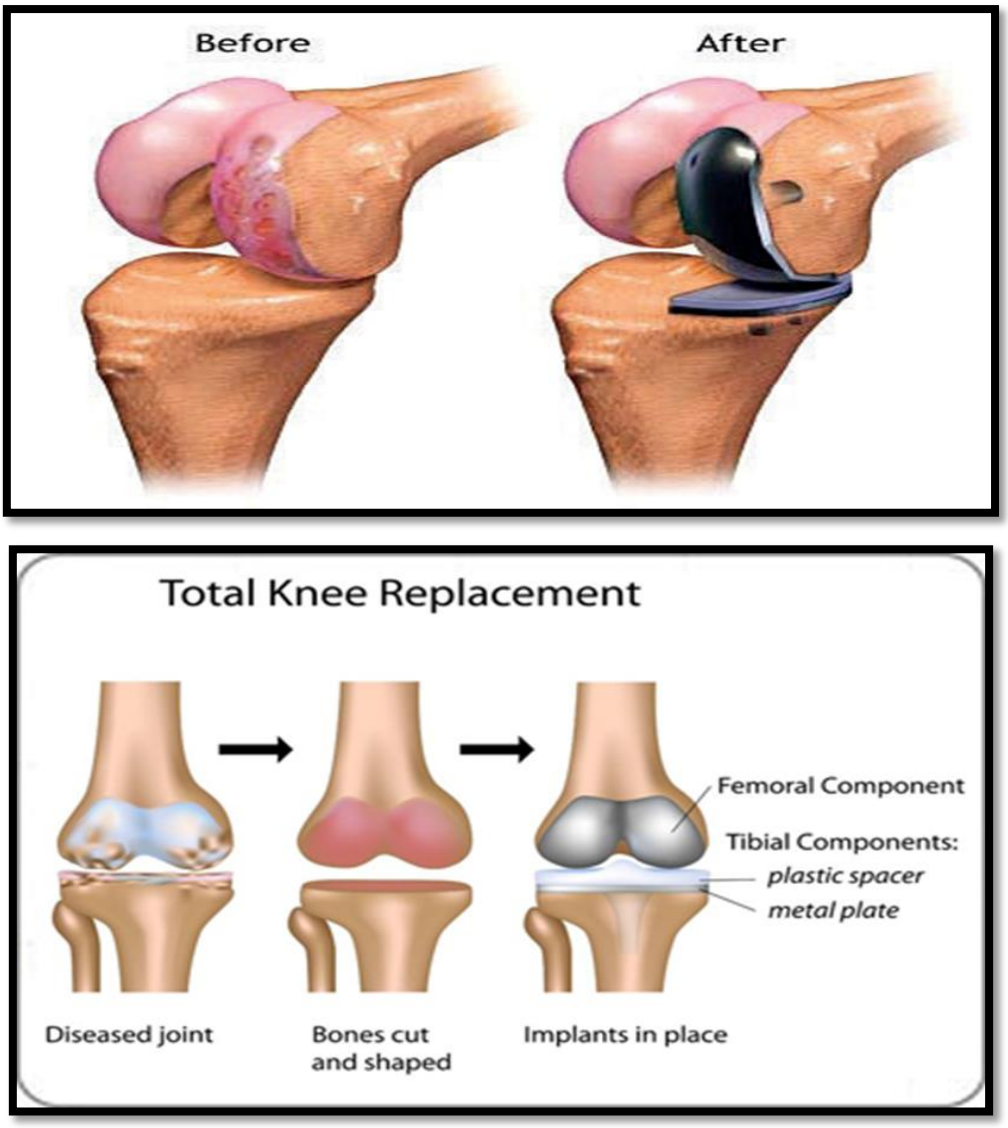

Figure (2-11) Knee replacement [83].

2.9 Literature Review

Materials utilized for biomedical applications cover a broad range and they must have higher particular properties. Metals which utilized as implants more than one century ago as bone fracture fixation from metal plate which first found it in 1895. At the start, metal implants be exposed with unsatisfactory strength complexities .

The history of human joint substitutions come back to the nineteenth century; the first permanent implantation of a large joint for human was completed in 1890. The first planting is made of natural

substances. The first knee joint-prosthesis was produce from ivory and is based to the bones . In 1930 began implant of metal joint for prosthesis .

Miguel Sampaioa, et. al., 2015 [84] In dentistry, prosthetic structures must be able to support masticatory loads combined with a high biocompatibility and wear resistance in the presence of a corrosive environ- ment. In order to improve the simultaneous wear and corrosion response of highly biocompatible prosthetic structures, a veneering poly-ether-ether-ketone (PEEK) to Ti6Al4V substrate was assessed by tribocorrosion analyses under conditions mimicking the oral environment. Samples were synthesized by hot pressing the PEEK veneer onto Ti6Al4V cylinders. The tribocorrosion tests on Ti6Al4V or PEEK/Ti6Al4V samples were performed on a reciprocating ball-on-plate tribometer at 30 N normal load, 1 Hz and stroke length of 3 mm. The tests were carried out in artificial saliva at 37 1C. Open circuit potential (OCP) was measured before, during and after reciprocating sliding tests. The worn surfaces were characterized by scanning electron microscopy. The results revealed a lower wear rate on PEEK combined with a lower coefficient of friction (COF), when compared to Ti6Al4V. In fact, PEEK protected Ti6Al4V substrate against the corrosive environment and wear avoiding the release of metallic ions to the surrounding environment.

Jayasheelan Vaithilingam, et. al. , 2016 ,[85] Selective laser melting (SLM) has previously been shown to be a viable method for fabricating biomedical implants; however, the surface chemistry of SLM fabricated parts is poorly understood. In this study, X-ray photoelectron spectroscopy (XPS) was used to determine the surface chemistries of (a) SLM as-fabricated (SLM-AF) Ti6Al4V and (b) SLM fabricated and mechanically polished (SLM-MP) Ti6Al4V samples and compared with (c) traditionally manufactured (forged) and mechanically polished Ti6Al4V samples. The SLM–AF surface was observed to be porous with

an average surface roughness (Ra) of 17.6 ± 3.7 μm. The surface chemistry of the SLM-AF was significantly different to the FGD-MP surface with respect to elemental distribution and their existence on the outermost surface. Sintered particles on the SLM-AF surface were observed to affect depth profiling of the sample due to a shadowing effect during argon ion sputtering. Surface heterogeneity was observed for all three surfaces; however, vanadium was witnessed only on the mechanically polished (SLM-MP and FGD-MP) surfaces. The direct and indirect 3T3 cell cytotoxicity studies revealed that the cells were viable on the SLM fabricated Ti6Al4V parts.

E. Almanza, et. al., 2017,[86] The electron beam melting (EBM) is a useful technique for fabricating alloys that are diffi- cult to machine and require expensive tools as well as the presence of inert atmosphere for further treatments. Under vacuum, EBM provides a controlled environment, reducing the drawbacks of the alloys of their processing in a conventional manner and thereby improv- ing their microstructure, which can enhance corrosion resistance. The corrosion resistance of the Ti-6Al-4V alloy was evaluated by using the Tafel extrapolation technique . The corrosion speci- mens were submerged in a Hank solution to simulate the corporal fluid. The specimens were characterized before and after the corrosion tests by optical microscopy and scanning electron microscopy, as well as a chemical microanalysis by EDS. The microstructural char- acterization before the corrosion tests revealed a dual phase (alph +beta) microstructure in the Ti-6Al-4V alloy. Corrosion resistance increased in the Ti-6Al-4V alloy due to the formation of a TiO2 passive layer.

Matthew K., et. al., 2018,[87] In near-net-shape manufacturing methods, such as powder metallurgy, additive manufacturing, and metal in- jection molding, porosity has historically been viewed as the sole

limiting factor for fatigue life. This is because pores tend to act as stress concentrators. However, in this work, a fractographic analysis of Ti-6Al-4V produced through several powder metallurgy techniques has shown that microstructural faceting due to slip can cause fatigue failure, even in the presence of porosity. The probability of pore related failure was found to be dependent on microstructure size and morphology. Additionally, a minimum pore size threshold was found to exist for each microstructure, under which pores will not cause fatigue failure. A simple model was developed to determine this threshold based on the microstructural characteristics of the material.

Shunyu Liu , et al.,2018,[88] The Ti6Al4V fabricated by three mostly developed additive manufacturing (AM) techniques-directed energy deposition (DED), selective laser melting (SLM) and electron beam melting (EBM)-is thoroughly investigated and compared. Fundamental knowledge is provided for the creation of links between processing parameters, resultant microstructures and associated mechanical properties. Room temperature tensile and fatigue properties are also reviewed and compared to traditionally manufactured Ti6Al4V parts. The presence of defects in as-built AM Ti6Al4V components and the influences of these defects on mechanical performances .

Jose Luis Cabezas-Villa , et al.,2018,[89] Ti6Al4V powders with three different particle size distributions (0–20, 20–45, and 45–75 μm) were used to evaluate the effect of the particle size distribution on the solid-state sintering and their mechanical properties. The sintering kinetics was determined by dilatometry at temperatures from (900 to 1260) ^{o}C. The mechanical properties of the sintered samples were evaluated by microhardness and compression tests. The sintering kinetics indicated that the predominant mechanism depends on the relative density

irrespective of the particle size used. The mechanical properties of the sintered samples are adversely affected by increasing pore volume fraction. The elastic Young's modulus and yield stress follow a power law function of the relative density. The fracture behavior after compression is linked to the neck size devel- oped during sintering, exhibiting two different mechanisms of failure: interparticle neck breaking and intergranular cracking in samples with relative densities below and above of 90%, respectively. The main conclusion is that relative density is responsible for the kinetics, mechani- cal properties, and failure behavior of Ti6Al4V powders.

M F azel ,2019,[90] The performance of biomaterials in general and orthopaedic biomaterials in particular is dependent on both the chemistry and topography of their surfaces. It is therefore important to tailor both of those aspects through an appropriate surface modification technique. Here, we examined the influence of hydrothermal treatment on the surface characteristics and electrochemical behavior of Ti-6Al-4V specimens whose surfaces were modified using plasma electrolytic oxidation (PEO). Even though no calcium-phosphorous related crystalline compound was identified in the XRD spectra of PEO layers, hydroxyapatite crystals were clearly detectable after the applied hydrothermal treatment. The partial water absorption of the HA crystals and their needle-like morphology resulted in a significant increase in the wettability of the surfaces. However, the application of post-PEO hydrothermal treatment also decreased the corrosion resistance of the PEO layers. The numerical results of electrochemical impedance spectroscopy demonstrated that the optimized surface properties and corrosion resistance were achieved in one of the groups, namely PEO-HT3, where the HA nanocrystals homogenously covered the entire surface of the specimens.

L Olmos,et al.,2020,[91] The effect of Ta particle addition into a Ti6Al4V alloy processed by solid state sintering. The sintering kinetics of powder mixes are evaluated by dilatometry. Sintered materials are characterised by SEM and XRD, and their mechanical properties are obtained from microhardness and compression tests. Sintering behaviour and final microstructure are affected by Ta particles, which slow down the densification, lower the temperature of α-to-β phase transition and stabilise the β phase. Mechanical properties, as microhardness, Young's modulus and yield stress, depend on the microstructure reached after sintering and on the residual porosity. The materials with at least 20 vol.-% of Ta exhibited a high strength to modulus ratio, which is suitable for orthopaedic implants.

Keng Ho Cheung, **et al.,2020,[92]** TiO2 coatings were fabricated by anodizing unpolished and polished Ti6Al4V substrates . Dielectric breakdown and associated heating of the insulating TiO2 promoted trace rutile formation. Consequently, the presence of the amorphous TiO2 passivating layer (unpolished) resulted in thicker and more irregular coatings than when anodization was done on the bare metal surface (polished). Large-scale delamination steps were observed for the coatings on the unpolished substrates while localized delaminations occurred for the coatings on polished substrates; the amounts of both increased with increasing anodization time. 3D laser scanning confocal microscopy allowed distinction between the fine-scale morphology and the coarse-scale topography. These data showed that increasing time and acid concentration resulted in similar trends of increasing roughness (morphology) and unevenness (topography). The focusses on the effect of initial substrate surface characteristics and its modification to improve the quality of the coatings formed by anodization of titanium biomedical implants.

Chapter Three

Experimental Part

Chapter Three

Experimental Part

3.1 Introduction

This chapter refers to the equipment and materials that have been used gives a detailed description of the experimental methodology and the working conditions under which the tests were conducted. In the beginning explaining the steps of preparing the sample and producing it by the method of powder metallurgy P.M . All mechanical and physical tests such as hardness test, dry wear test, (density and porosity) calculation are described and mentioned Describe the phases by means of the microstructure and XRD. The corrosion and ion release tests are explained.

3.2 Program of the Present Study

Samples in table (3-1) were prepared in the present work, where the matrix alloy is based on ASTM F 136-02a [93]. Figure (3-1) shows a summary of the overall program used in the present work

Table (3-1) : Prepared samples in the Present study.

Samples N.	The weight percentage of element (%)				
	Ti	Al	V	Ta	Zr
1	90	6	4	0	0
2	89.5	6	4	0.5	0
3	89	6	4	1	0
4	88.5	6	4	1.5	0
5	88	6	4	2	0
6	89.5	6	4	0	0.5
7	89	6	4	0	1
8	88.5	6	4	0	1.5
9	88	6	4	0	2

Figure (3-1): The Experimental Part

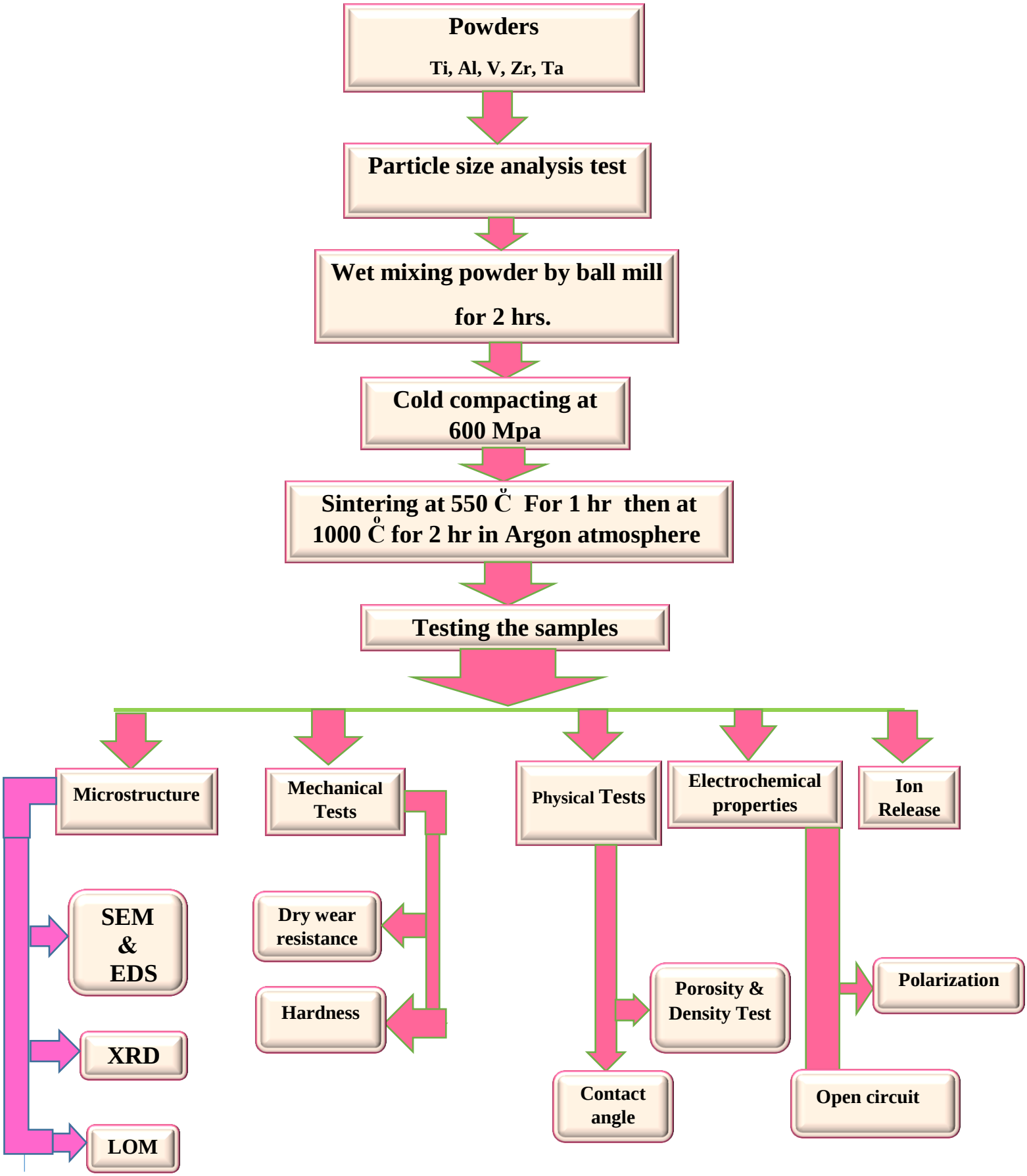

3.3 Materials and Tests

In this study the powders of (Ti, Al, V, Ta and Zr) , were used from the source for all these powders is (Lemandou Ltd. co. China) .

3.3.1 Particle size analysis

The test done to know difference in the grains size for powders used and thus to know for the interfere and homogeneity of the grains with each other. The carried out particles size was calculated by using device (Better size 2000 lazer particles size analyzer). Which is located in the Ceramic and Building Materials Laboratory in Materials Engineering - University of Babylon.

3.4 Preparation of Samples

To prepare the samples, the powder technology method was used, and the following steps are summarized for mixing, compacting and sintering The alloys used in this work are shown in table (3-2), which includes the code and composition of the alloys used

All samples prepared at the laboratories of Metallurgical Engineering Dept. / College of Materials Engineering / the University of Babylon

3.4.1 Powder Weight

Each quantity of powders done measurement weigh before mixing, a sensitive scale type (L220S - D) with an accuracy of (±0.0001) of Germane origin was used. In the preparation (Ti6Al4V) alloy and (Ti6Al4V)-XTa and (Ti6Al4V)-XZr alloys , powder for base alloy [90%Ti, 6%Al, 4%V], and the proportion the elements addtiton for each of the (Ta & Zr) to the base alloy as follows (0.5%, 1%, 1.5%, 2%) .

3.4.2 Powders Mixing

In the wet mixing process to the primary powders, an electric rolling mixer type mixer (STGQM-1/5-2) was used, was used, and alumina balls, and used different diameters of balls to ensure mixing and purification to the powders, and to reduce friction and oxidation resulting of mixing process added acetone to the powder particles before mixing. The mixing process was being carried out for (2) hours.

3.4.3 Powders Compacting

A one-way cylindrical mold is the mold used in the sample preparation process with diameters of (12 mm) and high (8 mm) as shown in Figure a (3-2) . Figure b (3-2) shown the shape of samples after compacting , the mold was used to sample was used for corrosion test, hardness test, microstructure test, compression test and dry wear tests. The preferred compacting pressure is determined by measuring the green densities at different compacting pressure . The pressure used is (260,380,485,600,700) Mpa , where the select pressure was specified as (600) Mpa based on the constancy of the green density at this value.

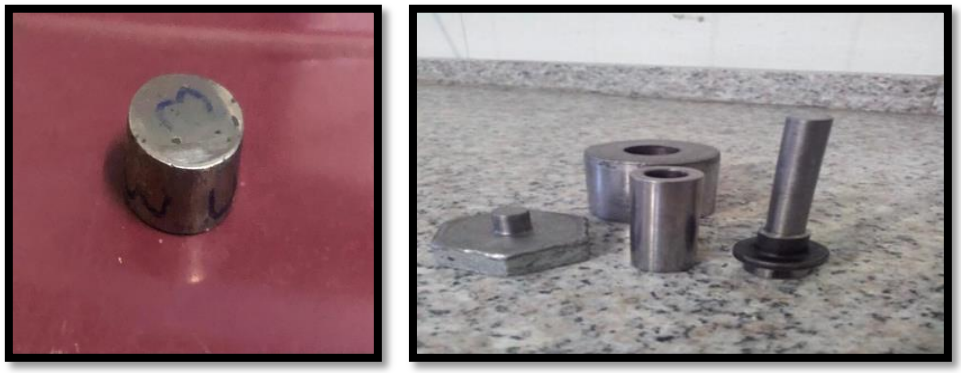

(a) **(b)**

Figure (3-2): (a)The die that used in samples preparation (12 mm) diameter die (b) The prepared samples.

3.4.4 Sintering of the Green Compacts

Using an electric tube furnace with a continuous stream of inert gas (Argon) as shown in the Figure (3-3) , the sintering process was carried out. In the laboratory of thermal transactions in the laboratories of the Department of Material Engineering - University of AL- KUFA, model (OTF-1200X) , under controlled atmosphere (Argon gas) to inhibit the specimens oxidation .

Figure (3-3): Tube furnace with a continued stream of argon.

The sintering process of samples includes the following steps as shown in Figure (3-4):-

1- Heating from room temperature to 550 $\overset{o}{C}$.
2- Staying for one hour at 550 $\overset{o}{C}$.
3- Heating from 550 $\overset{o}{C}$ to 1000 $\overset{o}{C}$.
4- Staying for two (2) hours at 1000 $\overset{o}{C}$.
5- When the sintering program finished, the samples were left inside the furnace to cool down until the sintered samples' temperature drops to room temperature again.

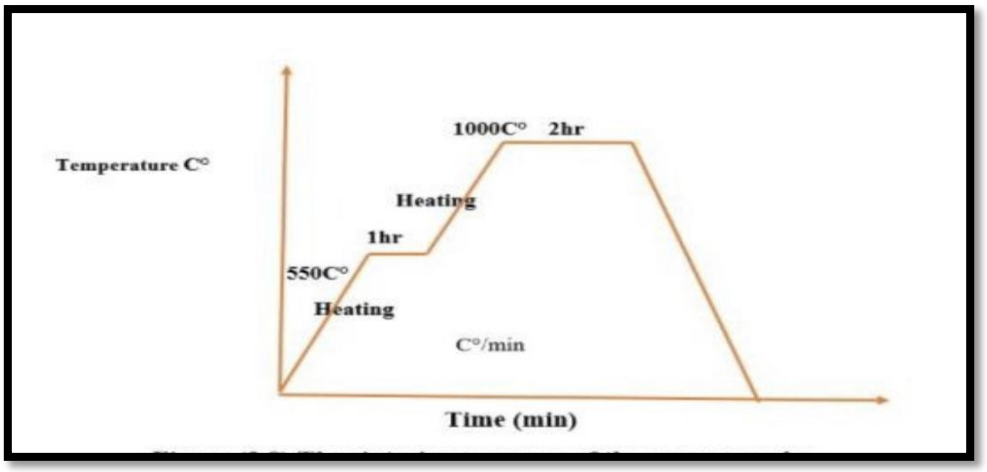

Figure (3-4) The sintering program of the green samples

3.5 Microstructure characterization

3.5.1 X-ray Diffraction (XRD)

The XRD test was conducted at Development and Continuous Education Centre/University of Baghdad - College of Education (Ibn Al-Haitham) (type xrd-6000 Shimadzu), in order to ,find out the composition and phases identification for Ti6Al4V base alloy , Ti6Al4V -XZr and Ti6Al4V -XTa alloys .The XRD generator with Cu aim at 40 KV and 30 mA, scanning speed (2°) per minute was used the scanning rate was (30 – 80) .

3.5.2 Light Optical Microscope (LOM)

The microscopic structure was studied using optical microscopy in order to identify the existing phases and to see the shape and size of the grains, after scratch in degrees as follows (180, 220, 400, 600, 800, 1500, 2000, 2500, 3000) by use scratch SiC paper, and then polishing by then to obtain a shiny surface were done by using diamond and then etched by a swab solution (swab) shown in table (3-3) [94] , and to wash and dry the samples, distilled water and an electric dryer were used. This test was done in the microscope is type (BEL PHOTONICS) . Located in the

laboratory of College Materials Engineering / Department of Metallurgy Engineering / University of Babylon .

Table (3-2) Chemical composition of swab solution [94]

NO.	Constituents	ml
1	HF	10 ml
2	HNO_3	5 ml
3	H_2O	85 ml

3.5.3 Scanning Electron Microscope (SEM) & Energy Dispersive Spectroscopy (EDS)

To get of obtaining surface composition and its topography, by using a scanning electron microscope . After sintering specimens then swab then polishing then etched by a etching solution then wash and dry the samples, where the specimens is imaged through a high-pack of electrons , where the analytical technique that has been used for chemical analysis and elemental analysis of surface of specimens was done by using energy-dispersive spectroscopy EDS. The EDS device was coupled with SEM and the inspection Was done at the same time of SEM observation. This test done in (University of Technology College of Applied Sciences in Baghdad) , model (INSPECT 550) as shown in Figure (3-5) .

Fig (3-5) SEM & EDX.

3.6 Physical and Mechanical tests

3.6.1 True Density and Porosity for Sintered Specimens

The porosity of sintered specimens can be calculated according to ASTM B328 [95].

1- The dry weight of the specimen is measured as mass (A).
2- At room temperature, using a suitable evacuating pump which was manufactured for this purpose. The pressure was reduced over the immersed specimen in oil for 30 min, and the specification of the oil used is (RL 68 H) .
3- After the oil immersion process, the weight of the specimen in the air is measured, which is mass (B).
4- The weight of the sample immersed in water is mass (F).
5- Finally, the porosity can be calculated through the following equation.

$$\mathbf{PF} = \left[\frac{\mathbf{B-A}}{\mathbf{(B-F)D^{\circ}}} * \mathbf{100}\right] \mathbf{Dw} \qquad \mathbf{\ldots (3\text{-}1)}$$

$$\boldsymbol{\rho}\mathbf{F} = \left[\frac{\mathbf{A}}{\mathbf{B-F}}\right] \mathbf{Dw} \qquad \mathbf{\ldots (3\text{-}2)}$$

Where:

PF : Porosity .

ρF : Density .

D_w =Density of water (0.9956 g/cm³)

D_0= Density of oil (0.977 g/cm³)

3.6.2 Contact angle Test

Contact angle test accomplished to evaluate wettability for Ti6Al4Vbase alloy, Ti6Al4V-XZr and Ti6Al4V-XTa .The used instrument is (SL 200C contact angle meter) which manufactured in (KINO Industry Co., Ltd., USA)with contact angle range (0 ° to 180 °).

This device makes calculation to contact angle for drops and monitoring changes of contact angle ,the device as show in Figure (3-6).

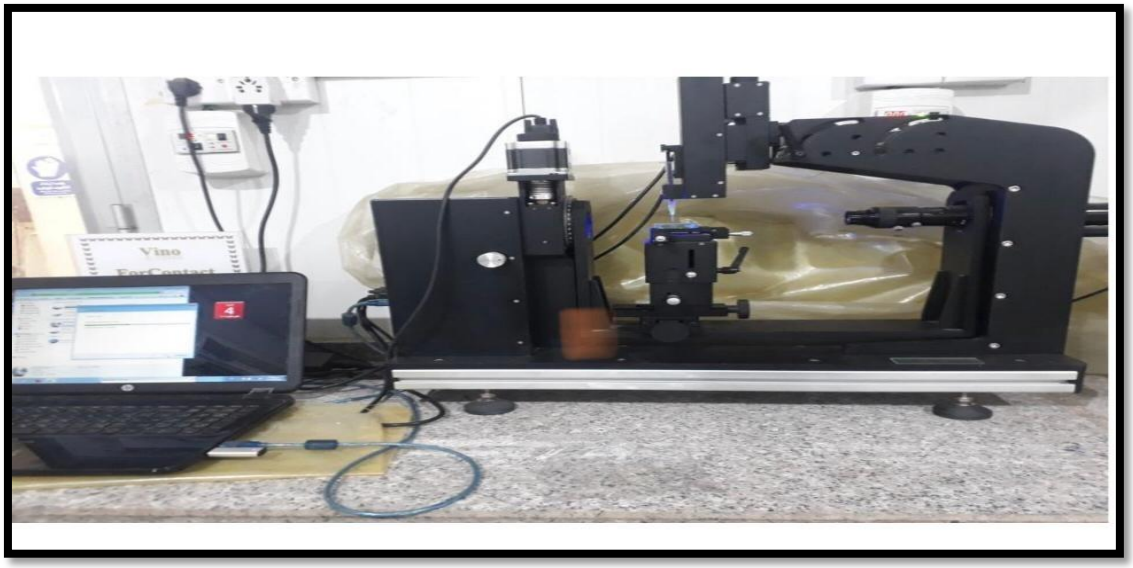

Figure (3-6) Contact angle device.

3.6.3 Macro Hardness Measurement

The macro brinell hardness test includes use of load (62.5 kg/ mm²) on the specimen to measure its hardness by a carbide ball diameter of (2.5 mm) for (10 sec) , located in the Laboratories of the College of Materials Engineering / Department of Metallurgical Engineering / University of Babylon. The average value used was taken for three readings for each specimen to analysis the behavior of the alloys. hardness measuring device brinell as shown in Figure (3-7).

Fig (3-7) Wilson hardness machine type (UH-250).

3.6.4 Dry Sliding Wear Test

According to (ASTMG99) [96] dry sliding wear test method is covered . On a precision tester (MT 4003 version 10) as shown in the Figure (3-16) the test was carried out . The test specimen is set as a pin against a rotating hard disk with a hardness of 850Hv . Where the slip distance between the center of the specimen and the center of the disc (radius) was constant 6.5 mm with different slip distances and the rotation speed was 950 rpm and a constant load of 10 N .The specimen was weighed before the start of the test using a sensitive scale , model (254a) with an accuracy of (±0.0001), as so after 5, 10, 15, 20,25, 30, 35 and 40 minutes where the specimen was weighed, and the dry wear rate according to the following equation was calculated :

$$\textit{Vol. loss } (cm^3) = \frac{weigth\ loss(g)}{\rho(\frac{g}{cm^3})} \qquad \ldots (3\text{-}4)$$

Where:

Weight loss (g)= Quantity loss after (5 ,10 ,15,20,25,30,35 and 40) min.

ρ (g/cm^3) = Account done from porosity and density test for each specimen.

The test was carried out at the University of Technology, materials engineering laboratories as shown in Figure (3-8).

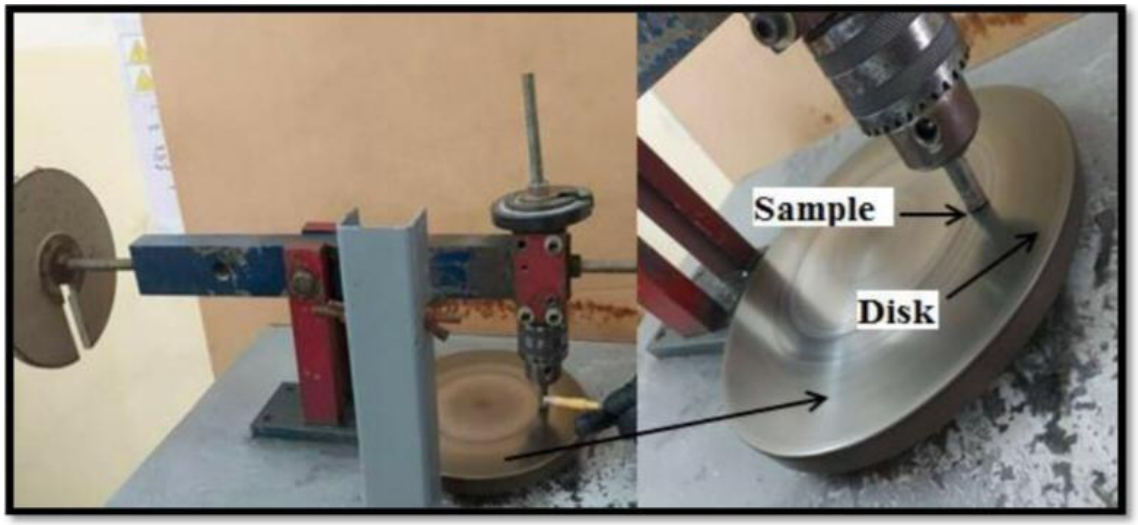

Figure (3-8) Wear tester device type (MT4003, version 10.0).

3.7 Electrochemical Corrosion Tests

3.7.1 The Open Circuit Potential

Used the Ti and its alloys as an implants within the human body, so corrosion tests should be done for specimens to determine the behavior of corrosion of specimens in the human body. This test was done in corrosion laboratory in the laboratories of the Department of Metallurgical Engineering – College Engineering Materials - University of Babylon. In this test were used two different body solutions artificial saliva and Hank's solutions. The chemical composition of artificial saliva and hank's solutions is illustrated in table (3-4). The pH of artificial saliva and hank's solution at 37±1°C were 6.7 and 7.4 respectively. The electrochemical tests was conducted at temperature 37±1°C on the all specimens. The test was performed as shown:

1. Preparation of specimens.
2. Calculation of the OCP (open circuit potential), the experimental arrangement for the measurement of open circuit potential is shown in Figure (3-9) in which describes the experimental situation. A 500 ml capacity glass electrolytic cell is used. The tests are carried out with the specimens immersed in artificial saliva and hank's

solutions. Through the standard calomel electrode (SCE), the working electrode potential can be measured.

A voltmeter is connected between the working electrode and the reference electrode. The specimen from (0 up to 60min) open circuit potential measurements were performed. The first record was taken immediately after immersion then the voltage was monitored for the intired period of test at an interval of (5min) .

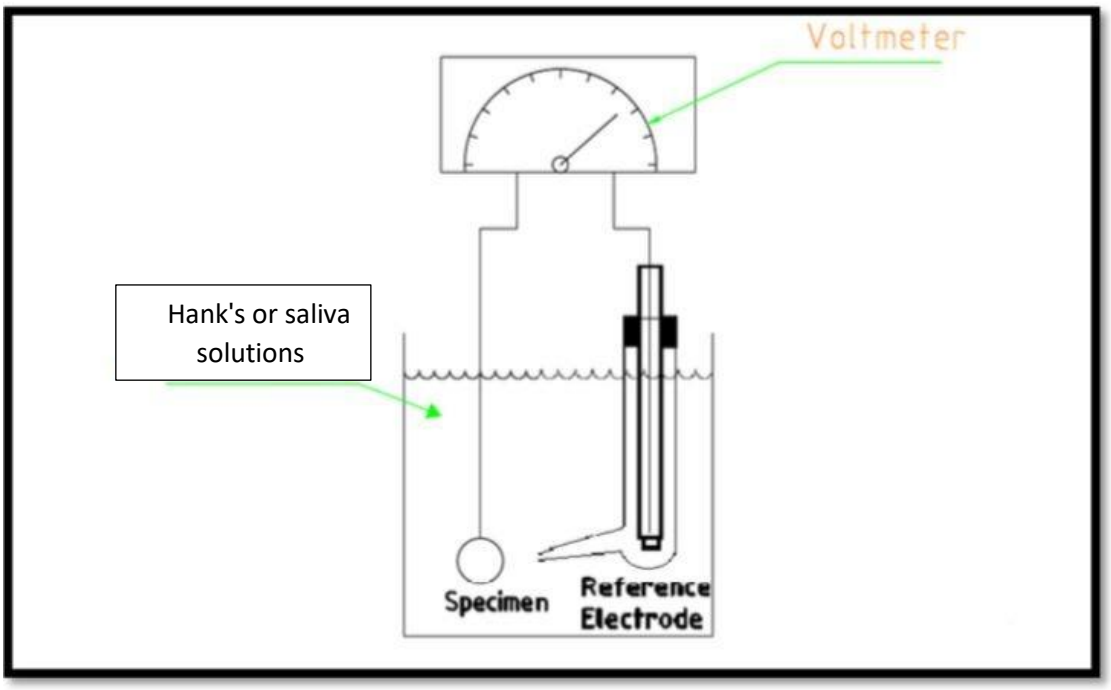

Figure (3-9): Illustrates a schematic drawing describes the experimental situation for the open circuit potential Measurement.

3.7.2 Potentiodynamic polarization

Potentiodynamic polarization, electrochemical tests were carried out in three-electrodes cell and containing electrolytes similar to nature artificial saliva and Hank's solutions. The counter electrode was Pt electrode and the reference electrode was SCE and working electrode specimen according to the american society for testing and materials ASTM F746-04[97].

.

The potentiodynamic polarization curves were plotted and both corrosion current density ($I_{corr.}$) and corrosion potential ($E_{corr.}$) were estimated by tafel plots by using anodic and cathode branches. The electrochemical system used is shown in Figure (3-10). The following equation can calculate the rate of corrosion [98]:

Corrosion rate (mpy) = 0.13 I_{corr} (Ew) / A.ρ …… (3-4)

Where:

0.13 = Metric and time conversion factor.

$I_{corr.}$= Corrosion current density (μA/ cm^2).

E.W= Equivalent weight (g/eq.).

A= exposed specimen area (cm^2)

ρ= Density (g/cm^3) measured by porosity and density test.

mpy = Corrosion rate (mils per year).

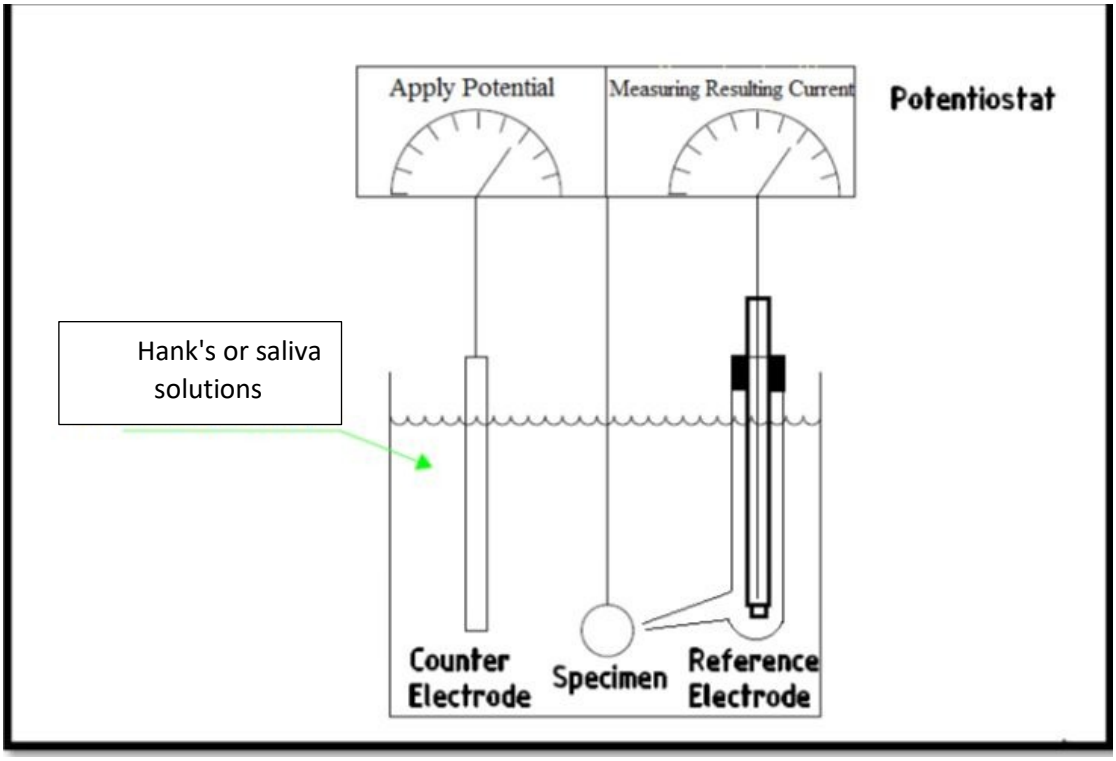

Figure (3-10) Shows a schematic diagram of potentiostatic polarization cell

Table (3-3) Chemical composition of artificial saliva and Hank's solutions [99].

No.	Constituents	Hank's solution	artificial saliva
		(g/L)	(g/L)
1	KCl	0.4	1.5
2	CaCl2	0.14	-
3	NaHCO3	0.35	1.5
4	NaCl	8	-
5	NaH2PO4H2O	-	0.5
6	HSCN	-	0.5
7	MgCl2.6H2O	0.1	-
8	Glucose	1	-
9	Na2HPO4.2H2O	0.06	-
10	KH2PO4	0.06	-
11	MgSO4.7H2O	0.06	-
12	Lactic acid	-	0.9

3.8 Ions Release

The static immersions test (metals ions rlease) of both Ti6Al4V alloy, Ti-6Al4V-Ta and Ti-6Al4V-Zr alloys in vitro by immersing in artificial saliva and Hank's solutions are illustrated in table (3-4).

The test of static immersions is recognized in agreement with the currently specified JIS T- 0304 standards for metallic biomaterial [100].

Specimens are immersed in plastic containers with 50 ml of each solutions saliva and Hank's for 21 days. The test has been done at the Ministry of Science and Technology .

Chapter Four

Results and Discussion

Chapter Four
Results and Discussion

4.1 Introduction

In this chapter, the experimental results were presented, which include the properties related to the specimens. These samples were prepared using the metal powder technique. Microstructure was tested by light optical microscope, SEM and EDX. The mechanical and physical properties tests that included hardness, dry wear test , the brazilin test , density & porosity and contact angle test . Electrochemical test (open circuit voltage, potentiodynamic polarization). Phase analysis results from XRD technique. Release of metal ions Ti, Al , V , Zr and Ta from alloys Ti6Al4V ,Ti6Al4V-XZr and Ti6Al4V-XTa .

4.2 Particles Size Analyzer

As shown in Figures (4-1) the particle size analysis test reports is shown, which shows the size of the powder particles for each element separately (Ti, Al, V, Ta , Zr) and for all these elements together (Ti, Al, and V) as base alloy and their analysis , where the blue curve shows the cumulative particle size distribution while the red curve shows the normal distribution of particle size , in table (4-1) the average particle size of the used powders is shown.

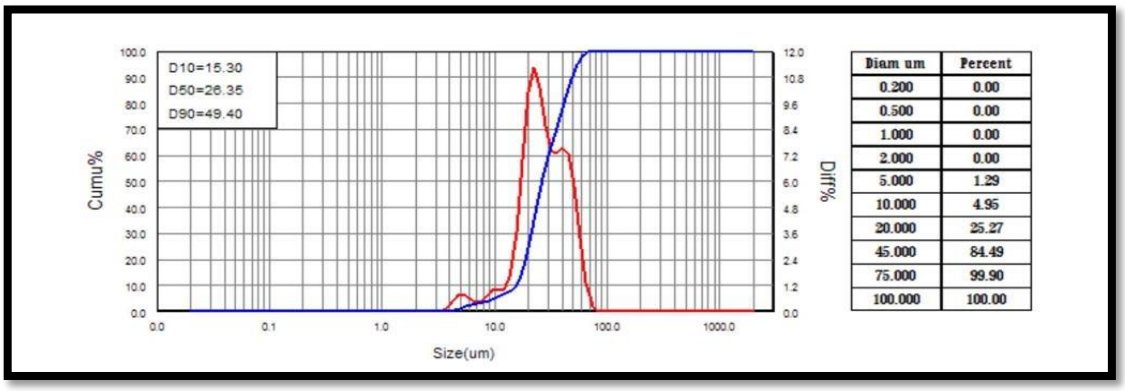

Diam um	Percent
0.200	0.00
0.500	0.00
1.000	0.00
2.000	0.00
5.000	1.29
10.000	4.95
20.000	25.27
45.000	84.49
75.000	99.90
100.000	100.00

(Ti element)

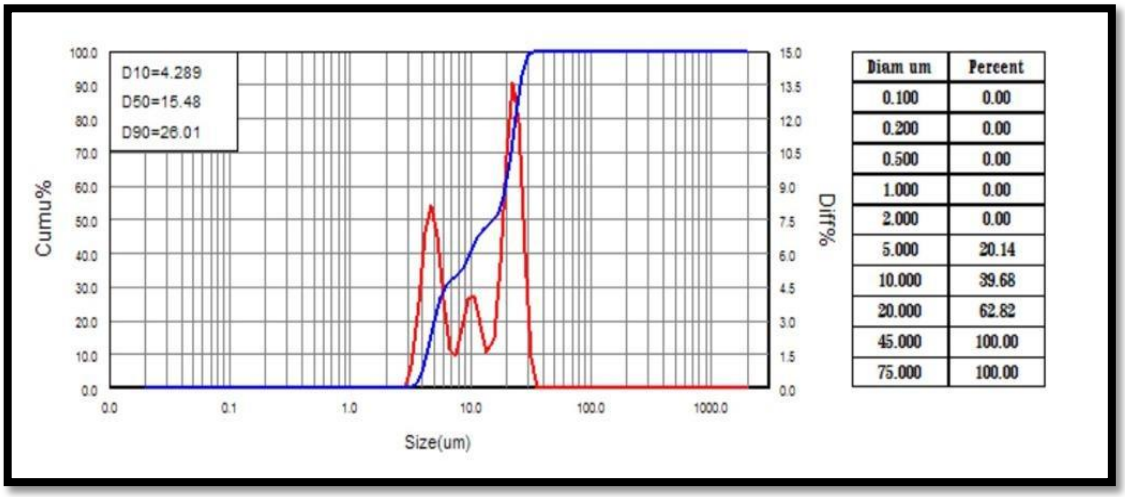

Diam um	Percent
0.100	0.00
0.200	0.00
0.500	0.00
1.000	0.00
2.000	0.00
5.000	20.14
10.000	39.68
20.000	62.82
45.000	100.00
75.000	100.00

(Al element)

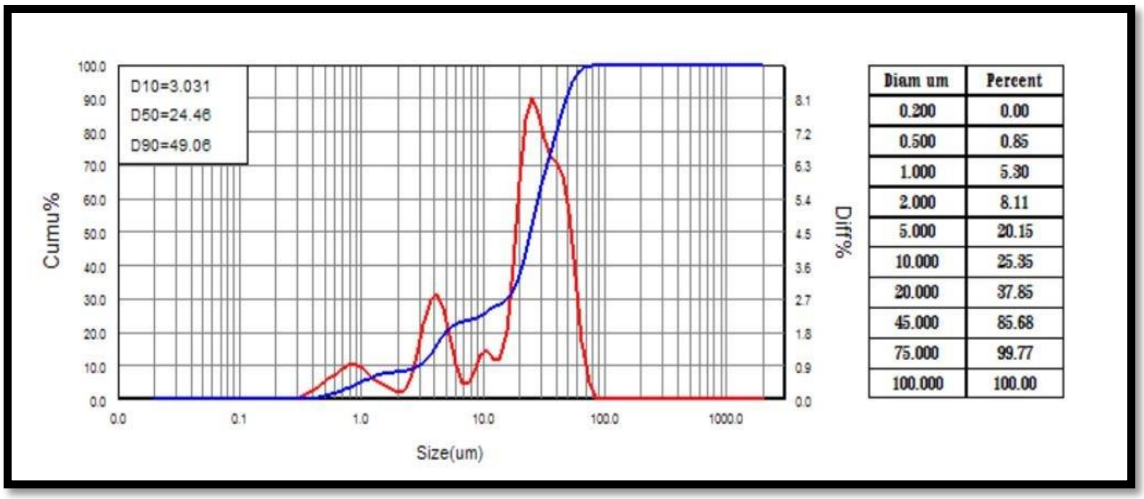

Diam um	Percent
0.200	0.00
0.500	0.85
1.000	5.30
2.000	8.11
5.000	20.15
10.000	25.35
20.000	37.85
45.000	85.68
75.000	99.77
100.000	100.00

(V element)

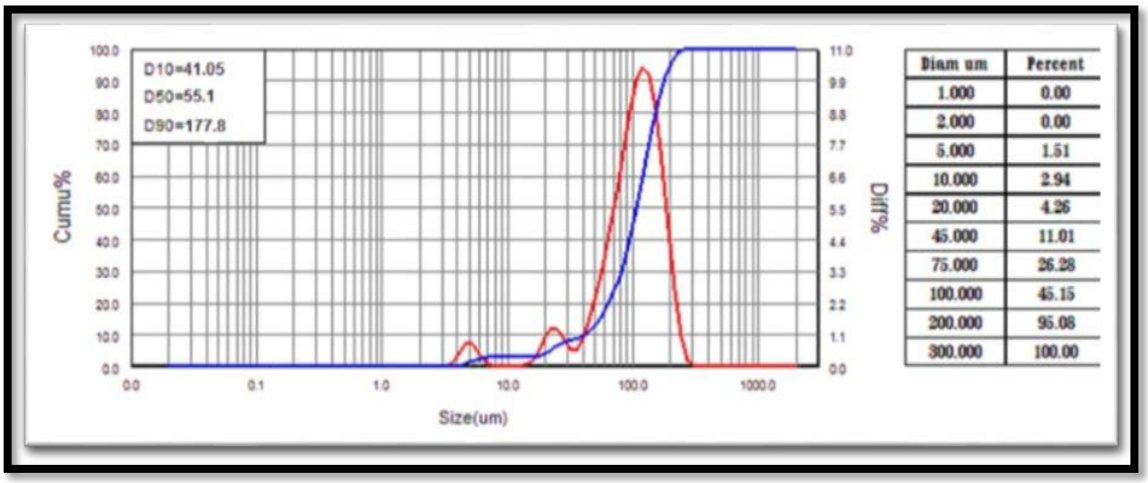

Diam um	Percent
1.000	0.00
2.000	0.00
5.000	1.51
10.000	2.94
20.000	4.26
45.000	11.01
75.000	26.28
100.000	45.15
200.000	95.08
300.000	100.00

(Ta element)

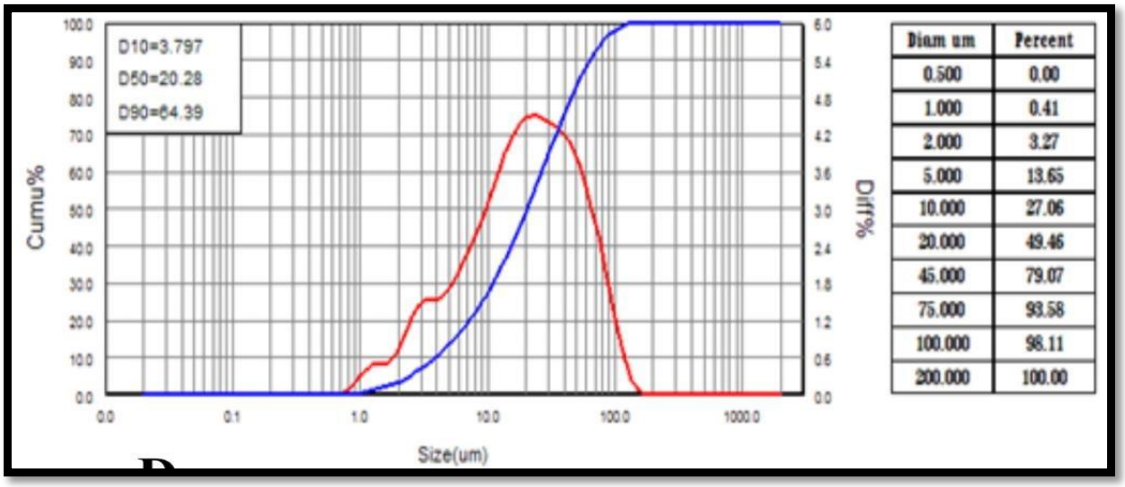

Diam um	Percent
0.500	0.00
1.000	0.41
2.000	3.27
5.000	13.65
10.000	27.06
20.000	49.46
45.000	79.07
75.000	93.58
100.000	98.11
200.000	100.00

(Zr element)

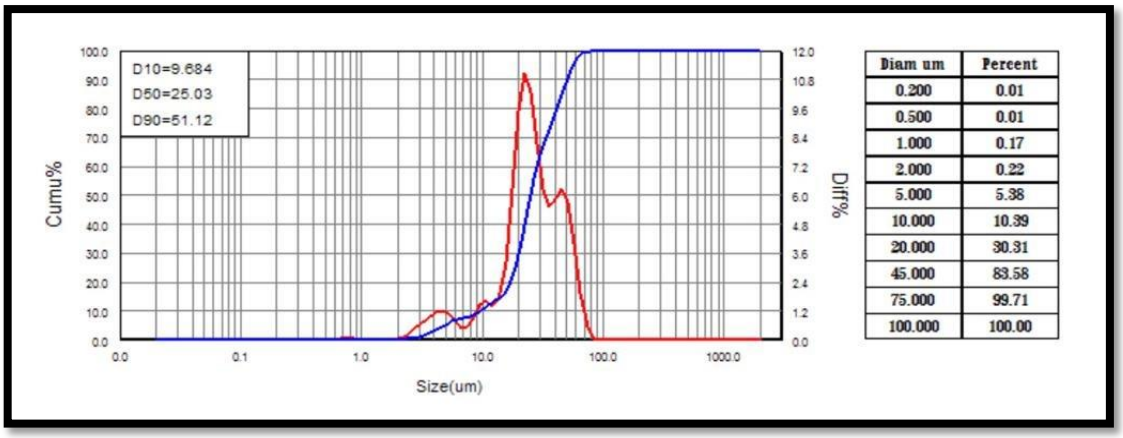

Diam um	Percent
0.200	0.01
0.500	0.01
1.000	0.17
2.000	0.22
5.000	5.38
10.000	10.39
20.000	30.31
45.000	83.58
75.000	99.71
100.000	100.00

Base (Ti,Al,V) alloy

Fig (4-1) Particles size analyzer for (Ti,Al,V,Base,Ta,Zr)

Table (4-1) Purity % and average particle size of powder materials

Material (powder)	Purity%	Average partials size (µm)
Titanium	99.93	26.35
Aluminum	99.9	15.48
Vanadium	99.99	24.46
Tantalum	99.95	55.1
Zirconium	99.95	20.28
Base	-	25.03

4.3 Effect of Compacting Pressure on Density

Figure (4-2) shows the effect of the compacting pressure on the green samples. This done using the electric hydraulic piston shown in figure (3-5). The loading rate was (0.3 ton /min), incubation time was (3min) in state applied stress. The graphite powder used as lubricator to the mold.

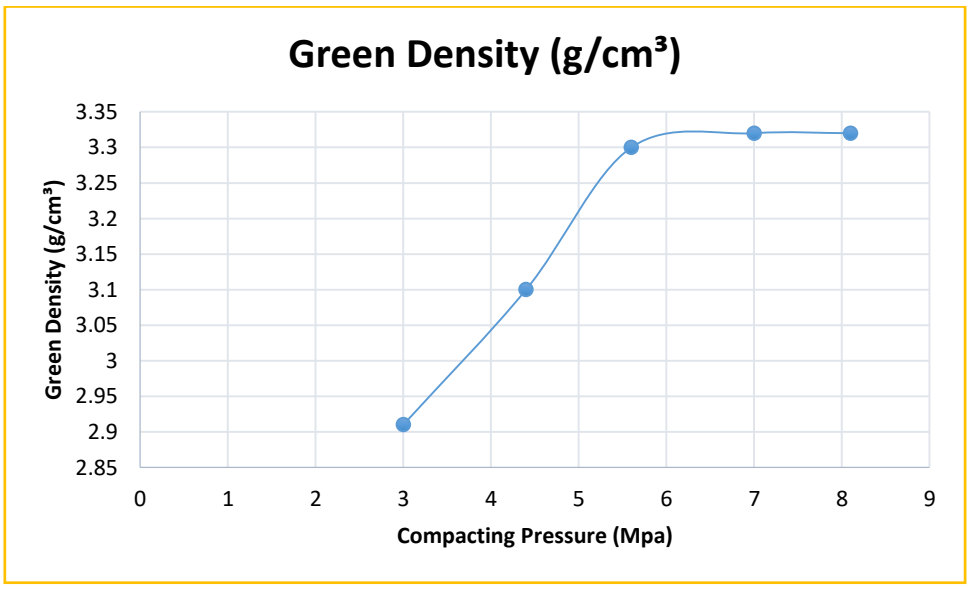

Figure (4-2): Effect of compacting pressure on the green density of the base alloy samples

Various values for compacting pressure were used in preparing these compacts. Figure (4-2) shows increasing the pressure, increases value of the green density until it reaches a constant value does not change with the increase in pressure, so was taken pressure values when the stability of the green density is 600 Mpa This compacting pressure was used for all studied specimens.

4.4 Microstructure Characterization

4.4.1 X-Ray Diffraction Analysis

The main objective to analyze X-ray diffraction was to determine the phases present in sintered specimens to analyze the microstructure of the studied Ti6Al4V base alloy, Ti6Al4V -XTa and Ti6Al4V -XZr after sintering process, because in general, the mechanical and physical properties of the alloys are affected by phase transition [101].

Phase transformation is a diffusion process and needs a high temperature to occur. Figure (4-3) illustrates the XRD patterns for base alloy after sintering at 550 C° for 1hr then 1000 C° for 2hr under Argon gas. It can be observed that all Ti , Al and V transformed to (αTi) , (βTi) phases [102]. Where Al is an alpha stabilizer and V is a beta stabilizer [103].

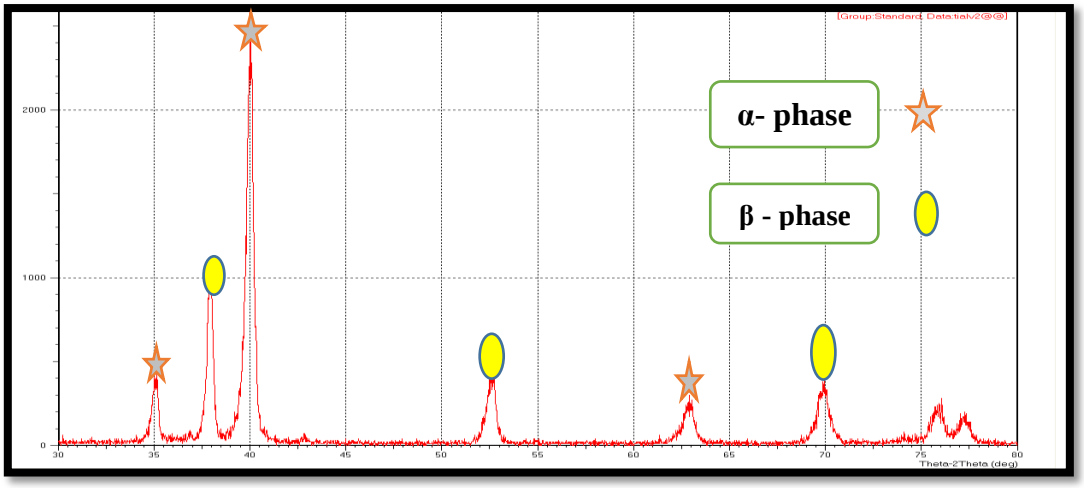

Figure (4-3) XRD test for the Ti6Al4V alloy.

Figure (4-4) illustrates XRD pattern for Ti6Al4V-2Ta alloy after the sintering process , all amount of Ti , Al, and V transformed to (αTi and βTi) phases and metallic Ti, Al and V peaks dose not appears in the Figure (4-4) . This means that 550 ˚C for 1h and then 1000 ˚C for 2h under Argon gas was enough to complete the sintering process due to the enhancement of the inter diffusion between Ti, Al, and V. The Ta was added at maximum percentage 2wt%, the XRD pattern for Ti6Al4V-2Ta alloy shown peak additional for beta phase at 2θ approximately 42-43. This means that the proportion of the beta phase increased in the alloy because Ta is one of the stabilizing elements for the beta phase.

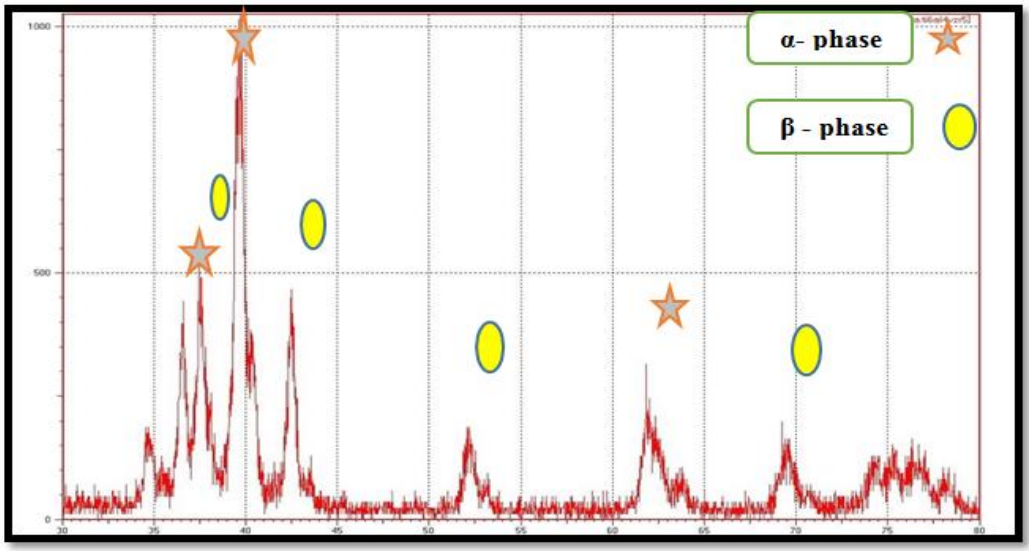

Figure (4-4) XRD test for the Ti6Al4V-2Ta alloy.

Figure (4-5) illustrates XRD pattern for Ti6Al4V-XZr alloy after the sintering process , all amount of Ti , Al, and V transformed to (αTi and βTi) phases. This means that 550C˚ for 1h and then 1000C˚ for 2h under argon gas was enough to complete the sintering process due to the enhancement of the inter diffusion between Ti, Al, and V. The Zr was added at maximum percentage 2wt%, the XRD pattern for Ti6Al4V-2Zr alloy shown peak additional for beta phase at 2θ approximately 40-55.

This means that the proportion of the beta phase increased in the alloy because Zr although it is neutral but Zr one of the stabilizing elements for the beta phase when present with installed elements for beta phase [104].

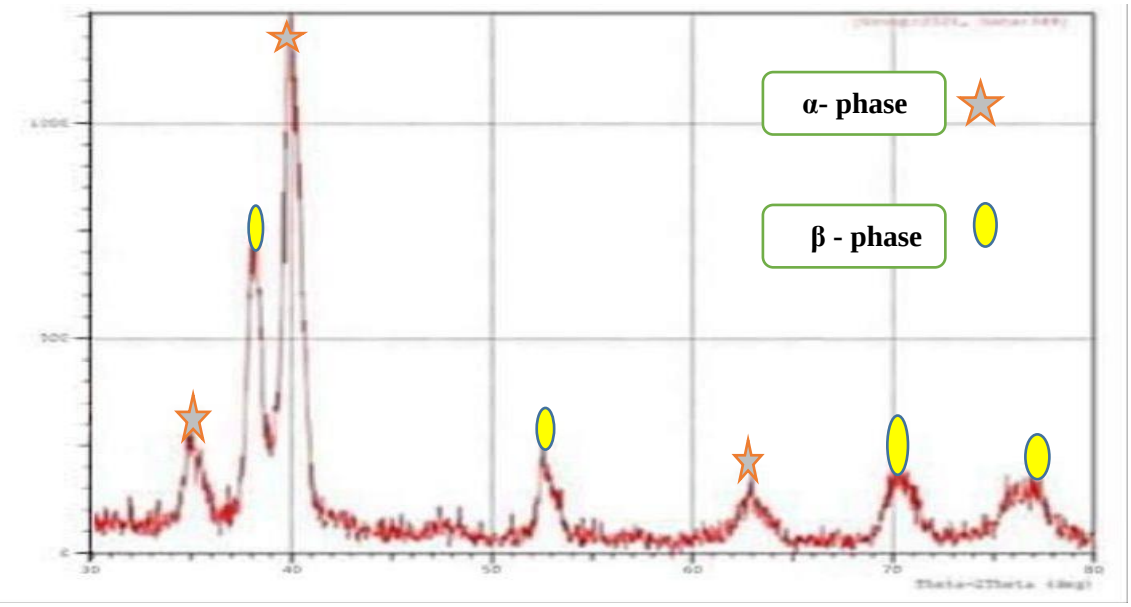

Figure (4-5) XRD test for the Ti6Al4V-2Zr alloy.

This means that the sintering process period at 550C° for 1hr then at 1000C° for 2hr was enough to complete the phases transformation process, the longer period of stay, lead to the greater diffusion of powders elements. The absence of free element is necessary in the alloys which used as biomaterials due to it toxicity effect into body.

4.4.2 Light Optical Microscope

The microstructure of an alloy is an essential parameter that determines its mechanical properties, physics and electrochemical as hardness, wear and corrosion resistance .The Figure (4-6) shows the microstructure of the etched alloys Ti6Al4V, Ti6Al4V-XTa and Ti6Al4V-XZr, after the sintering process with magnification of 400 x The boundaries of the grains and the current phases were revealed by testing the microstructure of the mentioned alloys. The specimens after sintering process, shown through this test that they contain microstructure as

shown in Fig (4-6) all specimens alloys consisting of two regions (a duplex microstructure), represents the regions of the light (bright) (α-Ti phase) and the other regions are dark which indicates the beta phase .

Generally compared with the base alloy , the addition of Ta and Zr elements leads to increase the spread (β- phase) due to the effect of Ta and Zr [104] as the beta stabilizer elements. This fact is similar to alpha beta and beta alloys , some equilibrium of beta phases are present at room temperature [105].

Where from Fig (4- 6) of the microstructure when adding Ta to the base alloy at proportion (0.5% wt Ta) shown that it led to a reduction in the size of grains for alloy compared to the size of grains the base alloy Ti6Al4V where was size grains medium not small or large in base alloy , and also shown the presence of a large beta phase compared to the base alloy, also that the beta phase at proportion of addition of (1,1.5%wt Ta) shown smaller and it begin spread on microstructure where the spread of the beta phase gradually increases in microstructure with increasing percentage of tantalum addition especially when the percentage of max addition (2%wt Ta) that is being accessed reached , where the beta phase was smaller and more diffuse on microstructure.

While when adding Zr to base alloy at proportion (0.5 % wt Zr) the size of the alpha particles increased compared to the grain size of the base alloy whose grain size is medium neither small or large ,also shown presence of a large beta phase compared with the base alloy, and when adding proportions of (1, 1.5%wt Zr) shows the spread of beta phase, which diffuse gradually increases with the increasing the percentage of zirconium addition and at arrival to the highest percentage of addition , where it found that the alpha phase increased and the beta phase spread more when adding (2% wt Zr) to the base alloy and with compared to

adding Ta 2% to the base alloy , shown the behavior of zirconium added it affect the beta phase diffusion more than the behavior of tantalum additive because element (Zr) which leads more beta phase spread so the mechanical properties of the microstructure at adding Zr improve and increase compared to mechanical properties the base alloy Ti6Al4V. Therefore, due to this clear spread of the beta phase as in the Figure (4-6) with addition Zr especially at an added proportions of 2%Zr , the alloy Ti6Al4V-XZr will have better mechanical properties than the base alloy Ti6Al4V and better than the base alloy with the addition of tantalum (Ti6Al4V-XTa) and this is confirmed by the Figure (4-6) of the microstructure when Zr is added, This is because the beta phase is more widespread than the alpha phase at adding Zr and the beta phase is a solid phase , as well Zr form Zro which is frome ceramic material that increases mechanical properties.

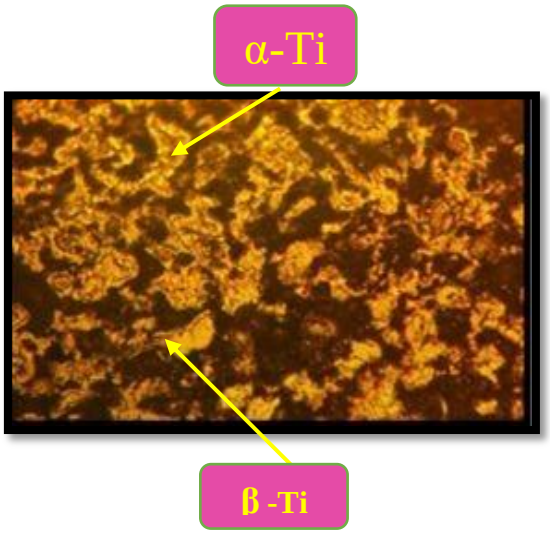

Base (400X)

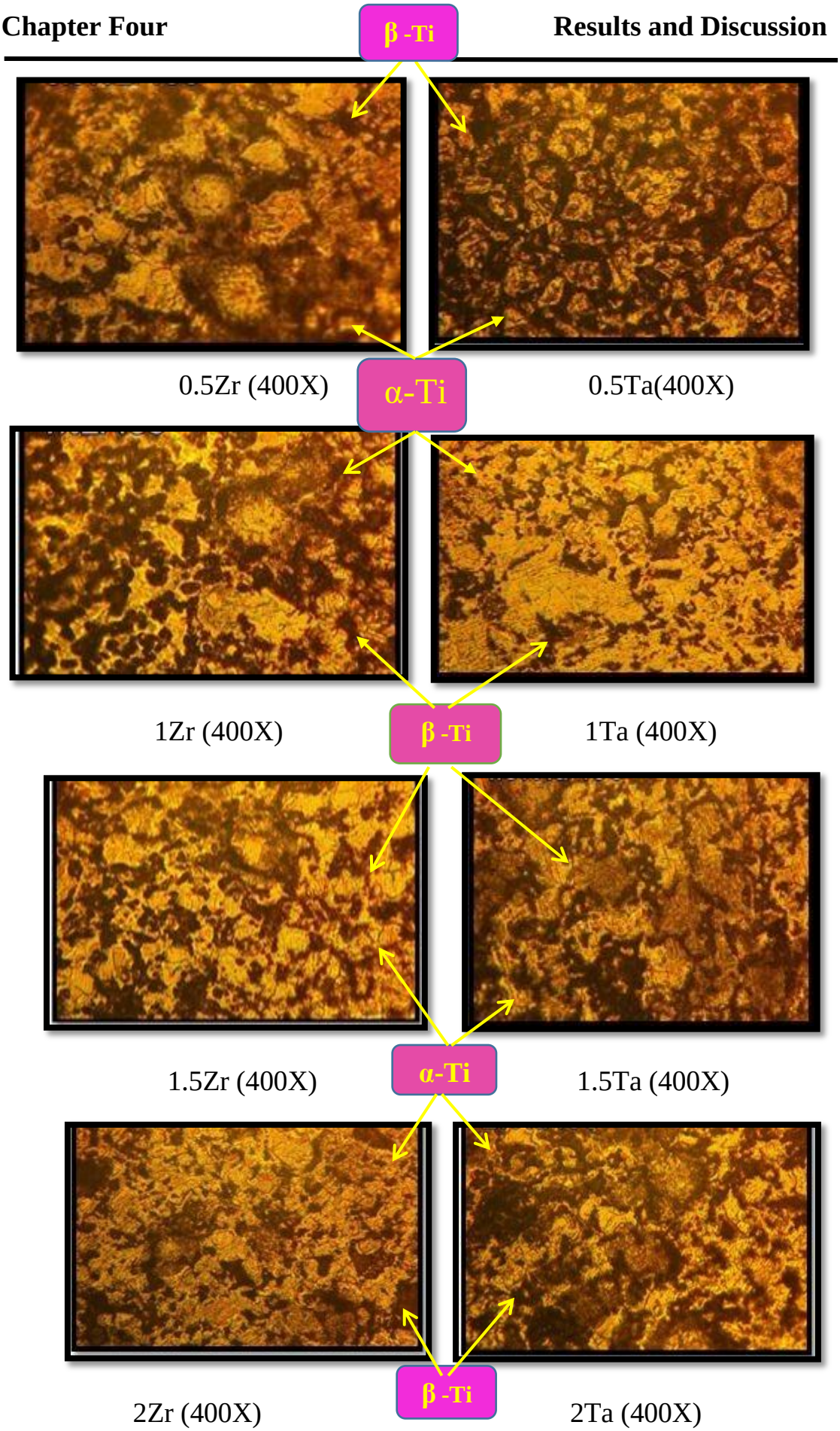

Fig(4-6 **Fig(4-6) Microstructure for (base,base -XTa,base-XZr)**

4.4.3 Scanning Electron Microscope (SEM)

Scanning electron microscope (SEM) has been used to get the microstructure of the etched specimens. The specimens have been etched by used etching solution to reveal the phases , pores and grain boundaries in the microstructure. The most common types of microstructure features in metallic materials are the boundaries between crystalline grains and the boundaries between different solid phases in multiphase alloys. The metallography can give a simplified idea about the relationships between the microstructure of the material and the material properties because the size grains directly affect the behaviour of the material [106].

SEM images are susceptible to chemical composition which is very sensitive to chemical composition [107] as a result, sintered specimens' microstructure shows a multiphase structure in which the (α Ti and β Ti) phase , this is confirmed by the XRD results.

SEM images of etched alloys showed phases (α Ti and β Ti) , grain boundaries , pores in different sizes and because the method used in preparing the specimens is the metal powder technique, there are pores that can be seen on the surface by test (SEM) that shows few pores on the surface of the samples with an increase in the percentage of additions to the element zirconium and tantalum , because of the role of these elements in reducing the pores gradually with a gradual increase for the addition, especially when adding zirconium reduces the porosity more than tantalum compared with Ti6Al4V base alloy , as indicated in Figures (4-7) illustrates the microstructure of Ti6Al4V, Ti6Al4V-XTa, Ti6Al4V-Zr alloys after sintering process with magnification 1700x. Its also clear that the spread of the beta phase increases with the addition of zirconium and tantalum, and its spread increases with the addition of zirconium more , as in the LOM test.

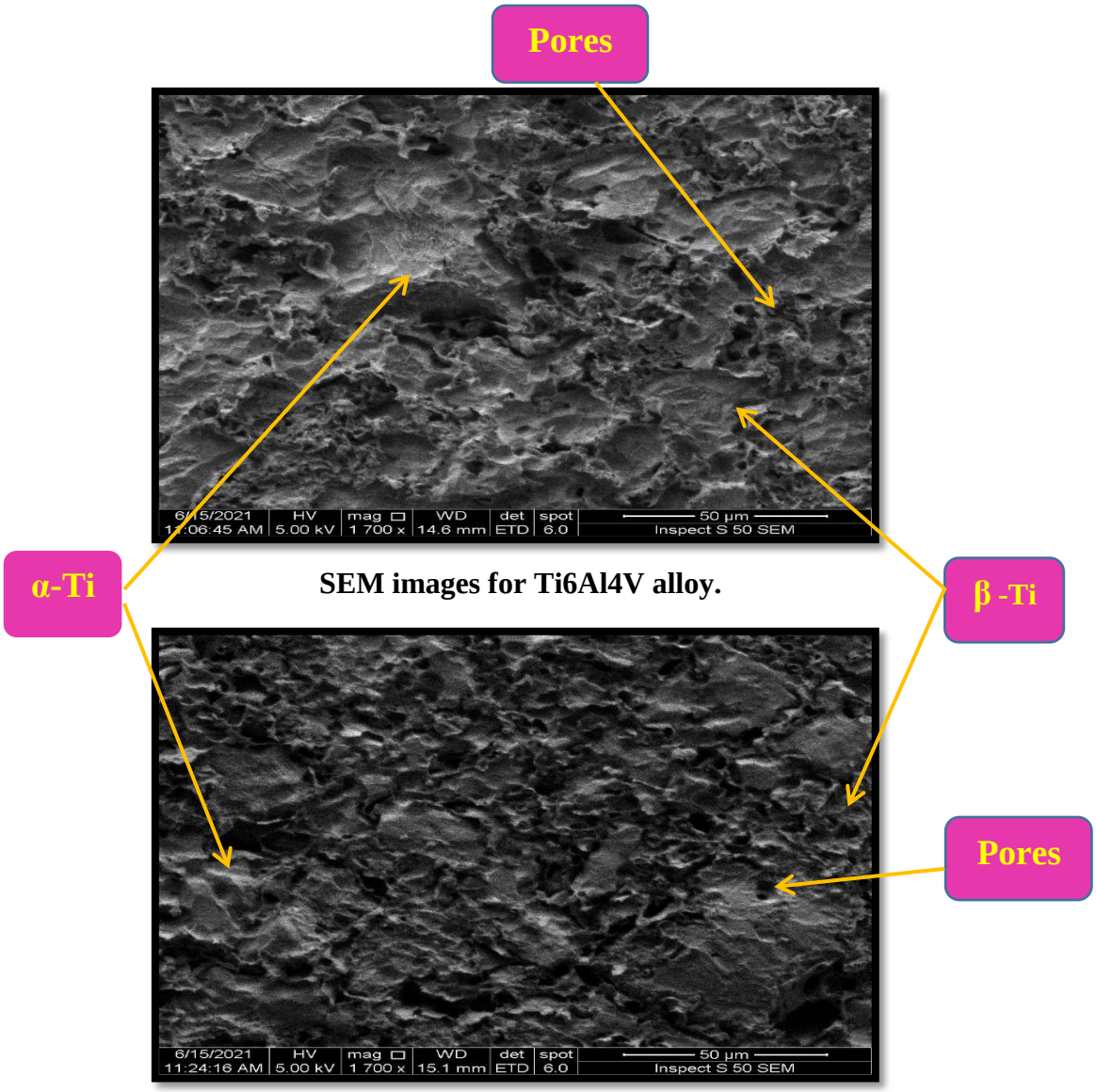

SEM images for Ti6Al4V alloy.

SEM Images for Ti6Al4V-0.5Ta alloy.

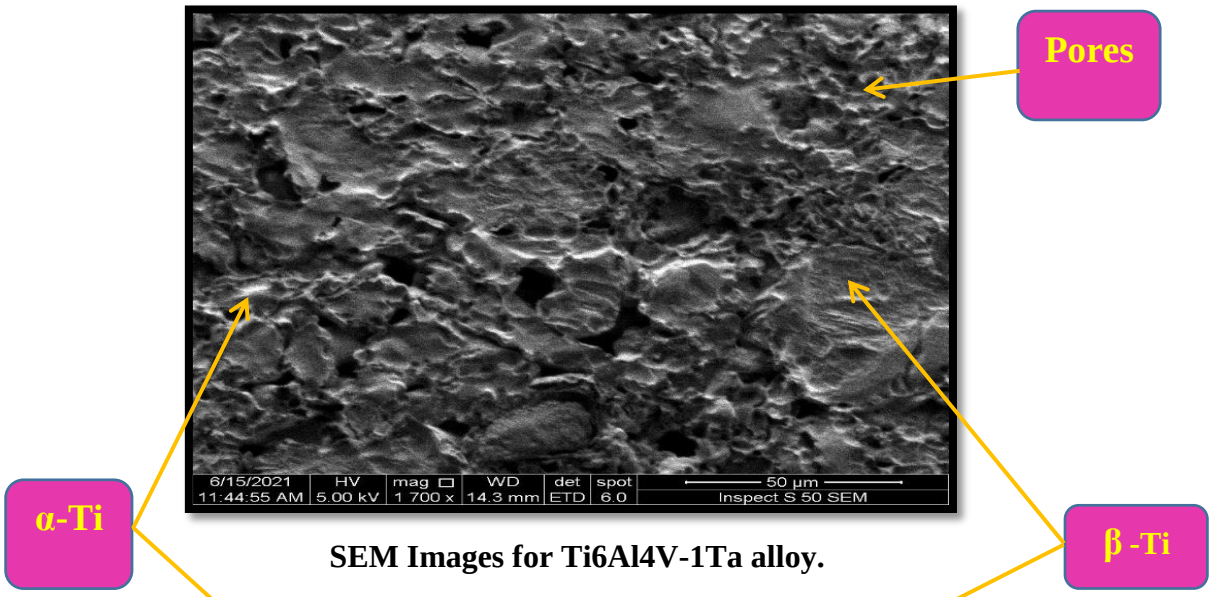

SEM Images for Ti6Al4V-1Ta alloy.

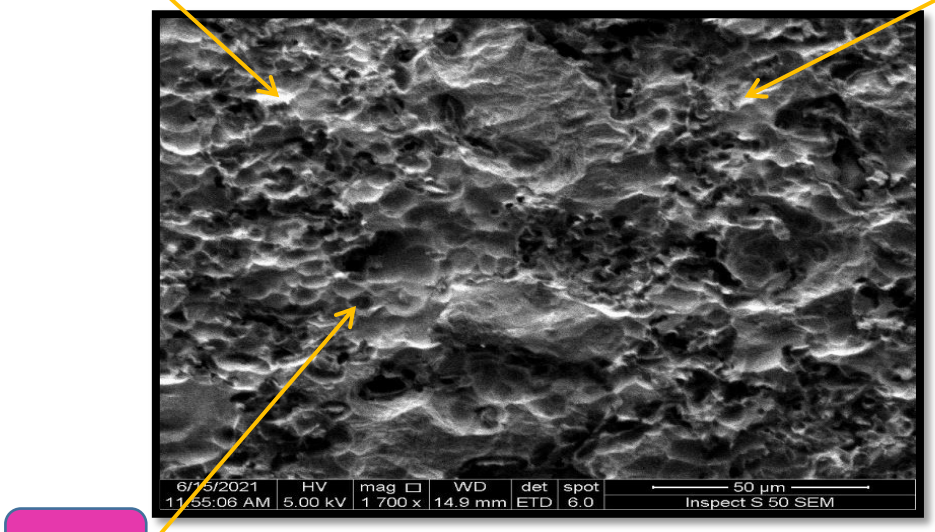

SEM Images for Ti6Al4V-1.5Ta alloy.

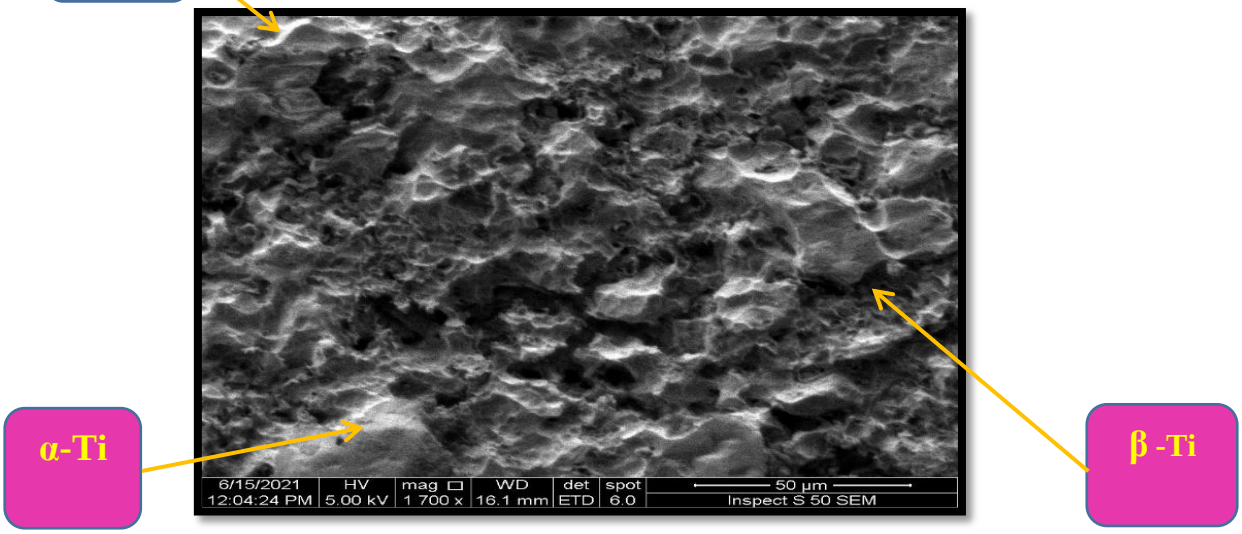

SEM Images for Ti6Al4V-2Ta alloy.

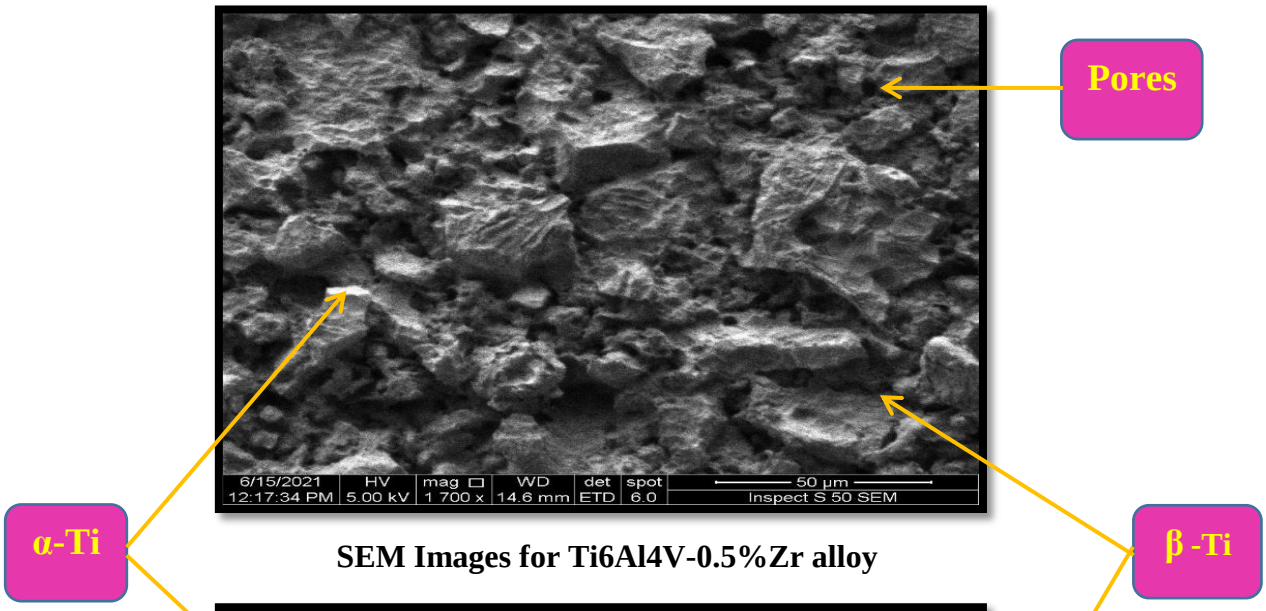

SEM Images for Ti6Al4V-0.5%Zr alloy

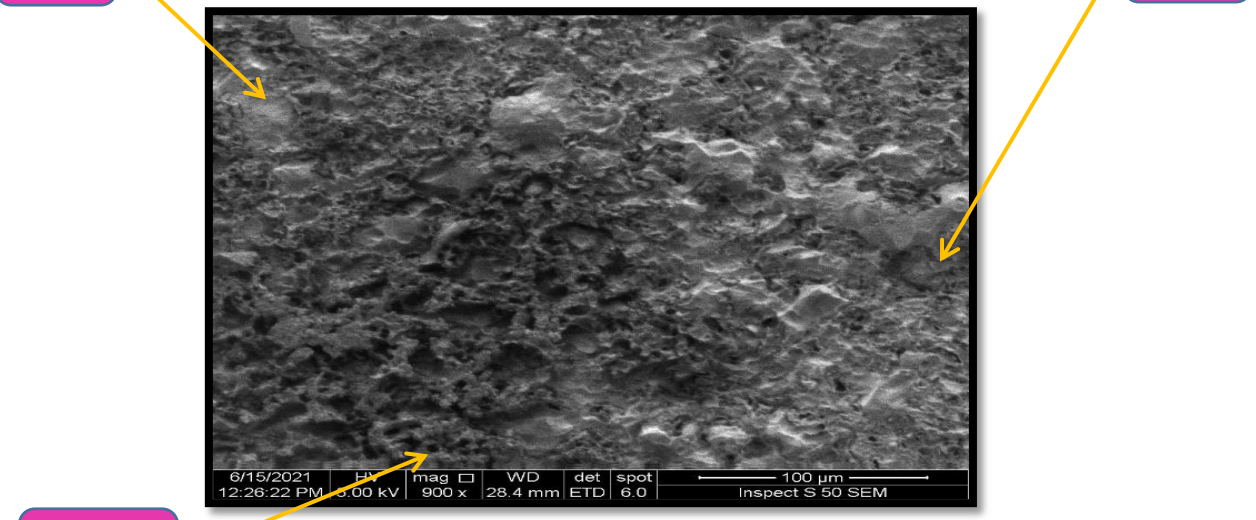

SEM Images for Ti6Al4V-1%Zr alloy.

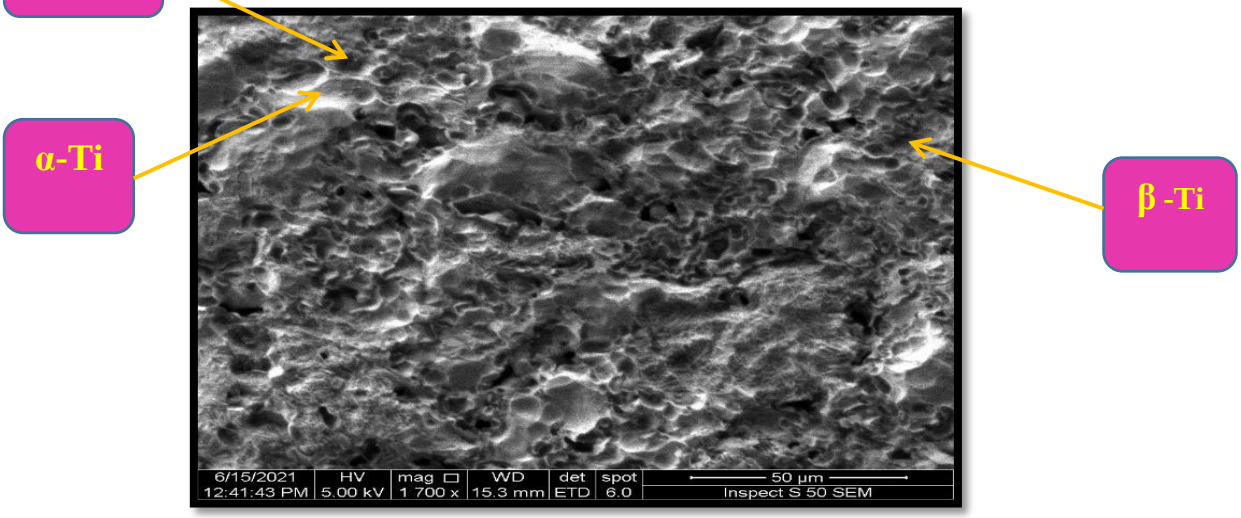

SEM Images for Ti6Al4V-1.5Zr alloy.

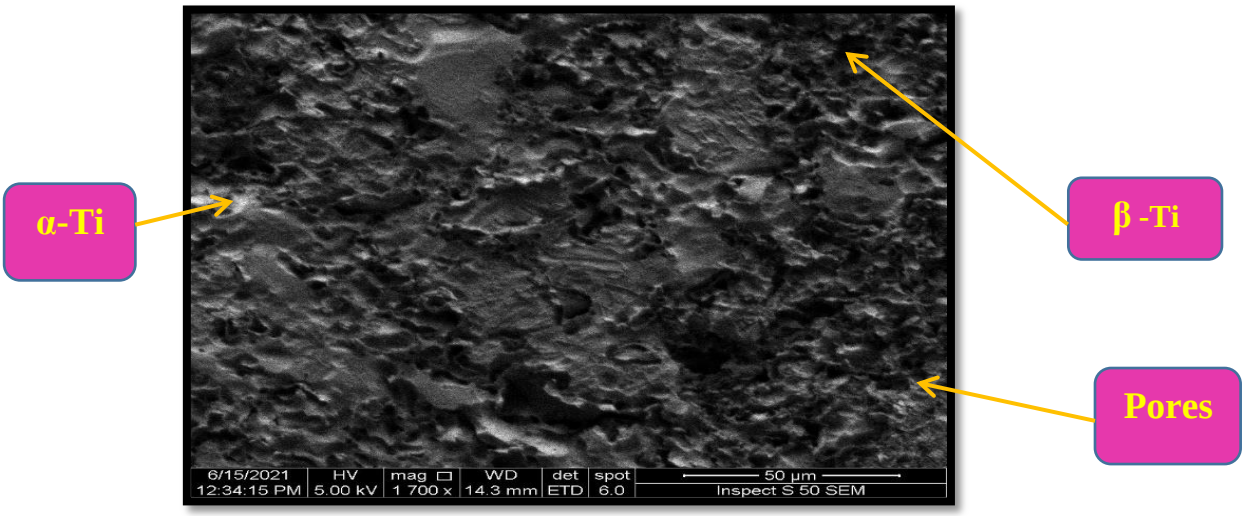

SEM Images for Ti6Al4V-2%Zr alloy.

Fig (4-7) SEM for(base,base -XTa,base-XZr).

4.3.4 Energy Dispersive X-Ray Analyzer (EDX)

The punctual chemical analysis by EDX aimed to determine microstructural details, quantitatively, through percentage values in weight, based on the choice of the best analysis points that would allow an understanding of the results obtained in terms of hardness, corrosion resistance , compressive strength, among others [108]. Such results were conclusive in determining the applicability of the Ti6Al4V, Ti6Al4V-2Zr, and Ti6Al4V-2Ta alloy as a biomaterial

In this study, 9 alloys were analyzed , one prepared from the Ti6Al4V base and the rest from the base, adding different proportions of tantalum and zirconium done this test by used etching solution.

EDX uses a power dispersion spectrometer installed in SEM to determine the distribution of different elements in the Ti6Al4V base alloy,Ti6Al4V-XTa and Ti6Al4V-XZr alloys , where the best points of analysis were marked, aiming to have a better view of the microstructural detailed, and thus being possible to obtain essential information.

From Figure EDX for the nine prepared alloys from (Ti6Al4V) base alloy,(Ti6Al4V-XTa and Ti6Al4V-XZr) alloys , the Ti peak is more pronounced than other elements as (Al), (V) , (Ta), and (Zr). EDX was tested by taking two points for each specimen, as found that the base alloy contains percentages of (Al) , (V) and the role of these existing elements in determining the microstruture and their impact on determining the existing phases (α Ti and β Ti), this confirms results of the SEM, and confirms the results of the XRD test existence of Al which is an alpha phase stabilizer and existence of V which is a beta phase stabilizer, and when tantalum and zirconium are added in different proportions (0.5,1,1.5&2%Ta and Zr) to the base alloy, it appears that the percentage of their presence gradually increases with the increase in the percentage of addition, and that the elements tantalum and zirconium are stabilizer beta-phase, where an element (Zr) although it is neutral, but it works to stabilize the (beta phase) when there is elements with it works to stabilize the (beta phase) , and therefore the element (Zr) is also work on installed the (beta phase) [104].It is clear of points to test EDX, that the conditions for the mixing and sintering process were sufficient for the occurrences of the distribution and spread of the elements.

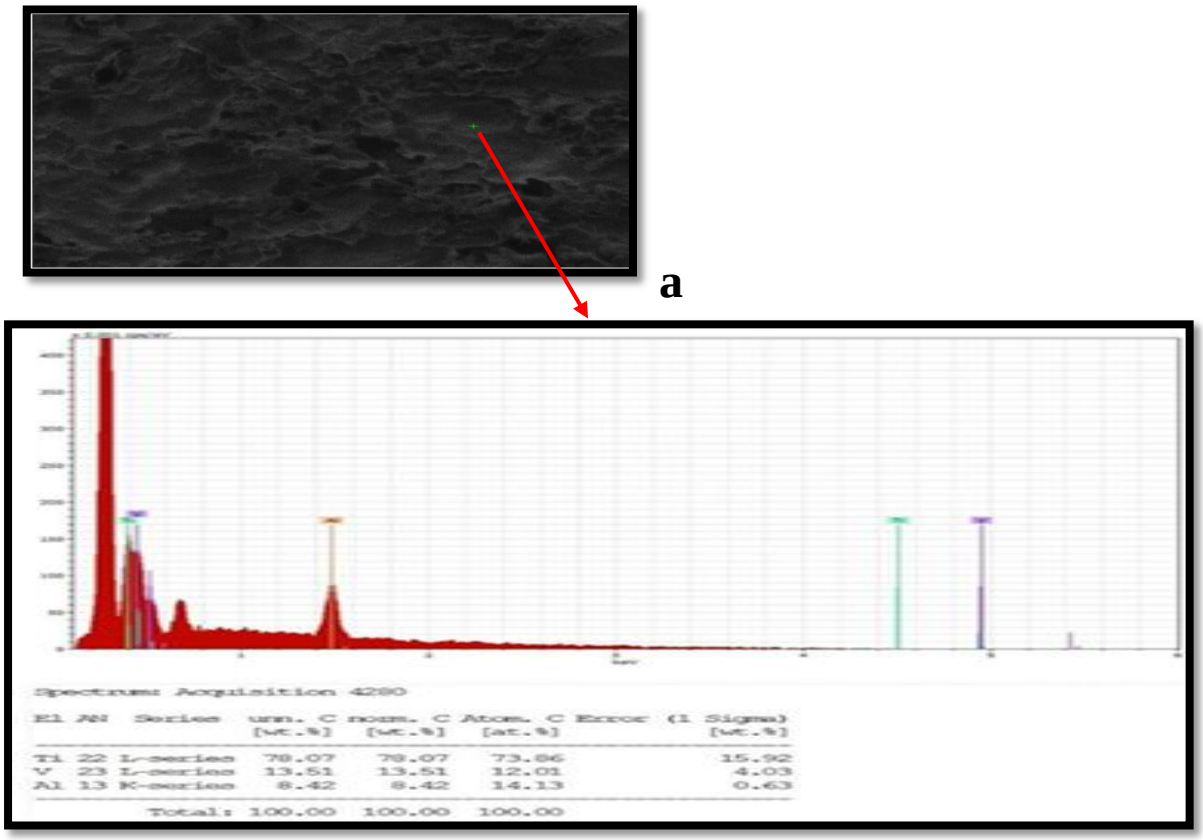

Figure (4-8) : a EDX for Ti6Al4V base alloy.

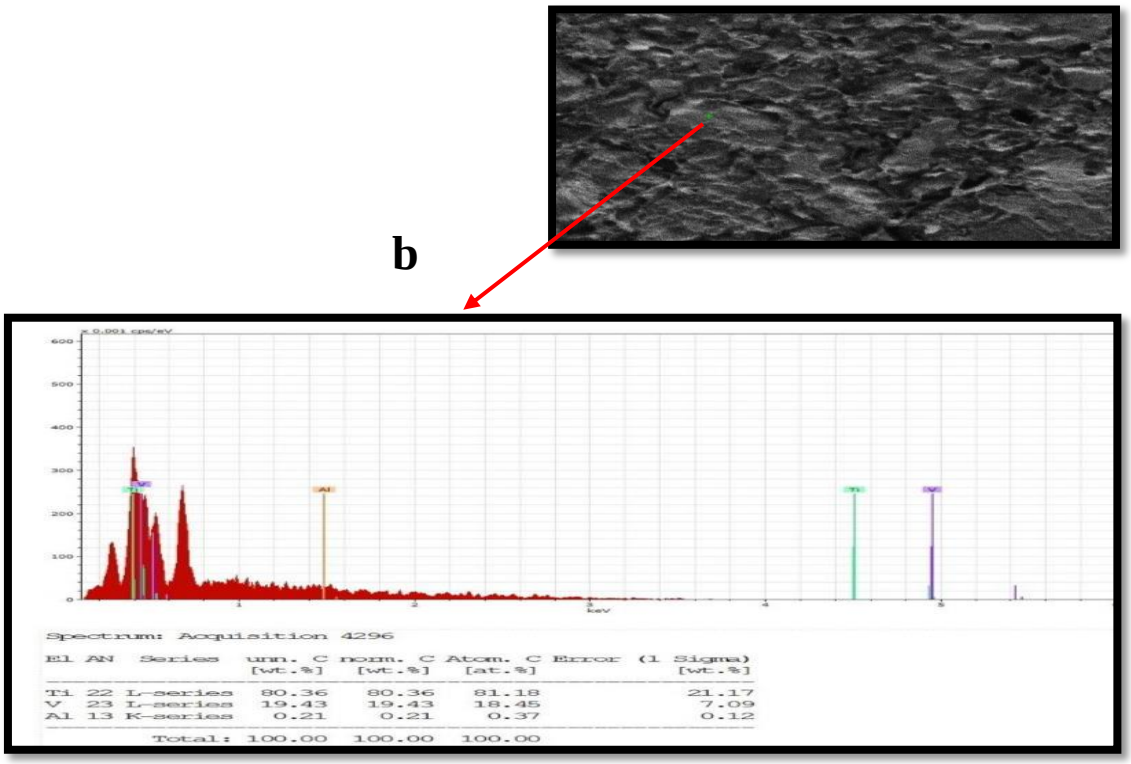

Figure (4-8) : b EDX for Ti6Al4V base alloy.

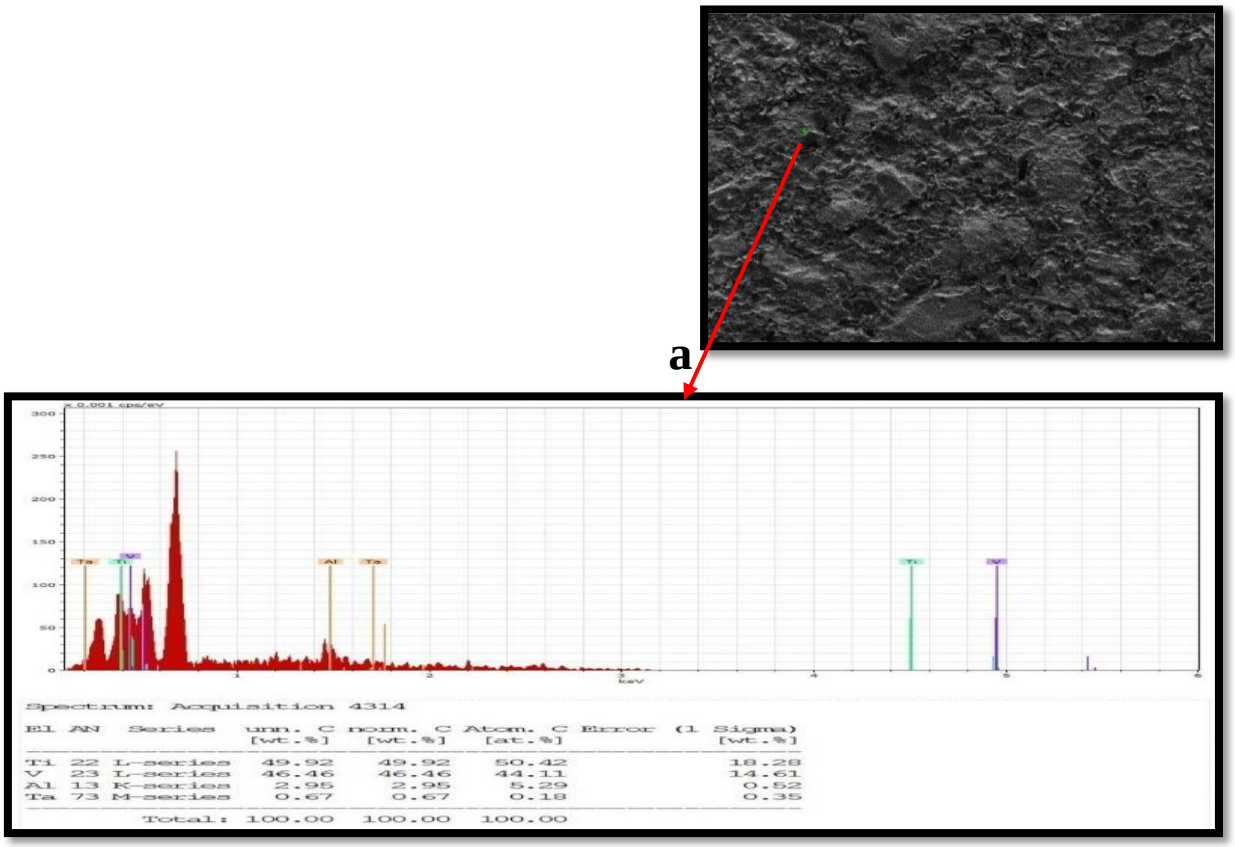

Figure a (4-9): EDX for Ti6Al4V-0.5Ta alloy.

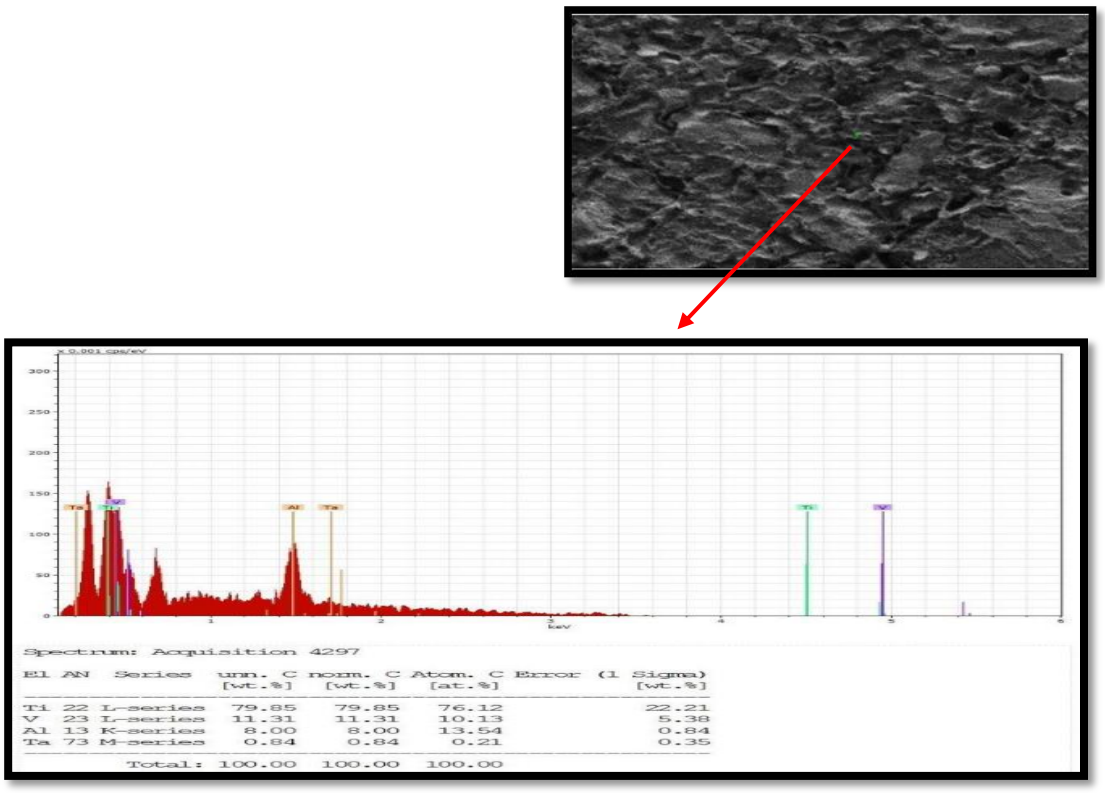

Figure b (4-9): EDX for Ti6Al4V-0.5Ta alloy

a

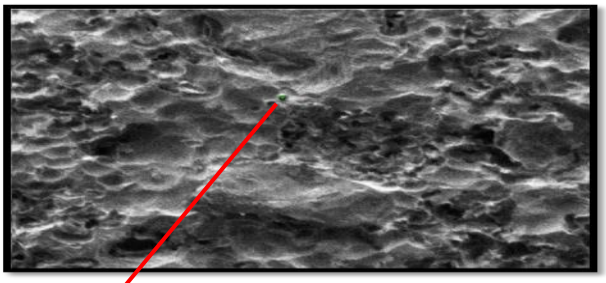

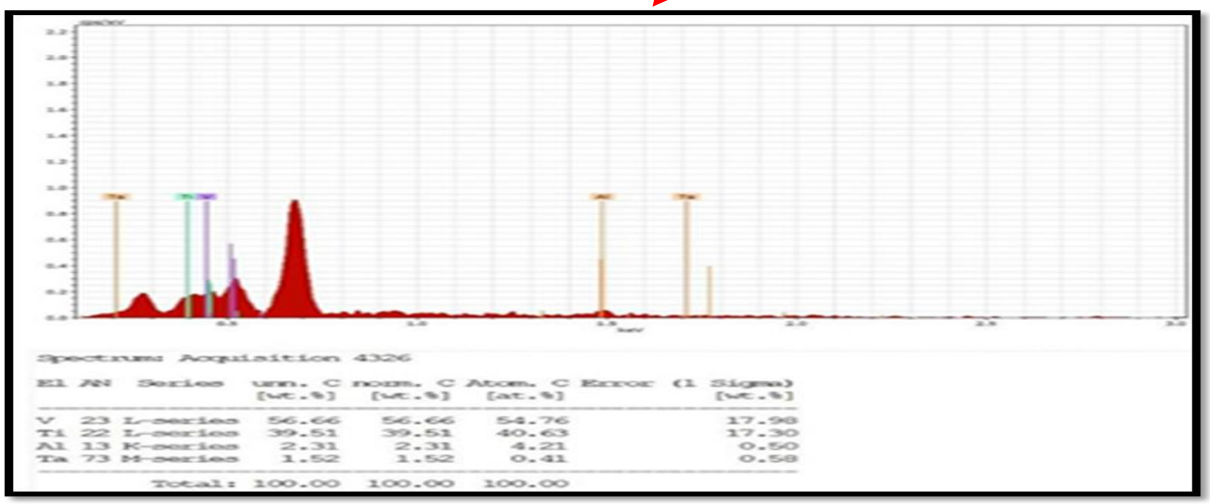

Figure a (4-10): EDX for Ti6Al4V -1 Ta alloy.

b

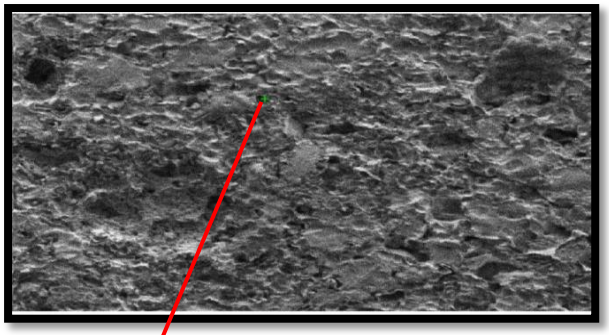

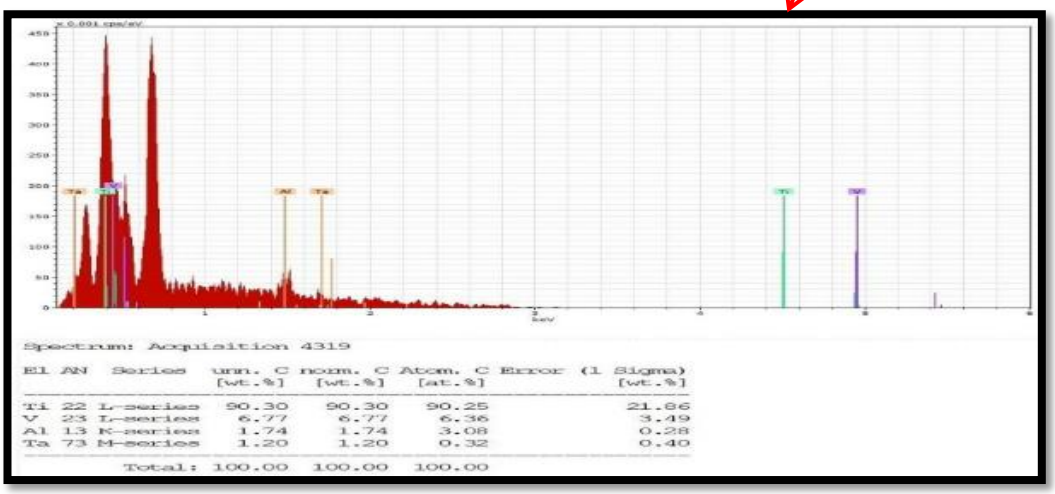

Figure b (4-10): EDX for Ti6Al4V -1 Ta alloy.

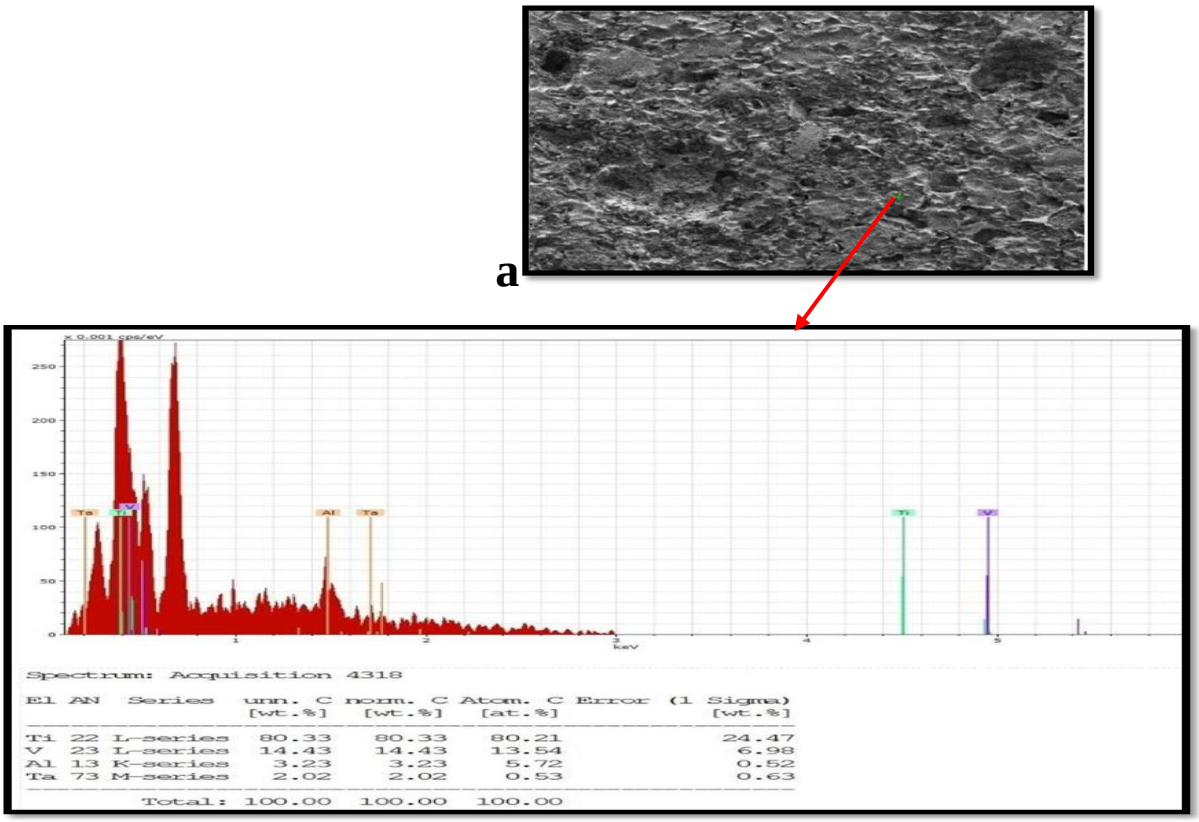

Figure a (4-11): EDX for Ti6Al4V-1.5Ta alloy.

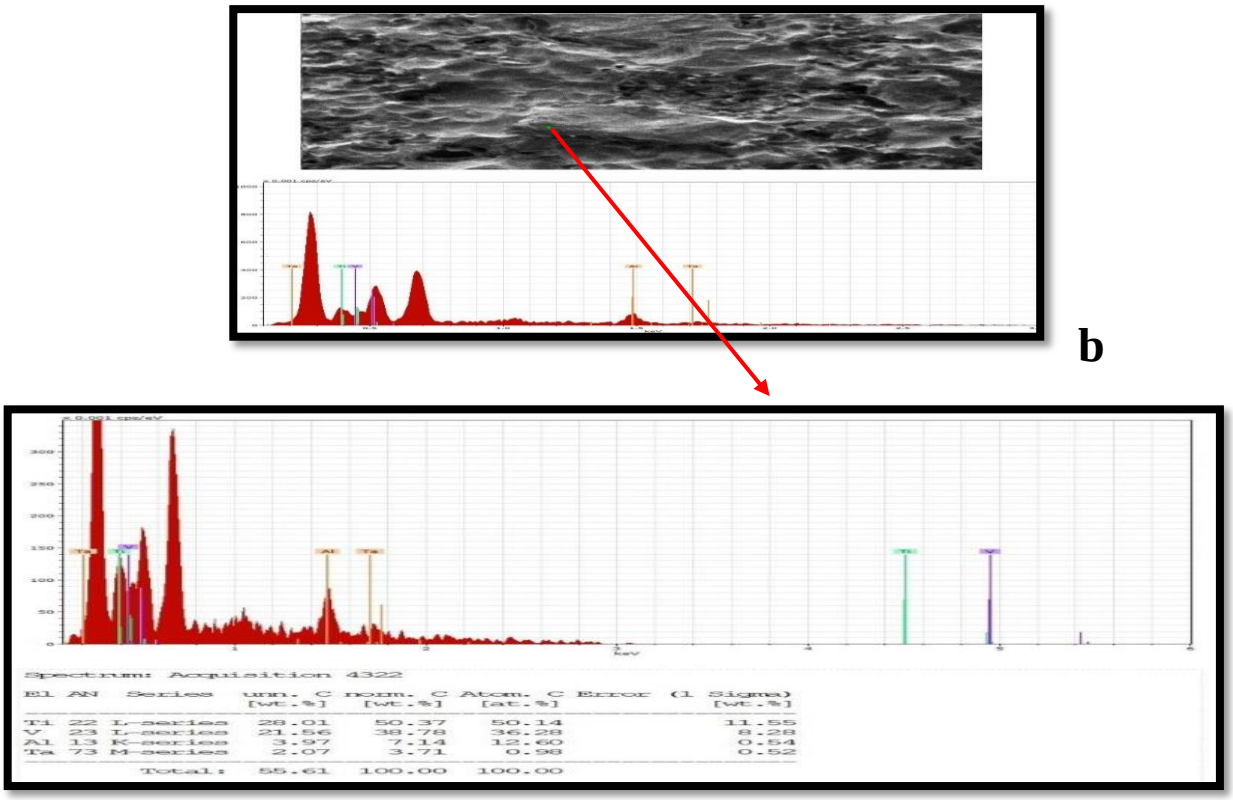

Figure b (4-12): EDX for Ti6Al4V-1.5Ta alloy.

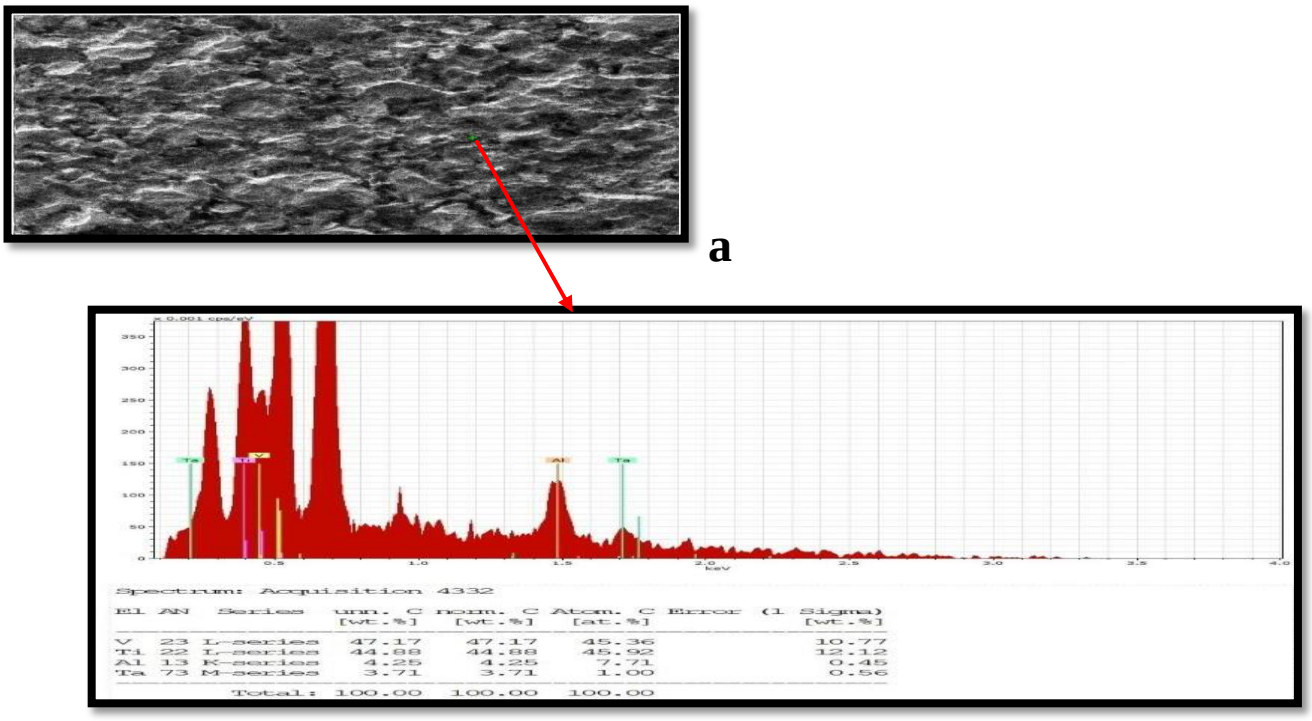

Figure a (4-13): EDX for Ti6Al4V-2Ta alloy.

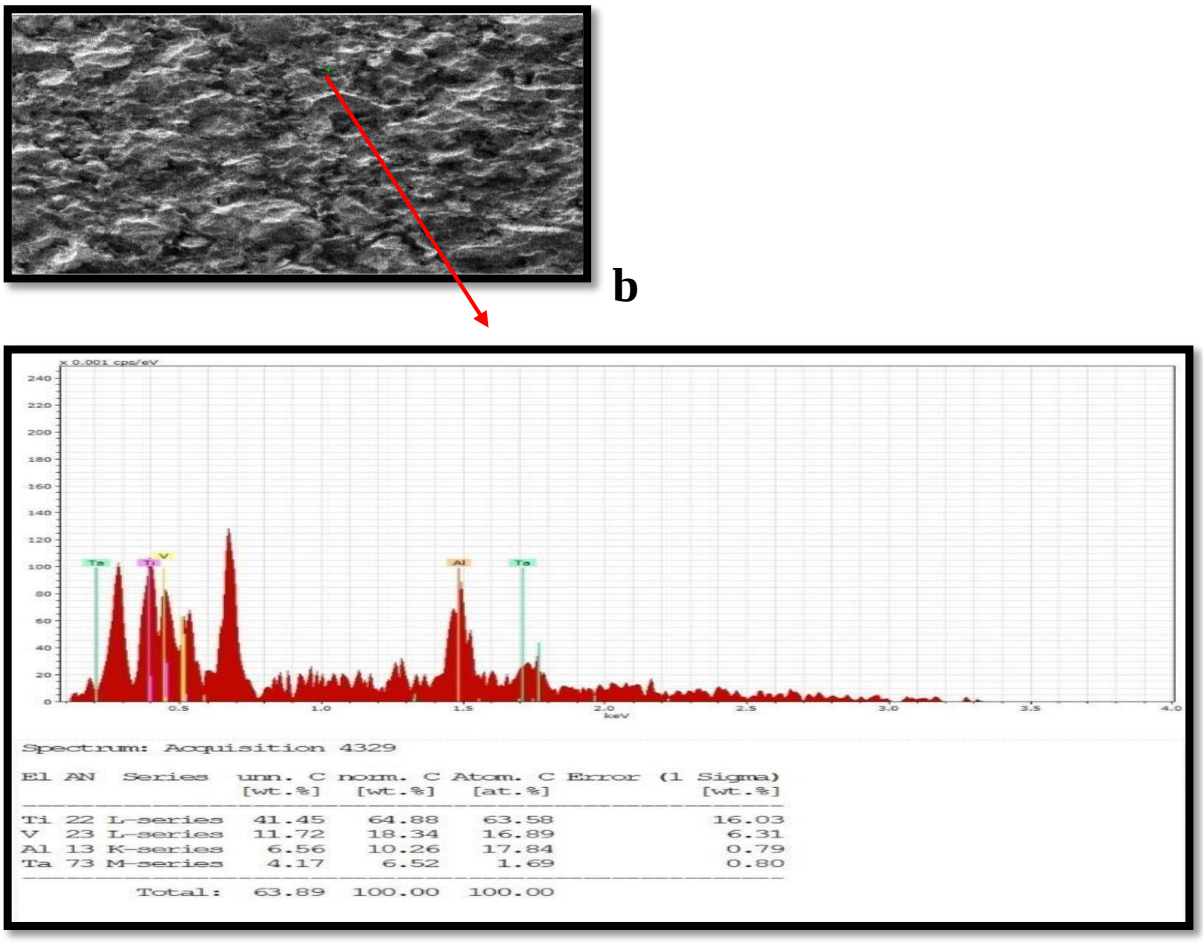

Figure b (4-13): EDX for Ti6Al4V-2Ta alloy.

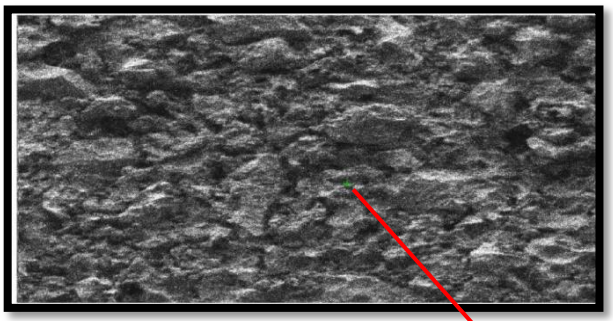

a

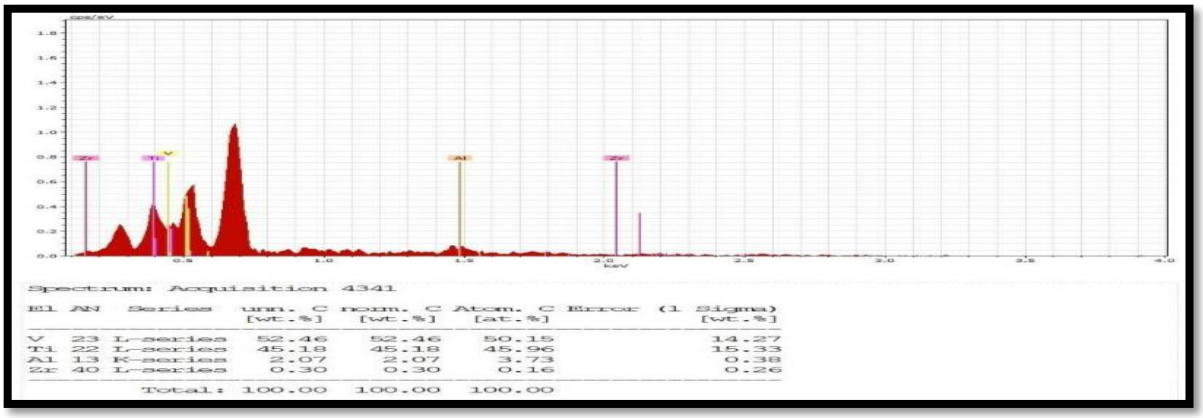

Figure a (4-14): EDX for Ti6Al4V-0.5Zr alloy.

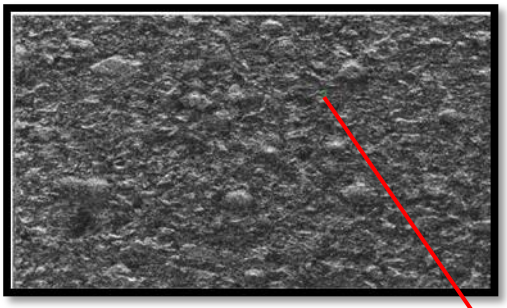

b

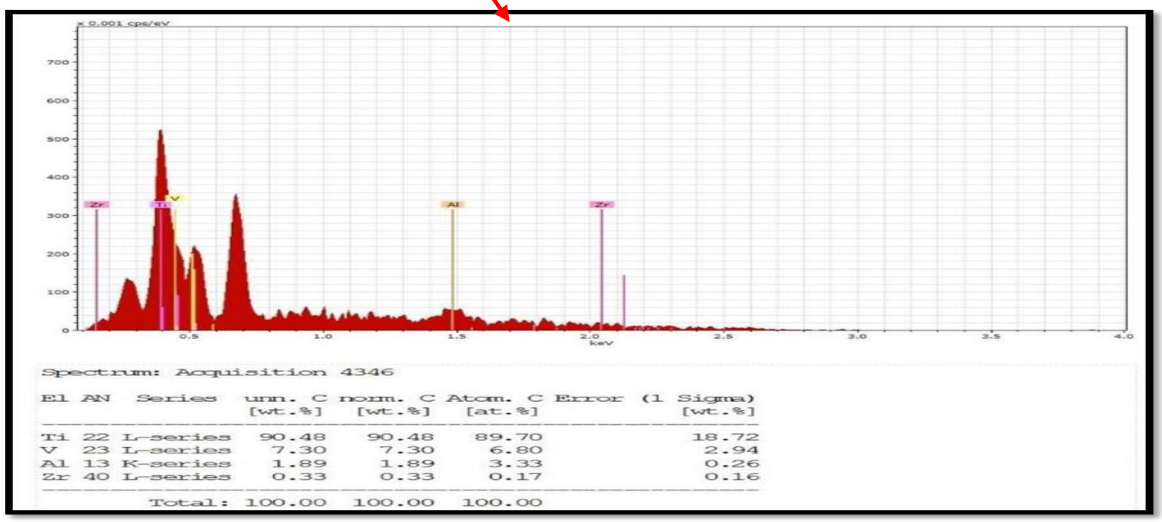

Figure b (4-14): EDX for Ti6Al4V-0.5Zr alloy.

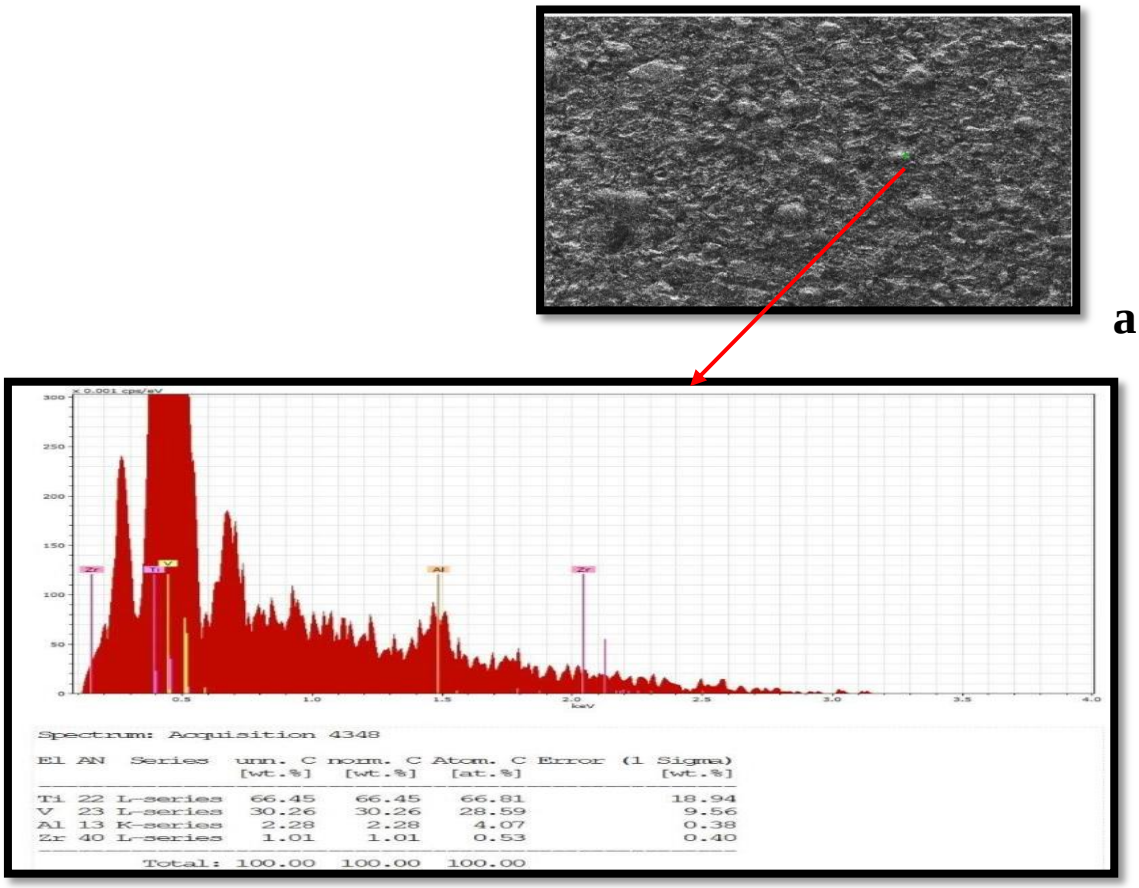

Figure a (4-15): EDX for Ti6Al4V-1Zr alloy.

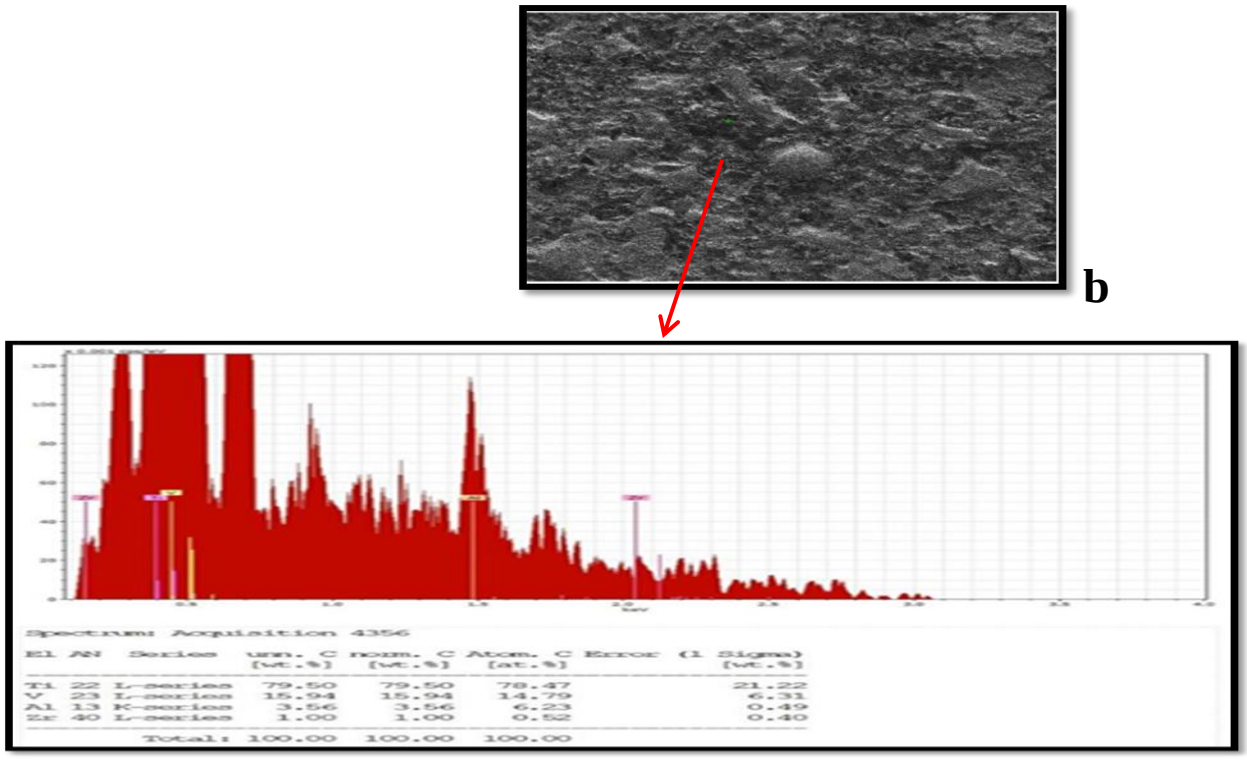

Figure b (4-15): EDX for Ti6Al4V-1Zr alloy.

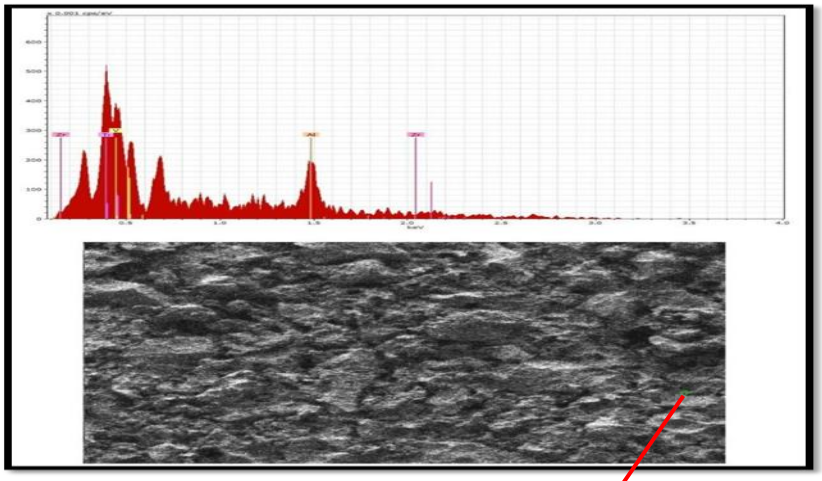

a

Spectrum: Acquisition 4343

El	AN	Series	unn. C [wt.%]	norm. C [wt.%]	Atom. C [at.%]	Error (1 Sigma) [wt.%]
Ti	22	L-series	76.74	76.74	74.26	21.79
V	23	L-series	15.27	15.27	13.89	6.51
Al	13	K-series	6.45	6.45	11.07	0.73
Zr	40	L-series	1.55	1.55	0.78	0.55
		Total:	100.00	100.00	100.00	

Figure a (4-16): EDX for Ti6Al4V-1.5Zr alloy.

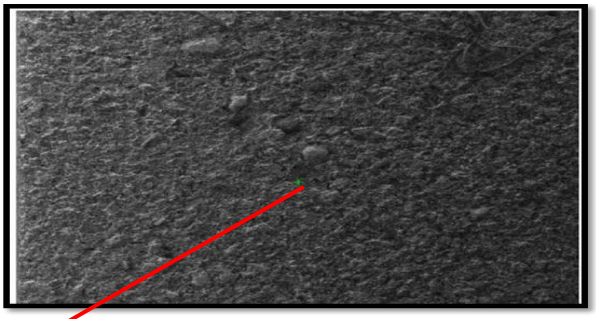

b

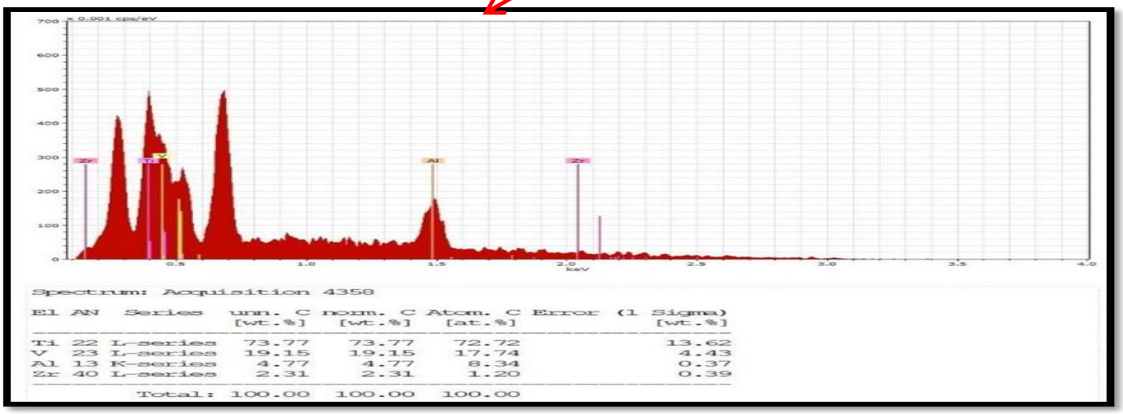

Spectrum: Acquisition 4358

El	AN	Series	unn. C [wt.%]	norm. C [wt.%]	Atom. C [at.%]	Error (1 Sigma) [wt.%]
Ti	22	L-series	73.77	73.77	72.72	13.62
V	23	L-series	19.15	19.15	17.74	4.43
Al	13	K-series	4.77	4.77	8.34	0.37
Zr	40	L-series	2.31	2.31	1.20	0.39
		Total:	100.00	100.00	100.00	

Figure b (4-16): EDX for Ti6Al4V-1.5Zr alloy.

a

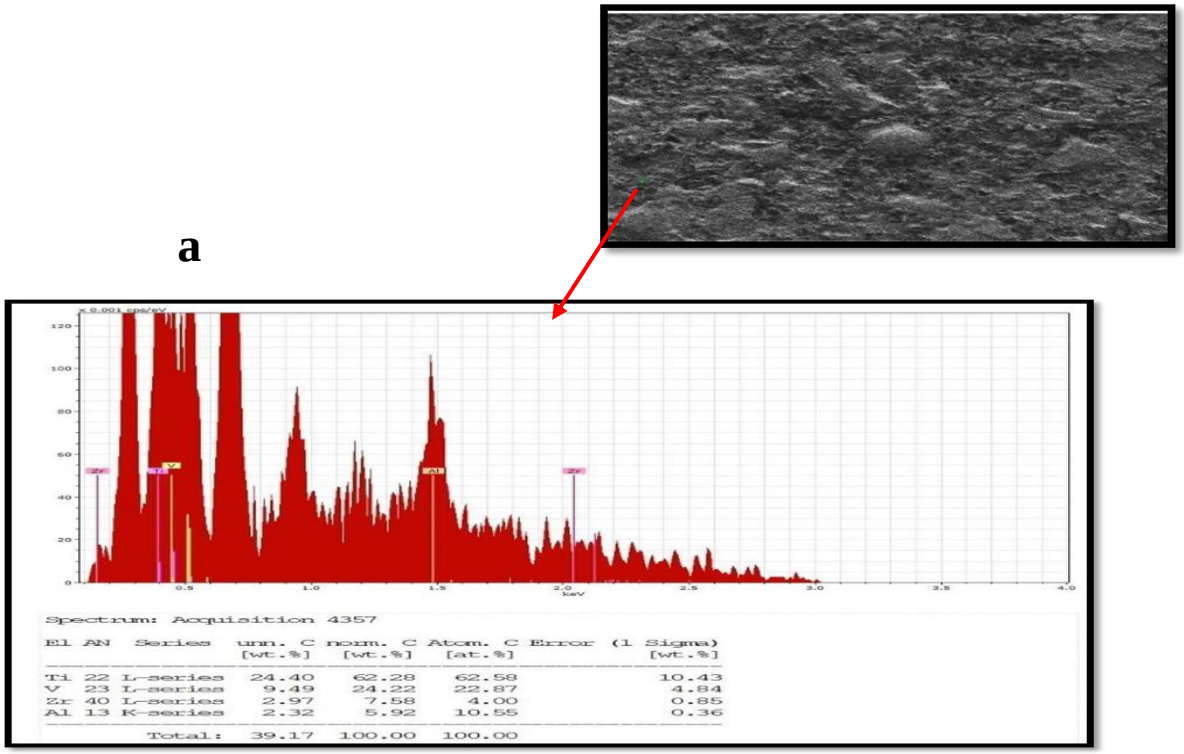

Figure a (4-17): EDX for Ti6Al4V-2 Zr alloy.

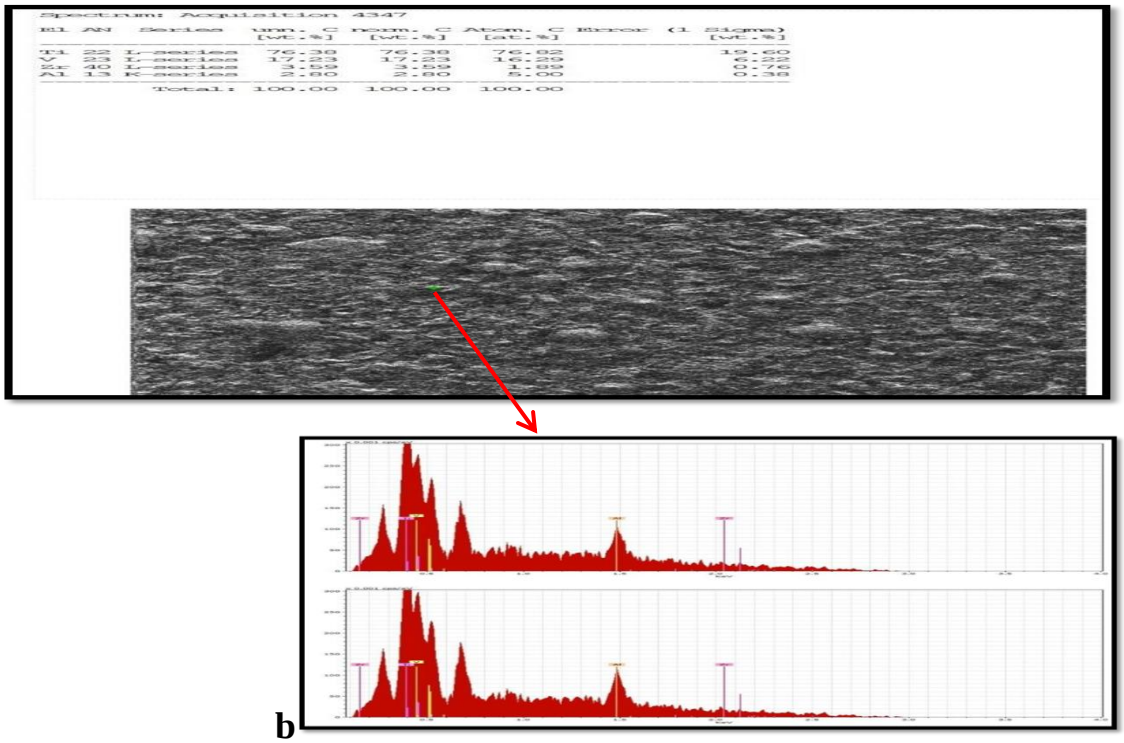

b

Figure b (4-17): EDX for Ti6Al4V-2 Zr alloy.

Fig (4-8) to Fig (4-17) EDX for Ti6Al4V alloy , Ti6Al4V-XTa alloy, Ti6Al4V-XZr alloy

4.5 The physical properties of the sintering

4.5.1 True Density and Porosity for sintered specimens

The porosity and density measured for all used alloys after sintering process , shown Figures (4-18) , (4-19) shown the effect additions of Zr and Ta on the (porosity and density) values for base alloy Ti6Al4V Where the porosity decreases gradually and density increasing gradually with the increasing the gradually for addition of (Zr & Ta) for base alloy.

Figure (4-18) showed the effect of adding (Ta) and (Zr) content on the porosity of sintered Ti6Al4V-XTa,Ti6Al4V-XZr and there is clear decreasing in porosity values of samples after sintering , this confirmed by the figures of the SEM test The porosity will gradually decreases for with the gradually increasing of (Ta) and (Zr) additions for base alloy Ti6Al4V, this is due to the better inter diffusion caused by these additives , as well the thermal expansion coefficient of zirconium and tantalum being less than the thermal expansion coefficient of titanium, and thus the thermal contraction causing porosity will be less or absent during cooling [109].

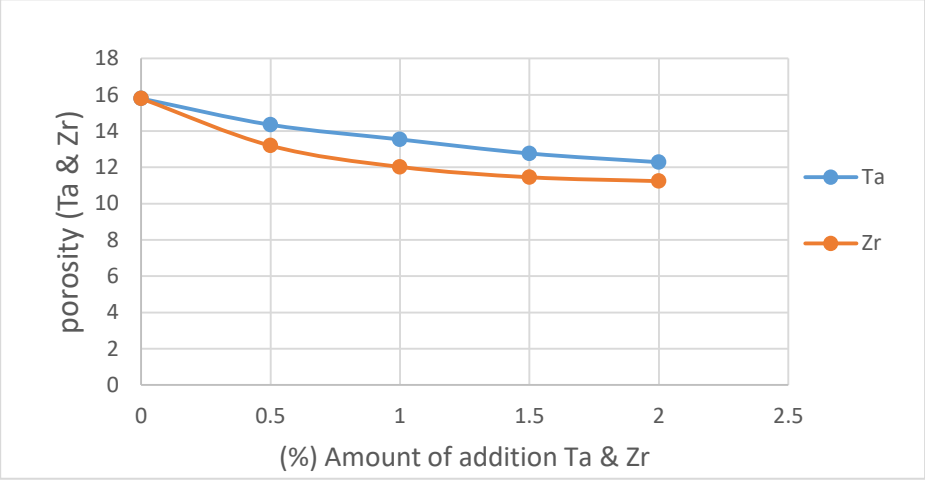

Figure (4-18): Effect of (Ta) and (Zr) content on the porosity after sintering of alloys (Ti6Al4V-XZr) and (Ti6Al4V-XTa).

Figure (4-19) shows that the density of the (Ti6Al4V-XZr) and (Ti6Al4V-XTa) alloys has a gradual increase according to the gradually rise in the concentration of Zr and Ta .The increase in the density of (Ti6Al4V-XZr) & (Ti6Al4V-XTa) alloys occurs due to the higher density of zirconium (6.51 g/ cm^3) and density of tantalum (16.69 g / cm^3) compared with density of titanium (4.51 g/ cm^3) [110] .

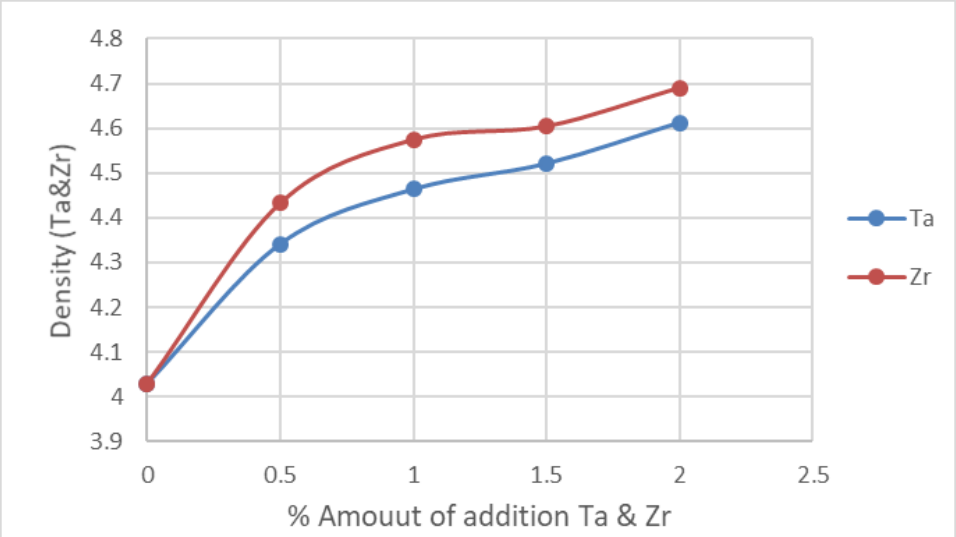

Figure (4-19): Effect of (Ta) and (Zr) content on the density after sintering of alloys (Ti6Al4V-XZr) and (Ti6Al4V-XTa).

4.5.2 Contact angle Test

The contact angle is measured to determine the wetting ability of surfaces. It was indicated that the contact angle is greatly affected by the phases and alloying elements [111], so the microstructure can be controlled as well as in the contact angle, in this work the microstructure was controlled by adding tantalum and zirconium to the base alloy in different proportions which leads to the spread of the beta phase on the surface of the alloys as shown in the LOM test, and thus the contact angle is also controlled, where the greater the beta phase on the surface, the greater the effect on the drop of solution, as the contact angle on the surface decreases with the increase in the beta phase on the surface [112],

and the beta phase forms a thicker oxide layer on the surface of the alloy, and due to the effect of the chemical composition of the oxide layer on the wettability, the contact angle values of the samples decrease through the formation of thicker oxide layer, where the contact angle of the material is determined by the chemical composition of the surface [113-114]. The excellent biocompatibility of titanium and its alloys is associated with the properties of the oxide layer on its surface. For this reason, titanium and its alloys are considered highly biocompatible materials [115-116] and because of the good compatibility of the titanium oxide layer with blood, it was found that its biocompatibility is related to its wettability [117] where whenever increase the thickness of the oxide layer ,its biocompatibility increases thus the contact angle decreases and the osseointegration increases As in the specimens (Ti6Al4V-2Zr and Ti6Al4V-2Ta) , which achieve the osseointegration higher and the osseointegration is more for (Ti6Al4V-2Zr) alloy because of its oxide layer on the surface which is thicker due to larger spread for beta phase

Where the results showed that the value of the contact angle of the base alloy Ti6Al4V is originally wettable, but after adding Ta and Zr gradually, the value of the contact angle became very small and gradually with the gradual increase of the addition of zirconium and tantalum and thus increasing wettable to the surface , and more increasing of hydrophilicity for base alloy Ti6Al4V with additions compared with contact angle value for base alloy Ti6Al4V without additions in the Hank's and saliva solutions.

Table (4-2) Value of contact angle for Ti6Al4V-XTa & Ti6Al4V-XZr in the Hank's solution.

Samples	Value of Contact angle	Contact angleHank's solution
Base	33.910	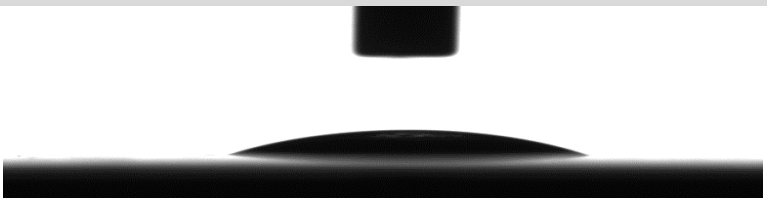
0.5%Ta	25.826	
1%Ta	21.413	
1.5%Ta	16.615	
2% Ta	12.181	
0.5% Zr	22.068	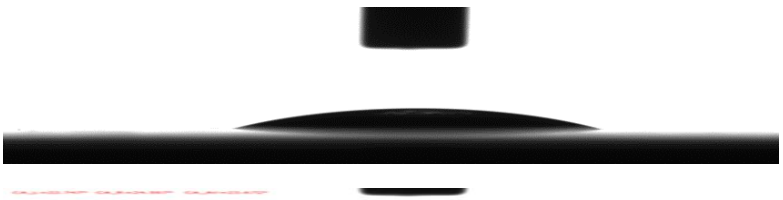
1% Zr	18.834	
1.5%Zr	14.964	
2%Zr	11.470	

Table (4-3) Value of contact angle for Ti6Al4V-XTa & Ti6Al4V-XZr in the saliva solution.

Samples	Value of Contact angle	Contact angle Saliva solution
Base	28.898	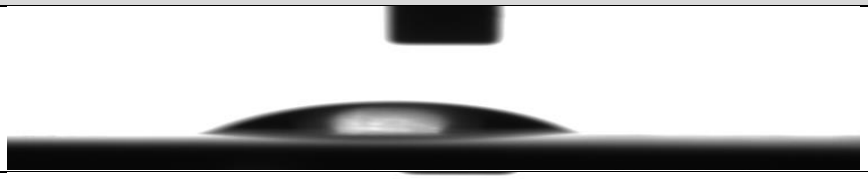
0.5% Ta	21.848	
1% Ta	17.624	
1.5%Ta	13.798	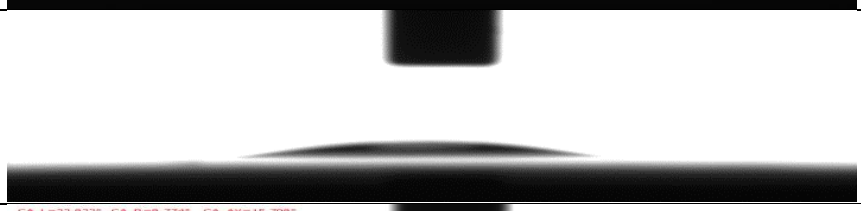
2%Ta	11.766	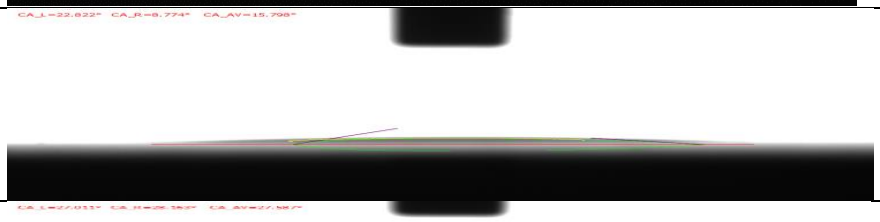
0.5%Zr	20.866	
1%Zr	16.662	
1.5%Zr	12.768	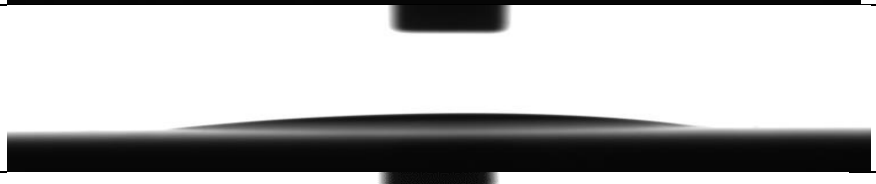
2%Zr	10.664	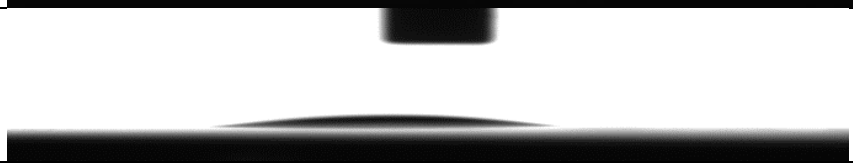

4.6 Mechanical Properties for Sintered Specimens

4.6.1 Hardness

Brinlle hardness was measured for all specimens of alloys (Ti6Al4V,Ti6Al4V-Ta,Ti6Al4V-XZr) as shown in Figure (4-20) and table (4-4).

From Figure (4-20) and table (4-4) , show that Ti6Al4V base alloy with Zr additive to it ,presented significantly higher hardness values in comparison with Ti6Al4V base alloys, Ti6Al4V base alloys with Ta additive to it , values of hardness shown increased gradully with the gradual incrreasd in the addition of Zr. Attributed the rise in hardness to the role of (Zr) in reducing porosity as shown in previously Figure 4-18 more than (Ta) by compared with porosity of Ti6Al4V base alloy , in addition to causes more decrease in ductility due to role Zr in dispersion and spread of the beta phase in the base alloy more than that of tantalum, its lead to the rising the hardness values of the specimens is attributed also to the relatively high hardness for the (Zr) compared with hardness of Ta and Ti.

The mechanical properties of Ti6Al4V alloys considerably depend on the microstructure and its present phases ,where elements (Ti , Al) stabilizer of phase (α) and elements (V, Ta) stabilizer of phase (β). element (Zr) Although it is neutral, but it works to stabilize the (beta phase) when there is elements with it works to stabilize the (beta phase) , and therefore the element (Zr) is also work on installed the (beta phase) [104] .

Ductility of Ti6Al4V alloy increases with increasing the (α) phase fraction that is favorable for plastic forming , as a result the hardness values considerably depend on the porosity and the percentage of these phases [118] and being tantalum from the elements that stabilizer the beta

phase and role it in decrease porosity as in previous figure (4-8), it causes decrease in ductility so have hardness more than base alloy but it stay less than hardness for Ti6Al4V-XZr because of role Zr it in decrease porosity larger.

The Zr & Ta have the same effect in the increase in the hardness values when added to the base alloy, and this denote the high hardness to Ta and Zr compared to hardness of the Ti titanium and because of the role of Ta and Zr in the reduce of the porosity it which causes a decrease in ductility, and thus the hardness value increases, as well as the tantalum and zirconium from the elements that stabilizer the beta phase In general , gradully increase the hardness values of the Ti6Al4V alloy with gradully increase in the content of tantalum and zirconium .

Table (4-4) Brinlle hardness values for specimens

NO.	Specimens	Brinell Hardness (HB)
1	Ti6Al4V	295.5
2	Ti6Al4V-0.5 Ta	299.5
3	Ti6Al4V-1 Ta	304
4	Ti6Al4V-1.5 Ta	310
5	Ti6Al4V-2 Ta	316
6	Ti6Al4V-0.5 Zr	313
7	Ti6Al4V-1 Zr	318
8	Ti6Al4V-1.5 Zr	323
9	Ti6Al4V-2 Zr	330

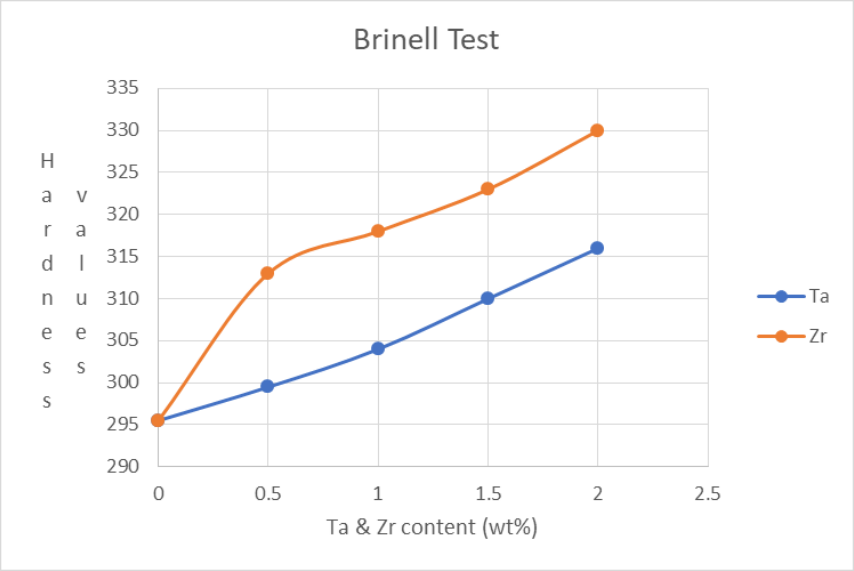

Figure (4-20) : Effect of Ta & Zr content on the hardness for Ti6Al4V.

4.6.2 Dry wear Test

The specimes with a diameter of (12) mm are subjected to dry wear test under constant load 10 N for different times (5, 10, 15, 20, 25, 30 , 35, 40) minutes, were chosen constant load and different times according to several experiments. The tested done at room temperature .

The results have been presented in the following Figures (4-21), (4-22) illustrate the dry wear rate vs time for all used alloys under constant load (10) N. From the mentioned figures, shown that the dry wear rate to (Ti6Al4V base alloy) is higher than dry wear rate for base alloys with additions (Ti6Al4V-XTa , Ti6Al4V-XZr).

Figure (4-21): Dry wear rate for Ti6Al4V – X Ta .

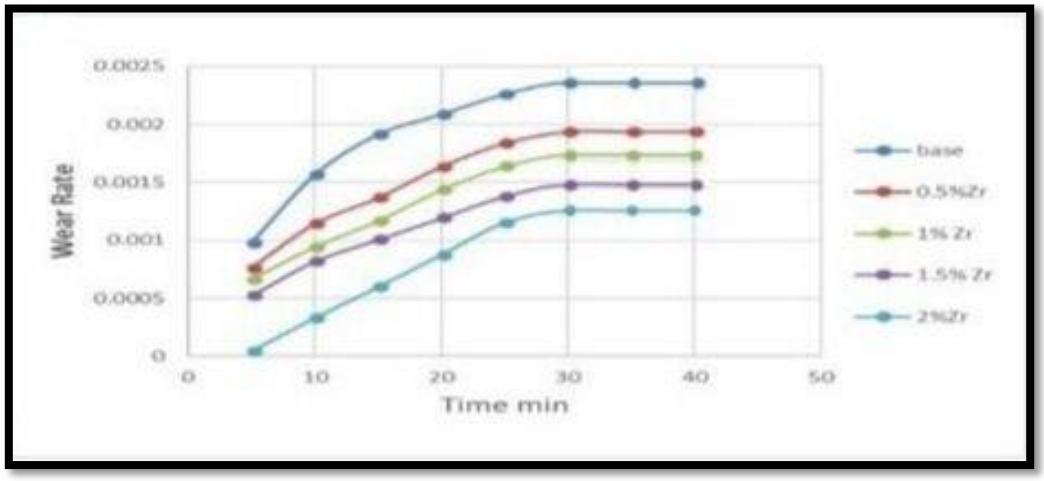

Figure (4-22): Dry wear rate for Ti6Al4V – X Zr .

The Figures (4-21), (4-22) shown the relationship between the loss of volume for Ti6Al4V base alloy without additions & with additions (0.5, 1, 1.5 and 2% wt. Ta & Zr) with time under constant load of 10 N From these figures, it's clear that weight loss gradually increased with increasing time regardless of the chemical composition and microstructure of alloys, it is true because more time tends to remove more materials from the surface and increases the rate of wear [119] as well as because of the increase in friction at the surface with increasing the time[120]. Loss of size of alloys (with + without added) increases with the increase of the time [121].

In addition , the figures (4-21) and (4-22) shown the dry wear rates where shown decreased wear rates with the increase in time for all specimes gradually, where the rate of dry wear decreases gradually as the increases in the time and the gradual increase in the percentage of addition (Ta and Zr) To reach the lowest dry wear rate value when adding (2%Ta) and (2%Zr), where the figures show the losses of volume as a function of time [121].

From Figures (4-21) and (4-22) shown there is simile to in loss of size for Ti6Al4V base alloy with the Zr & Ta addition for time from (5-40) min, but amount of loss in size Ti6Al4V base alloy with addition Zr, appear loss of size little less compared with base alloy with Ta addition, this is back to hardness of the alloy Ti6Al4V-XZr being higher in values of hardness compared with values hardness of Ti6Al4V base alloy at adding Ta, but remain loss of size for base alloys with Ta addition less than loss of size for the Ti6Al4V base alloy, so it is subjected to Archard's law which states weigh loss for material is inversely proportional to the hardness values the materials, in addition, the thickness of the oxide film formed on the surface of the specimen due to high hardness which is difficult to remove during time [122].

For the study effect addition of the Ta & Zr on dry wear rate for Ti6Al4V base alloy the dry wear rate vs (Ta & Zr) content under constant load (10) N for different times (5,10,15,20,25,30,35,40) as shown in Figures (4-21) and (4-22) respectively, The dry wear rate decreases with an increase in the addition of (Zr and Ta) but the dry wear rate decreases with an increase in the addition of (Zr) slightly more compared with the decrease in the dry wear rate with an increase in the addition of (Ta) .

The reason behind this decreases belongs to role the (Zr) addition which reduces the porosity and increases the hardness more than Ta addition, because of the effect of adding zirconium on the microstructure in spread of the beta phase more than Ta , so the dry wear rate will be reduced slightly more with adding (Zr).

Shown mentioned Figure (4-18) the decreases in the porosity with increases addition (Ta & Zr) content, that pores play an important role indicating the potential sites of the first micro cracks forming and that has positively influencing the wear process [121].

The addition of (Ta & Zr) to Ti6Al4V alloy increases the hardness as in mentioned Figure (4-20) then and the dry wear resistance increases as the hardness increases [123].

4.7 Electrochemical Tests

4.7.1 Open Circuit Potential (OCP)-Time Measuremen

The OCP-time is measured with respect to SCE in artificial saliva and Hank's solutions at 37±1 C° that simulated human body conditions carried out to examine the variation in time of corrosion potential behavior of the materials for all tested alloys (Ti6Al4V) base alloy, (Ti6Al4V-XZr) and (Ti6Al4V-XTa) alloys. Figures (4-23),(4-24),(4-25) and (4-26) and tables (4-6) , (4-7) displays the evolution of corrosion potential of the alloys throughout time of immersion until the tendency to a steady-state value .The time period from (0 up to 60 min) and with interval of 5 min between each reading were potentially reported The values of OCP were recorded using one sample for each alloy .

In order to understand the stability of an alloy Ti6Al4V in the solutions of the human body, it is necessary to know its behavior in the environment that simulates of body fluids to know the biocompatibility of these alloys, this is done by the open-circuit potential for by time during

immersion until the tendency to a steady-state value , it is one of the typical methods for studying the formation of a protective layer and passivation of implants in Hank's and saliva solutions and compared the stability of these (Ti6Al4V-XZr) ,(Ti6Al4V-XTa) alloys with the stability of the base alloy.

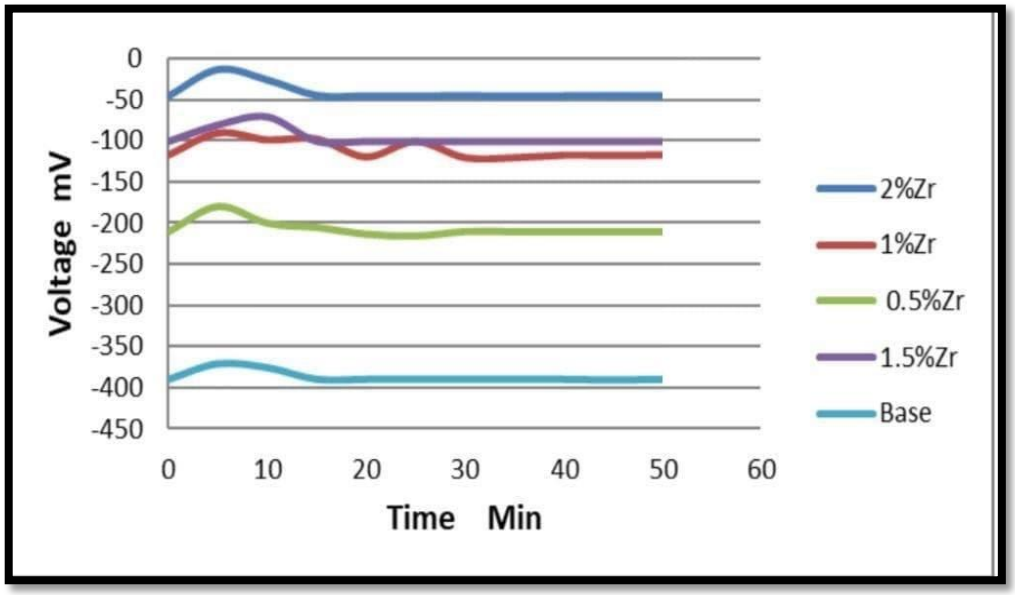

Figure (4-23): Open circuit corrosion potential measurements for Ti6Al4V-XZr in Hank's solutions.

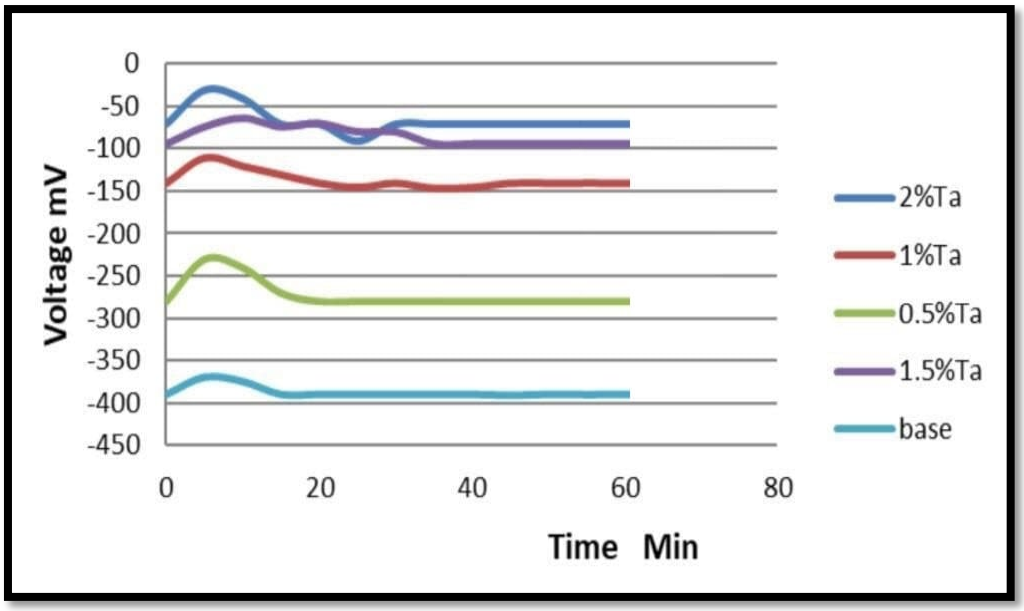

Figure (4-24) : Open circuit corrosion potential measurements for Ti6Al4V-XTa in Hank's solutions.

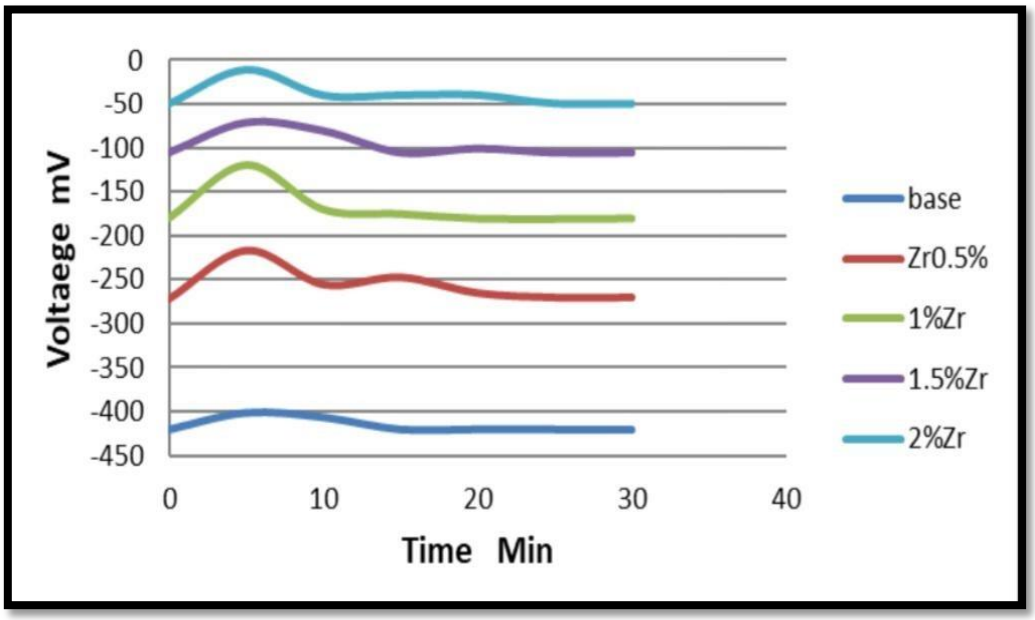

Figure (4-25) : Open circuit corrosion potential measurement for Ti6Al4V-XZr in saliva solution

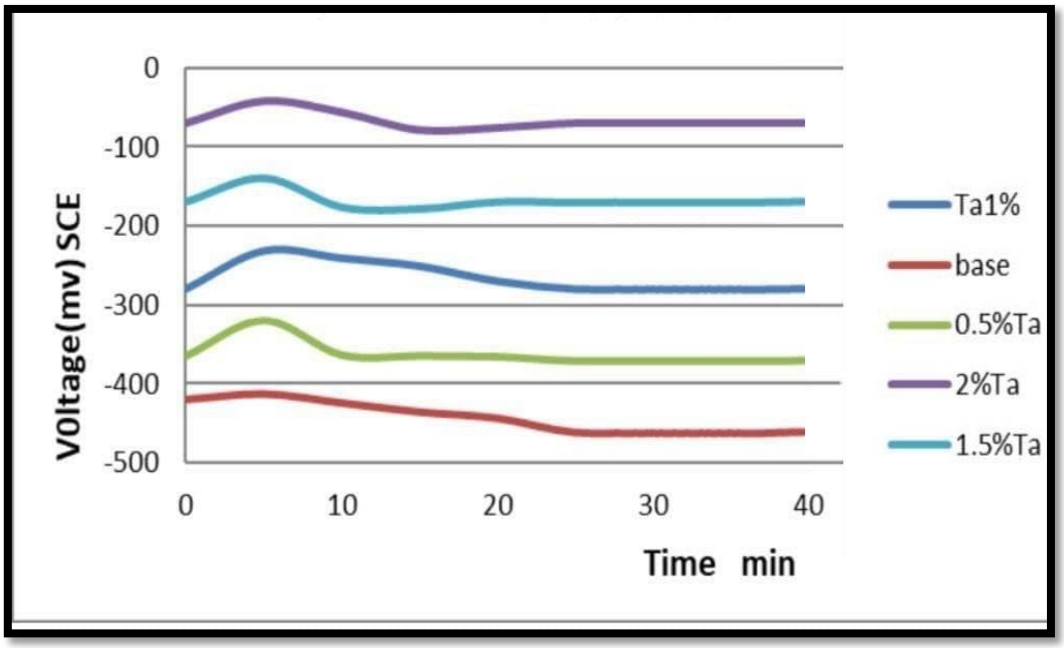

Figure (4-26) : Open circuit corrosion potential measurement for Ti6Al4V-XTa in saliva solution

The Figures indicate a rising of potential towards the positive direction where the surface of the implant is covered with a protective layer. Submerged alloys can be seen in the artificial saliva solution oriented to the negative direction and have a high negative value of ($E_{corr.}$) compared to the submerged alloys with Hanks solution is due to

the value of pH for each solution, where more number of pH represent more positive potential were pH of Hank's and saliva were (7.4) and (6.62) respectively [124] , and the OCP constant means that there is an equilibrium between dissolution and deposition [125] .

The evolution of ($E_{corr.}$) of (Ti6Al4V, Ti6Al4V-XTa and Ti6Al4V-XZr) alloys immersed in artificial saliva and Hank's solutions showed many deviations, suggesting that the oxide layer formed on the surface of the implant is collapsed and formed, is that attributed to the processes of dissolution and rebuilding the protective layer. The presence of sulfur ions and chlorides in hostile solutions, in which the implants are immersed, is the cause of this behavior [126].

Table (4-5) Shown the $E_{corr.}$ and improvement percentage% for alloys in artificial saliva solution.

Alloys	$E_{corr.}$ mV	Improvement Percentage%
Base	-420.32	-
0.5% Ta	-370.71	11
1% Ta	-280.48	33
1.5% Ta	-170.34	59
2% Ta	-70.93	83
0.5% Zr	-270.21	35
1% Zr	-180.15	57
1.5% Zr	-105.96	74
2% Zr	-50.30	88

Table (4-6) Shown the E_{corr} and improvement percentage% for alloys in Hank's solution.

Alloys	Ecorr. mV	Improvement Percentage%
Base	- 390.45	-
0.5% Ta	- 280.34	28
1% Ta	- 140.55	64
1.5% Ta	-100.37	74
2% Ta	- 70.72	81
0.5% Zr	-210.32	46
1% Zr	-117.73	69
1.5% Zr	-94.42	75
2% Zr	-45.74	88

From tables (4-6) & (4-7) as shown the effect of adding Zr and Ta to the Ti6Al4V base alloy through the improvement percentage for each specimes prepared in the saliva and Hank's solutions , where leads adding Zr and Ta for base alloy to making Ti6Al4V alloy more nobler and its tendency to corrode less because of the effect of adding Ta and Zr in enhancing passivation to the base alloy, through the formation of the protective inert negative oxide layer on the surface of the alloy and therefore osseointegration occurs , it was also found that the improvement of the percentage with the addition of Zr is higher than the improvement of the percentage with the addition of tantalum, as a result of the effect of Zr in increasing the diffusion of the beta phase and thus increasing the hardness for the alloy and thus strengthening the oxide layer where it which characterized being thicker, more stable, protective and resistant, and thus there is increase a noticeable and improvement in the corrosion resistance of the alloy as the resistance is enhanced by oxides the Zr element on the surface of the alloy, so it tends to passivating and corrode

less and the improvement percentage is higher, and the E_{corr} value for the base alloys with zirconium added is lower than the E_{corr} value for base with the addition of tantalum, where passivation is easier and faster in the saliva and Hank's solutions due to the presence of the more thick negative layer on the surface of (Ti6Al4V-XZr) alloys but the $E_{corr.}$ value is higher in saliva solution compared with Hank's solution.

4.7.2 Potentiodynamic polarization

The corrosion behavior of all alloys used in artificial saliva and Hank's solutions have been studied. By using Potentiodynamic polarization to give estimation about the corrosion behavior of alloys.

The corrosion parameters are corrosion current density ($I_{corr.}$), corrosion potential ($E_{corr.}$) and (corrosion rate) resulted from corrosion test for the specimens in mentioned solutions at 37 ± 1C° were illustrated in tables (4-8) and (4-9).

Table (4-7) : The corrosion current density ($I_{corr.}$), corrosion potential ($E_{corr.}$) and corrosion rate (C.R.) for all used alloys in saliva solution at 37°C ±1 .

Alloys	$I_{corr.}$ (µA/cm²)	$E_{corr.}$ (mV)	Corrosion rate (C.R.)mpy	Improvement Percentage%
Ti6Al4V	**14.25**	**- 420.32**	**0.077**	**-**
Ti6Al4V-0.5Ta	**7.16**	**-370.71**	**0.065**	**15**
Ti6Al4V-1Ta	**6.63**	**-261.42**	**0.058**	**24**
Ti6Al4V-1.5Ta	**5.51**	**-150.21**	**0.042**	**45**
Ti6Al4V-2Ta	**4.23**	**-70.93**	**0.031**	**59**
Ti6Al4V-0.5Zr	**5.58**	**-270.21**	**0.042**	**45**
Ti6Al4V-1Zr	**4.74**	**-160.36**	**0.036**	**53**

Ti6Al4V-1.5Zr	**3.23**	**-95.89**	**0.028**	**63**
Ti6Al4V-2Zr	**2.47**	**-50.30**	**0.017**	**77**

In saliva solution, from table (4-8) it shown that there is a significant improvement in corrosion resistance of the base alloys with different additives of (Ta) (0.5,1,1.5,2%wt) and $I_{corr.}$ for specimens are graded in decreases from 7.16 (μA/ cm²) for (Ti6Al4V-0.5Ta) alloy to 4.23 (μA/ cm²) for (Ti6Al4V-2Ta) alloy which are lower than $I_{corr.}$ for Ti6Al4V base alloy which is 14.25 (μA/ cm²). However the $E_{corr.}$ values for (Ti6Al4V-XTa) alloys is graded in decreases from (-370.71 mV) for (Ti6Al4V-0.5Ta) to (-70.93 mV) for (Ti6Al4V-2Ta) which are lower than $E_{corr.}$ for Ti6Al4V base alloy which is (-420.32 mV).

The data listed in table (4-8) shows significant an excellent improvement in corrosion resistance of base alloy with Zr additives (0.5,1,1.5&2% wt) and the $I_{corr.}$ for these alloys ranged between 5.58 (μA/ cm²) for (Ti6Al4V-0.5Zr) alloy to 2.47 (μA/ cm²) for (Ti6Al4V-2Zr). It can be shown that the $I_{corr.}$ for base alloy with Zr additives is lower than all of base alloy and base alloys with Ta additives However the $E_{corr.}$ values for Zr alloys are graded from (-270.21mV) for (Ti6Al4V-0.5Zr) to (-50.30 mV) for (Ti6Al4V-2Zr) which are lower than $E_{corr.}$ for (Ti6Al4V-XTa) alloys and base alloy Ti6Al4V where $E_{coor.}$ for base alloy is (-420.32 mV).

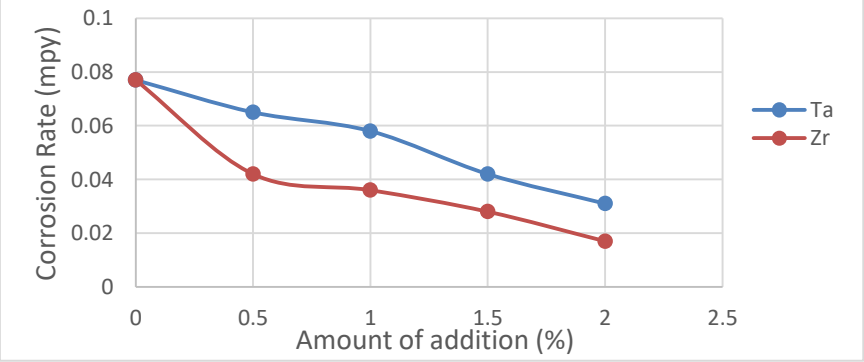

Figure (4-27) Effect of Ta and Zr content on the corrosion rate Ti6Al4V alloy in saliva solution.

Table (4-8): The corrosion current density ($I_{corr.}$), corrosion potential ($E_{corr.}$) and corrosion rate (C.R.) for all used alloys Hank's solution at 37°C ±1.

Alloys	$I_{corr.}$ (μA/ cm²)	$E_{coor.}$ (mV)	Corrosion rate (C.R.)mpy	Improvement Percentage%
Ti6Al4V	10.96	-390.45	0.023	-
Ti6Al4V-0.5Ta	6.69	-280.34	0.016	30
Ti6Al4V-1Ta	5.91	-170.24	0.0094	59
Ti6Al4V-1.5Ta	4.11	-105.32	0.0038	83
Ti6Al4V-2Ta	3.40	-70.72	0.0032	86
Ti6Al4V-0.5Zr	4.49	-210.32	0.011	52
Ti6Al4V-1Zr	3.93	-113.10	0.0038	83
Ti6Al4V-1.5Zr	2.15	-90.43	0.0021	90
Ti6Al4V-2Zr	1.79	-45.74	0.0019	91

In Hank's solution, from table (4-9) it shown the gradual improvement of corrosion resistance for Ti6Al4V base alloy with gradual increasing of different addition (0.5,1,1.5& 2%wt) from (Ta) also there is a noteworthy a significant improvement in corrosion resistance for Ti6Al4V base alloy with Zr additions (0.5,1,1.5& 2%wt) as compared with each Ti6Al4V base alloy and Ti6Al4V base alloy with (Ta) additives. $I_{corr.}$ for (Ti6Al4V-XTa) specimens are graded in decreases from 6.69 (μA/ cm²) for (Ti6Al4V-0.5Ta) alloy to 3.40 (μA/ cm²) for Ti6Al4V-2Ta alloy which are lower than $I_{corr.}$ for base alloy which is 10.96 (μA/ cm²). However, the $E_{corr.}$ value for the (Ti6Al4V-XTa) alloys are graded from (-280.34) mV for Ti6Al4V-0.5Ta to (-70.72) mV for Ti6Al4V-2Ta which are lower than $E_{corr.}$ for base alloy Ti6Al4V which is (-390.45) mV.

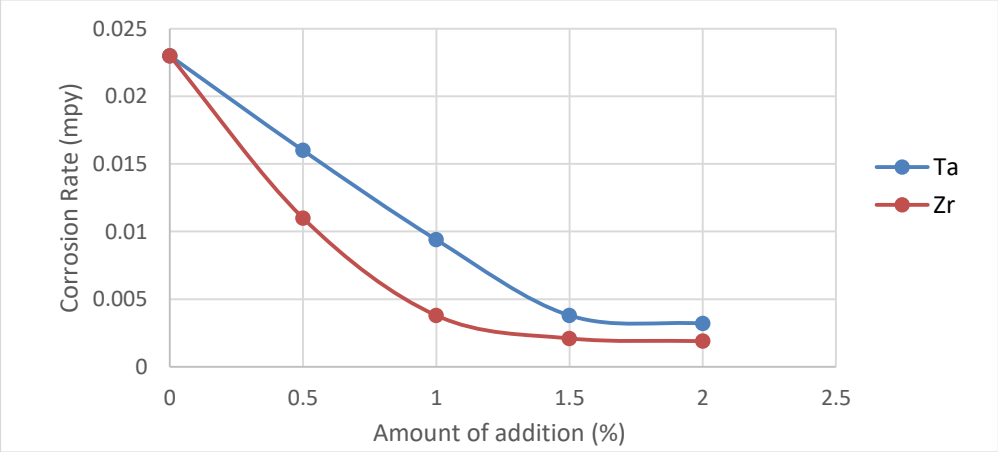

Figure (4-28) Effect of Ta and Zr content on the corrosion rate Ti6Al4V alloy in Hank's solution.

$I_{corr.}$ for Ti6Al4V-XZr alloys ranged between 4.49 (μA/ cm²) for (Ti6Al4V-0.5Zr) alloy to 1.79 (μA/ cm²) for Ti6Al4V-2Zr.It can shown that the $I_{corr.}$ of base alloys with Zr additives is lower than base alloy and base alloy with Ta additive . However the $E_{corr.}$ values for the Ti6Al4V-XZr alloys are graded from (-210.32) mV for Ti6Al4V-0.5Zr to (-45.74) mV for Ti6Al4V-2Zr which are more lower than $E_{corr.}$ for Ti6Al4V base alloy and Ti6Al4V-XTa alloys where $E_{corr.}$ for Ti6Al4V base alloy is (-390.45) mV.

The corrosion rate was found to be strongly related to pH, where corrosion rate decreases with the increase of pH, ie, an inverse relationship. Where, the pH of artificial saliva and Hank's solutions at 37 C° ±1 were 6.7 and 7.4 respectively [129]. From the two tables above it can be seen, that there is a clear decrease in corrosion current density and corrosion rate for (Ti6Al4V, Ti6Al4V-XTa and Ti6Al4V-XZr) specimens in Hank's solution as compared to specimens in artificial saliva solution at 37C° .

These results agree with the fact that the corrosion resistance of pure metal or an alloy strongly depends on the environment where it is exposed and the chemical composition [127].

From tables (4-8) & (4-9) show improvement in corrosion resistance of base alloys with different additives of (Ta and Zr), where whenever the high the percentage of addition (Zr and Ta) gradully (0.5,1,1.5,2 wt) will greater the corrosion resistance gradully as compared with base alloy. Also the corrosion rate and the corrosion current density decreases when (Ta and Zr) content increases for all specimens in two corroded solutions is especially in Hank's solution as compared with saliva solution, as shown in Figures (4-27)& (4-28), means in saliva and Hank solutions that Ta & Zr addition made the Ti6Al4V alloy nobler.

This can be attributed to the behavior of (Ta and Zr) as an anti-corrosion elements and noble elements, which enhances the corrosion resistance of the alloys added to it (Ti6Al4V-XZr) and (Ti6Al4V-XTa) alloys.

The listed data in tables (4-8) and (4-9) show by compared in improvement in corrosion resistance for adding Ta and adding Zr ,where shown an excellent improvement in corrosion resistance of Ti6Al4V alloys with different additives of (Zr) by compared with Ta additives. Where the rate of corrosion and the corrosion current density in the base alloy with the addition of zirconium are lower compared with corrosion rate and the corrosion current density of the base alloy with the addition of tantalum as compared with Ti6Al4V base alloy Also, the percentage of improvement in corrosion rate with the addition of zirconium is higher than percentage of improvement in corrosion rate with the addition of tantalum In two corroded solutions especially in Hank's solution as compared with Ti6Al4V base alloy ,this is due to the effect of zirconium

in the dispersion of beta phase more than tantalum and consequently the increase in the hardness more and this lead to the effect of (Zr) on surface by formation of a thicker oxide layer film , passivity which will lead to a higher protection against corrosion in the surface layer compared with tantalum.

Which enhances the corrosion resistance of Ti6Al4V alloy Therefore, the corrosion rate and the corrosion current density decreases, with adding (Zr) more compared with adding (Ta) for all specimens in two corroded solutions as shown in Figure (4-27) & (4-28).

For protection from corrosion, a more from noble potential and as low as possible current density are desired [126]. The current densities for (Ti6Al4V-XTa),(Ti6Al4V-XZr) alloys, in this study, were less in comparison with that of Ti6Al4V base alloy .

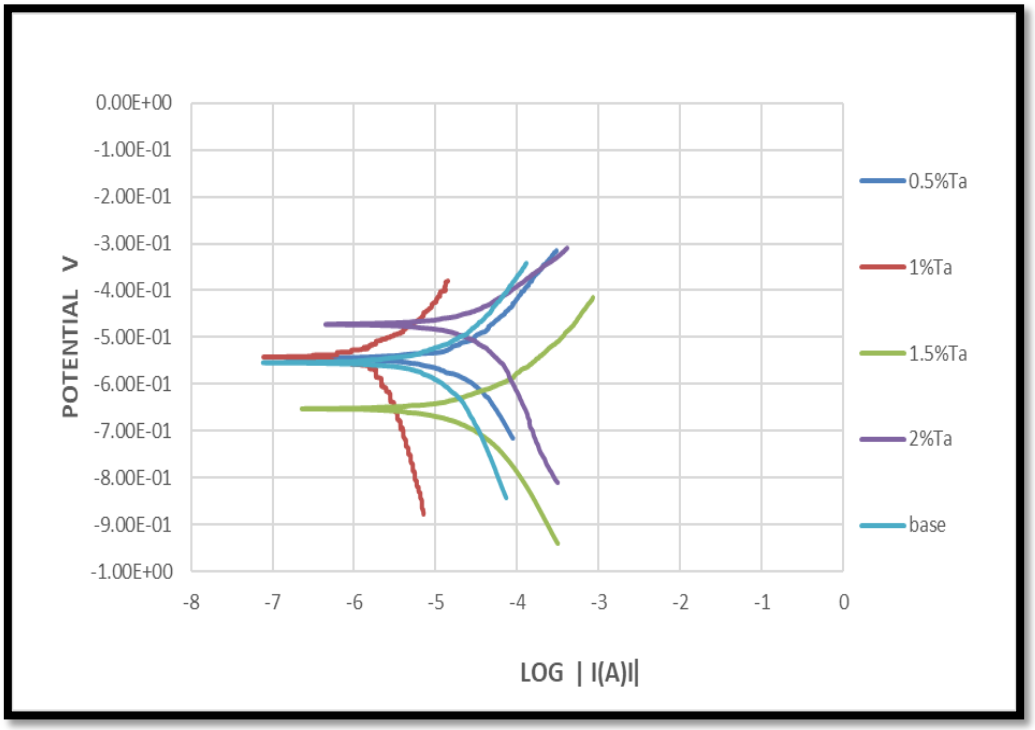

Figure (4-29): Potentiodynamic polarization for Ti6Al4V XTa in Hank's solution.

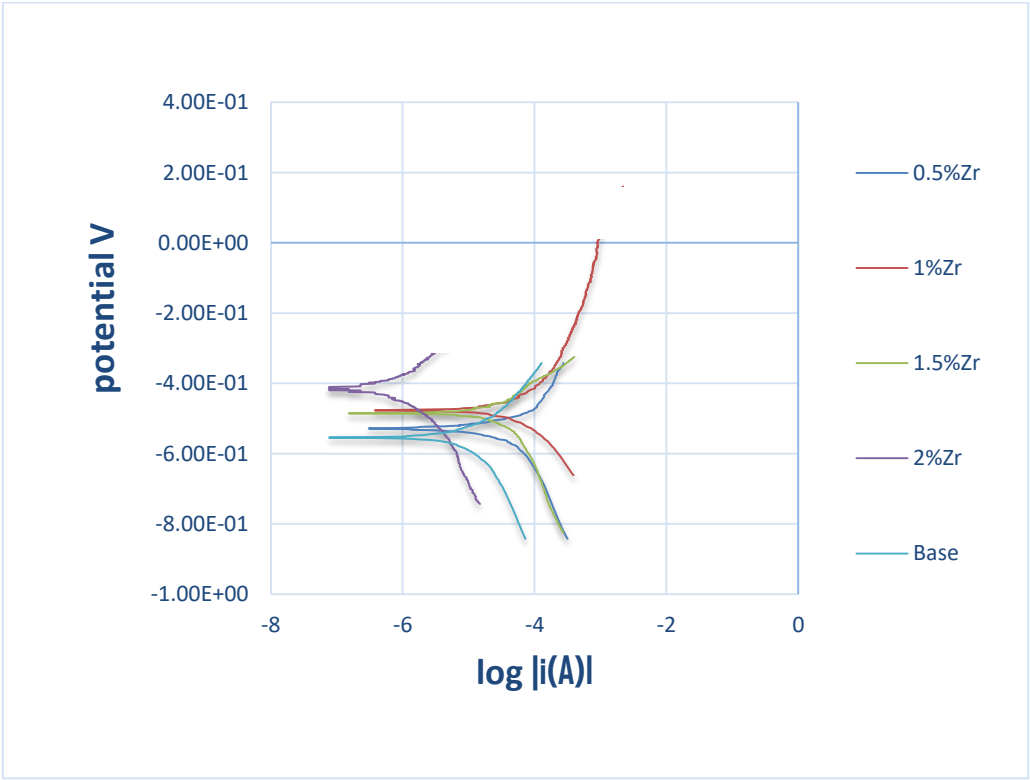

Figure(4-30): Potentiodynamic polarization for Ti6Al4V- XZr in Hank's solution.

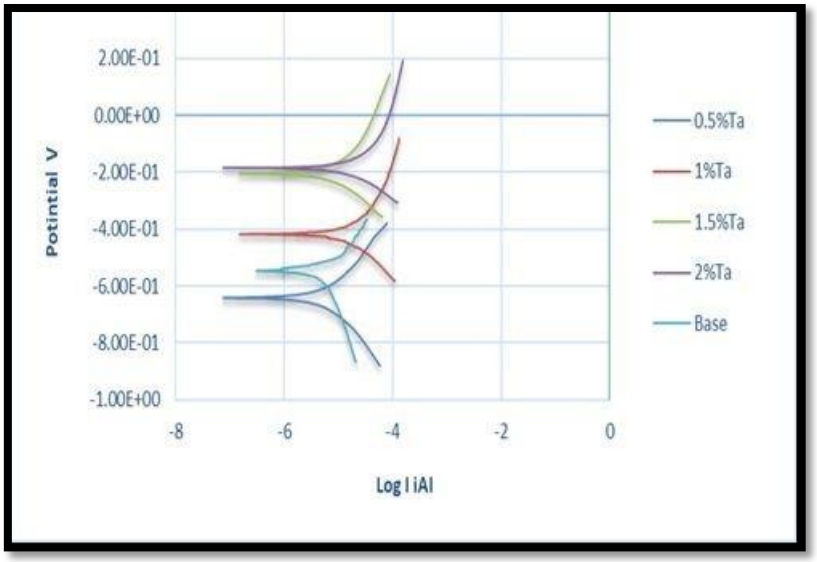

Figure (4-31) Potentiodynamic polarization for Ti6Al4V-XTa in saliva solution.

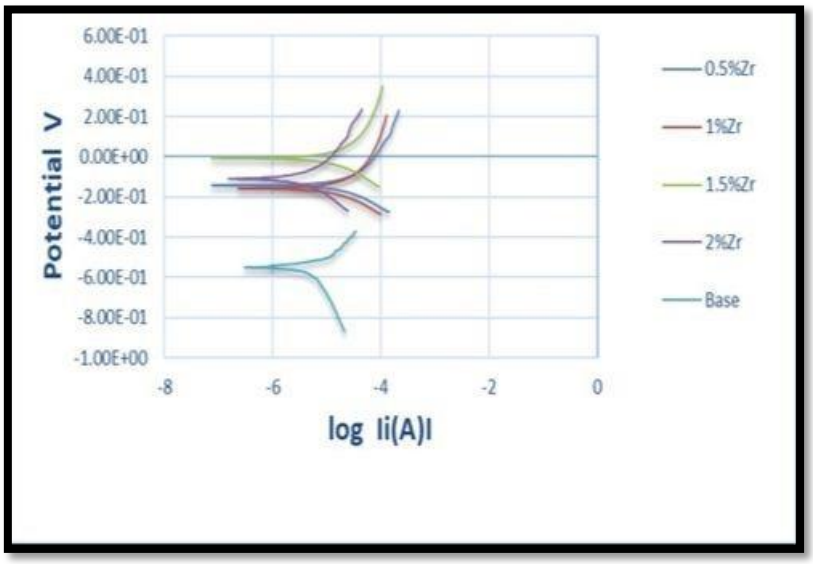

Figure (4-32): Potentiodynamic polarization for Ti6Al4V-XZr in saliva solution.

It's shown in figures (4-29), (4-30) , (4-31) and (4-32) which represents polarization curve for base alloy, Ti6Al4V-XTa and Ti6Al4V-XZr in (artificial saliva and Hank's solutions) In cathodic polarization, the corrosion current density decreases with increasing voltage until it reaches the lowest possible value In anodic polarization, the corrosion current density increases with increasing voltage until it reaches voltage at which it decreases suddenly that due to the formation of passive film [128].

As well , (Ti6Al4V ,Ti6Al4V-XTa and Ti6Al4V-XZr) alloys for until the low current density is obtained, the protective layer on the submerged specimens must be sufficiently integrated, so that the low current density is obtained [129]. Accordingly, the protective layer gradual increases, with gradual increasing for addition alloying elements (Ta , Zr) , but protective layer with addition Zr will be more thicker.

4.8 Metals Ions Release Test

Released metals ions from the metal orthopedic implants within surrounding tissue It causes a variety of problems involve wear and

corrosion such as corrosion fatigue, stress corrosion, fretting corrosion, etc. [130].

This metal ion release has been related with clinical implants deterioration, osteolysis and cause allergic reaction. There requirement for lengthened use for implant, with fewer metals ions release. So, the behavior of metal ion release of each from base alloy and alloys with elements addition Zr and Ta , is being studied by using different solutions from Hank's and artificial saliva [131].

The stability of passive film is strongly affected the metals ions release, when the film undergoes pitting corrosion, through this degraded film, metal will release. The configuration of pits is associated with the stability potentials of (passive) film which represent as a guide for the happened activities [132] .

Where the use of two solutions (Hank’s solution and artificial saliva) to be performed immersion tests with Ti6Al4V alloy to known the ion release concentration quantitative data , and that is to known the biocompatibility of materials to the select the appropriate biomaterials for different medical applications .

Figures (4-33), (4-34) and (4-35) show the amount of metals ions released after immersion in Hank’s solution and artificial saliva solution for 21 days at 37 ^{o}C ±1.

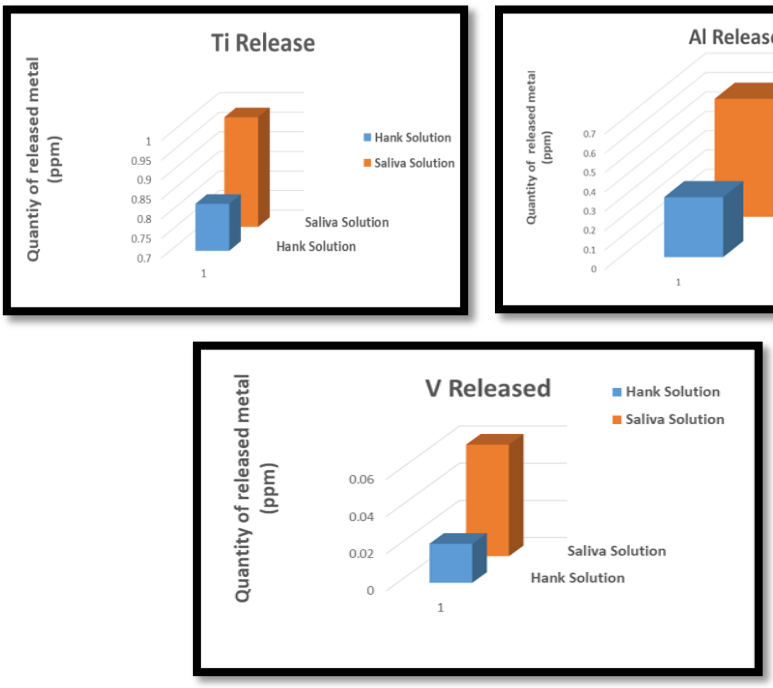

Figure (4-33) Quantity of each metal ion released from base alloy in artificial saliva and Hank's solutions and 37 °C ±1 after 21 days.

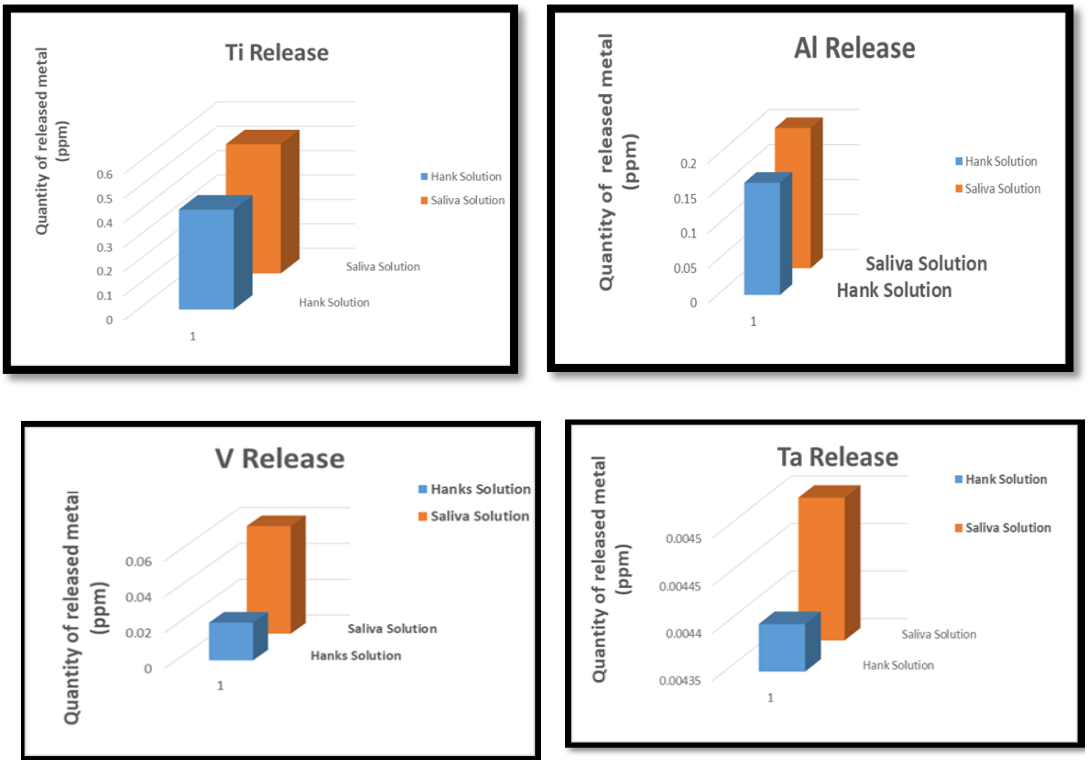

Figure (4-34) Quantity of each metal ion released from (T6Al4V2Ta) alloy in artificial saliva and Hank's solutions at 37 °C ±1 after 21 days.

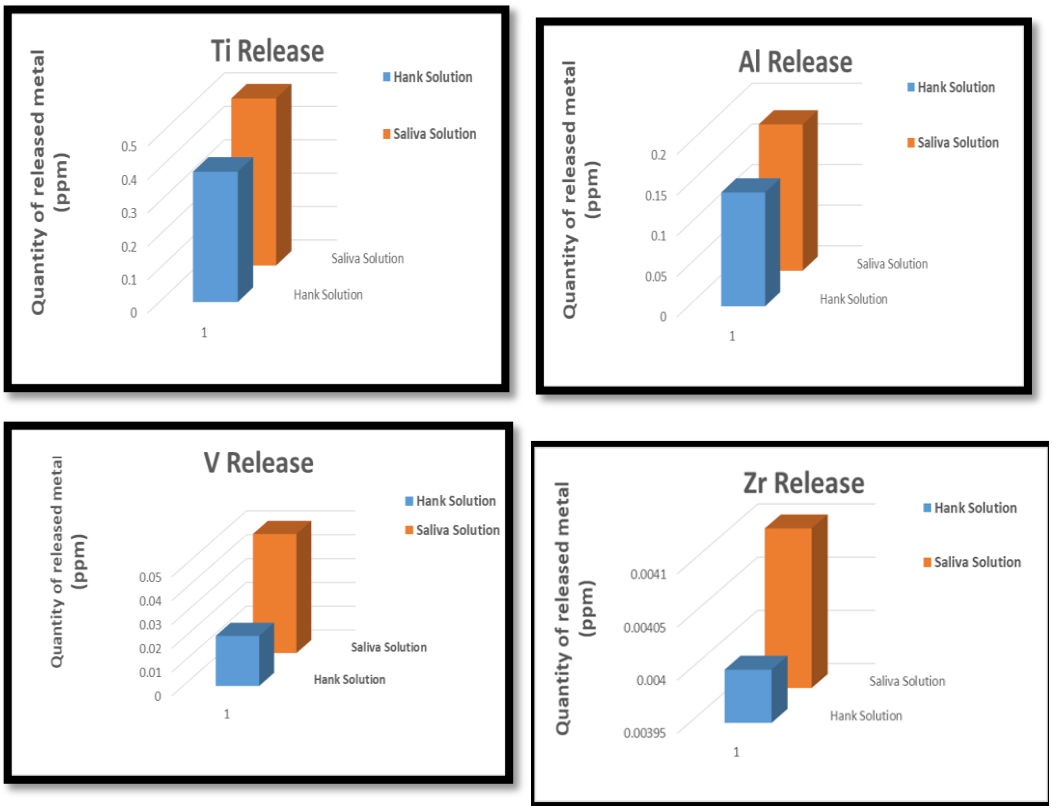

Figure (4-35) Quantity of each metal ion released from (Ti6Al4V2Zr) alloy in artificial saliva and Hank's solutions at 37°C ±1 after 21 days.

From table (4-10) and Figures (4-33), (4-34) , (4-35) where can be observed base alloys with Ta additives, ions are released from specimens ,slightly higher as compared to with base alloys with Zr additives which releases a little less percentage of ions compared with Ti6Al4V-XTa ,this is due to the role of Zr in spreading the beta phase more than Ta, and therefore it is more hardness, thus the oxide layer is more stable in Ti6Al4V-XZr alloys and Zr also shows a decrease in the inflammatory responses in the soft tissues surrounding the implant [133] , but both Ti6Al4V-XTa and Ti6Al4V-XZr lower than base alloy (Ti6Al4V) in ion release which indicates that it is (Ta , Zr) addition useful for long-term implantation [134], and thus the base alloy Ti6Al4V was developed by adding Zr and Ta elements in different proportions (0.5,1,1.5&2) to each of them separately to the base alloy, and their advantage as being

elements non-toxic to the human body and are more compatible with human tissues, thus (alpha-beta) alloys lead to superior biocompatibility and improved mechanical properties. Thus, adding these elements did not cause a negative response to tissues as the most biocompatible metal .

In the Figures (4-33), (4-34) , (4-35) , it is possible to observe that titanium ions are more released in all the alloys as compared with the release of other element ions (V, Al, Ta and Zr). In addition, shown the release of the elements in the artificial saliva solution are increased compared with the Hank's solution which be less ion release. This is due to the pH of the artificial saliva solution (6.7) less than the pH of the Hank's solution (7.4) where the less degradation in the solution which have the highest pH [135].

Moreover, the Ti-ion release from the (Ti6Al4V-0.5 Ta), (Ti6Al4V-0.5 Zr) alloys was slightly lower than that of base Ti6Al4V alloy. In addition, when gradual increase the(Ta) and (Zr) addition until reached max (2wt.%), the ion release of all elements reduced; this result indicates that the corrosion resistance of the (Ti6Al4V-2 Ta) , (Ti6Al4V-2 Zr) alloys was better than the corrosion resistance of base Ti6Al4V alloy, consistent with the results of the potentiodynamic polarization.

Table (4-9) Metal ions release concentrations in Hank's solution & saliva solutions at 37°C.

Alloy	Hanks Solution Ppm					Saliva Solution ppm				
	Ti	Al	V	Ta	Zr	Ti	Al	V	Ta	Zr
Ti6Al4V	0.82	0.31	0.08	-	-	0.98	0.61	0.11	-	-
Ti6Al4V-0.5Ta	0.72	0.27	0.018	0.00111	-	0.81	0.50	0.09	0.0011	-
Ti6Al4V-1Ta	0.62	0.22	0.015	0.00223	-	0.73	0.41	0.08	0.0022	-
Ti6Al4V-	0.52	0.19	0.013	0.00334	-	0.61	0.32	0.07	0.0033	-

1.5Ta										
Ti6Al4V-2Ta	0.41	0.16	0.011	0.0044	-	0.53	0.21	0.06	0.0045	-
Ti6Al4V-0.5Zr	0.70	0.25	0.017	-	0.00109	0.79	0.48	0.08	-	0.009
Ti6Al4V-1Zr	0.60	0.20	0.014	-	0.00220	0.70	0.39	0.07	-	0.0020
Ti6Al4V-1.5Zr	0.49	0.17	0.012	-	0.00330	0.58	0.29	0.05	-	0.0030
Ti6Al4V-2Zr	0.39	0.14	0.010	-	0.0040	0.50	0.18	0.05	-	0.0041

Chapter Five

Conclusions

&

Recommendations

5.1 Conclusions

According to the obtained results, the following conclusions are made and some suggestions or recommendations also mentioned for future work **:-**

1- Ti6Al4V base alloy, and base alloy with the different addition ratios (0.5 , 1, 1.5 , 2%wt Zr & Ta) , was prepared by powder metallurgy (P/M) method. XRD results showed that the sintering temperature was 550°C for 1 hours then 1000°C for 2 hours enouph to ensure the transformation of the used elements into alloys structure. Just two phases structure appear in base alloy (with additives &without additives), (αTi) and (βTi) at room temperature.

2 -The gradually less porosity with gradual increases in the addition of elements (Ta, Zr) to (Ti6Al4V) base alloy compared to the porosity of the (Ti6Al4V) base alloy without additives.

3-The contact angle values gradually decrease with the gradual increase in adding Ta and Zr to the base alloy Ti6Al4V in the artificial saliva solution and Hank's solution . It means that the addition of (Zr and Ta) increased the wettability of this alloy

4 -The alloys, the hardness values gradually increase with the increase addition of Ta and Zr to the base alloy compared to the hardness value to the base alloy without additions.

5-Gradual increases in the addition of elements (Ta, Zr) to (Ti6Al4V) base alloy gradually reduces the dry wear rate of these alloys compared with wear rate of the Ti6Al4V alloy without additives.

6-The corrosion improvement of (Ti6Al4V) base alloy significant improvement and gradually with a gradual increases in elemental addition of Ta and Zr in artificial saliva and Hank’s solutions.

7- The base alloys with Ta and Zr additives exhibited enhances the passive layer to more area by reduce the ionic release gradually with

gradual increases in the addition of elements (Ta , Zr) to (Ti6Al4V) base alloy.

5.2 Recommendations

For future work, the following suggestions:-

1. Study the microstructure and mechanical properties of the surface of Ti6Al4V alloy the catalyst by laser before and after implantation in the body of animals.
2. Study of the effect of heat treatment on the corrosion fatigue of the Ti6Al4Valloy.
3. Study of the effect of porous percentage on the mechanical properties of the Ti6Al4V alloy
4. Perform in vitro tests to assess the geno toxicity of the studied alloy
5. Study a new alloy, increasing the percentage of Nb or mix Ta with Zr, changing it to10%, decreasing the titanium rate, changing it to 75% ."

References

References

1. Al-Humairi, A.N.S., et al., BIOMATERIALS: A Multidisciplinary approaches and theirrelated applications. White Falcon Publishing.
2. Vallet-Regí, M.J.C.R.C., Evolution of bioceramics within the field of biomaterials. 2010. 13(1-2): p. 174-185.
3. Kunčická, L., Kocich, R., & Lowe, T. C. (2017). Advances in metals and alloys for joint replacement. *Progress in Materials Science*, *88*, 232-280.
4. Niinomi, M. (2002)‘ Recent metallic materials for biomedical applications’ Metallurgical and materials transactions A, 33(3), 477-486.
5. Hanawa, (2010)‘Overview of metals and applications T. Tokyo Medical and Dental University’, Japan .
6. Park, J. B., & Bronzino, J. D. (Eds.). (2002)‘ Biomaterials: principles and applications’. crc press.
7. Ostomel, T. A., Shi, Q., Tsung, C. K., Liang, H., & Stucky, G. D. (2006). Spherical bioactive glass with enhanced rates of hydroxyapatite deposition and hemostatic activity. *Small*, *2*(11), 1261-1265..
8. Guimaraes, Z.A., et al., *A Novel Porous Diamond-Titanium Biomaterial: Structure, Microstructure, Physico-Mechanical Properties and Biocompatibility.* 2017. **89**(4): p. 3111-3121.
9. da Rocha, D.N., et al., *Production and characterization of niobate apatite.* 2013. **2**(1): p. 24-29.
10. Wang, K.J.M.S. and E. A, *The use of titanium for medical applications in the USA.* 1996. **213**(1-2): p. 134-137.

11. Long, M. and H.J.B. Rack, *Titanium alloys in total joint replacement—a materials science perspective.* 1998. **19**(18): p.1621-1639.
12. Niinomi, M.J.M.S. and E. A, *Mechanical properties of biomedical titanium alloys.* 1998. **243**(1-2): p. 231-236.
13. Reinhold, E., et al., *EB-PVD process management for highly productive zirconia thermal barrier coating of turbine blades.* 1999.**120**: p. *77*-83.
14. Narayan, R. (2012) 'Fundamentals of medical implant materials', Materials for Medical Devices, Vol. 23, pp.6-17..
15. Cui, C., et al., *Titanium alloy production technology, market prospects and industry development.* 2011. **32**(3): p. 1684-1691.
16. Bin Jaafar , A.R., *Study of Selected Properties of Low Density Alloy After The Heat Treatment Process*, in *Faculty of Engineering Technology*. 2015, University Technical Malaysia Melaka (UTeM): Malaysia
17. Oldani, C. and A.J.R.a.i.a. Dominguez, *Titanium as a Biomaterial for Implants.* 2012. **218**: p. 149-162.
18. Gepreel, M.A.-H. and M.J.J.o.t.m.b.o.b.m. Niinomi, *Biocompatibility of Ti-alloys for long-term implantation.* 2013. **20**: p. 407-415.
19. Liu X, Chu PK, Ding C. Surface modification of titanium, titanium alloys, and related materials for biomedical applications. Mater Sci Eng. 2004;47(3-4):49–121.
20. Stadlinger B, Ferguson SJ, Eckelt U, et al. Biomechanical evaluation of a titanium implant surface conditioned by a hydroxide ion solution. Br J Oral Maxillofac Surg. 2012;50(1):74–79.

21. Subramani K, Mathew RT. Titanium Surface Modification. Techniques for Dental Implants – From Microscale to Nanoscale. Emerging Nanotechnologies in Dentistry. 2012;85–102.
22. Long, M.; Rack, H.J. Titanium alloys in total joint replacement–a materials science perspective. Biomaterials 1998, 19, 1621–1639. [CrossRef]
23. Abbasi, M.; Ahmadi, F.; Farzin, M. Production of Ultrafine-Grained Titanium with Suitable Properties for Dental Implant Applications by RS-ECAP Process. Met. Mater. Int. 2020. [CrossRef]
24. C.E. Campbell, U.R. Kattner, and Z.-K. Liu, Integr. Mater. Manuf. Innov. 3, 12 (2014).
25. I. Ansara, A.T. Dinsdale, and M.H. Rand, COST 507 Thermochemical Database For Light Metal Alloys, vol 2 (Luxembourg: Office for Official Publications of the European Communities, 1998).
26. H. Okamoto: J. Phase Equilibria, 1993, vol. 14 (1), pp. 120-21.
27. Li, X.-W.; Sun, H.-F.; Fang, W.-B.; Ding, Y.-F. Structure and morphology of Ti-Al composite powders treated by mechanical alloying. Trans. Nonferr. Metals Soc. 2011, 21, s338–s341. [CrossRef].
28. F. Ermanis, P.A. Farrar, and H. Margolin, Trans. Met. Soc. 221, 904 (1961).
29. N. Saunders, in: P. Bleckinsop, W.J. Evans, H.M. Flower (Eds.), Titanium'95: Science and Technology, Institute of Materials, London, 1996, p. 2167.
30. V.V. Molokanov, D. Chernov, and P. Budberg, Met. Sci. Heat Treat. 19, 704 (1977).
31. J.L. Murray, Phase Diagrams Bin. Vanadium Allloys, ed. J.F. Smith (Cambridge: ASM International, 1989), pp. 297–306.

32. Callings, E. W., J. Less-Common Met., 39, 63 (1975). "Magnetic Studies of Omega Phase Precipitation and Aging in Titanium-Vanadium Alloys."

33. Li, Y., Yang, C., Zhao, H., Qu, S., Li, X. and Li, Y. (2014), 'New developments of Ti-based alloys for biomedical applications', Materials, Vol. 7, No. 3, pp.1709-1800.

34. Nugroho, A.W. (2013) 'Investigation of the Production and Mechanical Properties of Porous Beta Titanium Alloy Compacts Prepared by Powder Metallurgy Processes for Biomedical Applications', Doctoral dissertation, Curtin University.

35. F.H. Froes, C. Suryanarayana, et al., Synthesis, properties and applications of tita- nium aluminides, J. Mater. Sci. 27 (19) (1992) 5113–5140.

36. P.K. Chaudhury, M. Long, et al., Effect of vanadium on elevated temperature phase relations in titanium aluminides containing 44 at.% Al, Mater. Sci. Eng., A 152 (1)(1992) 37–40.

37. S.C. Huang, E.L. Hall, Characterization of the effect of vanadium additions to TiAl base alloys, Acta Metall. Mater. 39 (6) (1991) 1053–1060.

38. Z. P, J.D. Shi, Z. Zhong, Improving the ductility of γ(TiAl) based alloy by in-troducing disordered β phase, Scr. Metall. Mater. 27 (1992) 1331–1336.

39. V.T. Witusiewicz, A.A. Bondar, et al., The Al–B–Nb–Ti system: IV. Experimental study and thermodynamic re-evaluation of the binary Al–Nb and ternary Al–Nb–Ti systems, J. Alloy. Comp. 472 (1–2) (2009) 133–161

40. B. Lindahl, X.L. Liu, et al., A thermodynamic re-assessment of Al–V toward an as-sessment of the ternary Al–Ti–V system, Calphad 51 (2015) 75–88.
41. Marsumi, Y. and Pramono, A.W. (2014) 'Influence of Niobium or Molybdenum in Titanium Alloy for Permanent Implant Application', In Advanced Materials Research, Trans Tech Publications, Switzerland, Vol. 900, pp. 53-63.
42. Radecka, A. (2015) 'Ordering and the deformation mechanisms of Ti-Al alloys', PhD thesis, Imperial College London/ Department of Materials.
43. Findik, F. (2017) 'Titanium Based Biomaterials', Engineering Biosciences, Vol. 7, No. 3, pp.1-3.
44. Leonhardt Å, Bergström C, Lekholm U.. Microbiologic Diagnostics at Titanium Implants. Clin Implant Dentistry Relat Res 2003;5:226–32. [PubMed] [Google Scholar]
45. Savoldi F, Visconti L, Dalessandri D. et al. In vitro evaluation of the influence of velocity on sliding resistance of stainless steel arch wires in a self-ligating orthodontic bracket. Orthodont Craniofac Res 2017;20:119–25. [PubMed] [Google Scholar]
46. Engh CAJ, Young AM, Engh CAS. et al. Clinical consequences of stress shielding after porous-coated total hip arthroplasty. Clin Orthop Relat Res 2003;417:157–63. [PubMed] [Google Scholar]
47. Vinarcik, E.J. (2002) 'High integrity die casting processes', John Wiley & Sons, New York, Published simultaneously in Canada.
48. Callister, W.D. and Rethwisch, D.G. (2011) 'Materials science and engineering', NY: John Wiley & Sons, Vol. 5.
49. Budinski, K.G. and Budinski, M.K. (2009) 'Engineering materials', 9th ed., Nature, Vol. 25.

50. Erdem, O. (2017) ‘The Development and Applications of Powder Metallurgy Manufacturing Methods in Automotive Industry’, Ul l ı Mü n l k A ş ı m v G l ş m D , Vol. 9, No. 3, pp.100-112.
51. Torralba Castello, J.M. and Campos Gómez, M. (2014) ‘Toward high performance in powder metallurgy’, Revista De Metalurgia, Vol. 50, No. 2.
52. Hammi, Y., Stone, T.W., Allison, P.G. and Horstemeyer, M.F. (2010) ‘Fatigue Modeling of a Powder Metallurgy Main Bearing Cap’, In SIMULIA Customer Conference.
53. Kipouros, G.J., Caley, W.F. and Bishop, D.P. (2006) ‘On the advantages of using powder metallurgy in new light metal alloy design’, Metallurgical and Materials Transactions A, Vol. 37, No. 12, pp.3429-3436.
54. Groover, M.P. (2012) ‘Introduction to manufacturing processes’, John Wiley & Sons, INC.
55. Groover, M.P. (2002) ‘Fundamentals of Modern Manufacturing’, 2nd ed., John Wiley & Sons, INC.
56. Sharma, P.C. (2007) ‘Production Technology (Manufacturing Processes): Manufacturing Processes’, S. Chand Publishing.
57. Rajput, R.K. (2007) ‘A textbook of manufacturing technology (Manufacturing processes)’, Firewall Media.
58. Groover, M.P. (2012) ‘Fundamentals of Modern Manufacturing Materials, Processes, and Systems’, 5th ed. Wiley Global Education, Hoboken, NJ.
59. Bhola, R., et al., Corrosion in titanium dental implants/prostheses–a review. 2011. 25(1): p. 34-46.
60. M.C. Shaw and G.J. DeSalvo, On the Plastic Flow Beneath a Blunt Axisymmetric Indenter, Trans. ASME, Vol 92, 1970, p 480.

61. Prof. G. O. Rading, Concise notes on Material Science, 2007, Victoria publishers.
62. Material science. Free download from: WWW. FaaDoOEngineers.com. Laboratory practical manual-Material Science. 71.
63. A.R. Fee, R. Segabache, and E.L. Tobolski, Introduction, Mechanical Testing, Vol 8, ASM Handbook, ASM International, 1985, p 72
64. SRM. (1978) Suggested methods for determining tensile strength of rock materials. Int. J. Rock Mech. Min. Sci. Geomech. Abst. 15, 99–103
65. Kutz, M., Materials and Mechanical Design. 2006: John Wiley and Sons.
66. Hayashi, K., et al., Quantitative analysis of in vivo tissue responses to titanium-oxide-and hydroxyapatite-coated titanium alloy. 1991.25(4): p. 515-523.
67. He, G., P. Liu, and Q.J.J.o.t.m.b.o.b.m. Tan, Porous titanium materials with entangled wire structure for load-bearing biomedical applications. 2012. 5(1): p. 16-31.
68. Elias, C., et al., Biomedical applications of titanium and its alloys. 2008. 60(3): p. 46-49.
69. G. Y. Lai. "High-Temperature Corrosion and Materials Applications". Chapter 9, 2007
70. F.H. Silver, Biomaterials, Medical Devices and Tissue Engineering: An Integrated Approach, Chapman & Hall, London, 1994, pp. 5–8.
71. G.R. Parr, L.K. Gardner, R.W. Toth, J. Prosthet. Dent. 54 (1985) 410–414.

72. Abd-elrhman, Y., et al., Compatibility assessment of new V-free lowcost Ti–4.7 Mo–4.5 Fe alloy for some biomedical applications 2016. 97: p. 445-453
73. Y. Li, C. Yang, H. Zhao, S. Qu, X. Li, Y. Li, New development of Ti-based alloys for biomedical applications, Materials, 7 (2014), 1709-1800.
74. W.F. Ho, C.P. Ju, J.H. Chern Lin, Structure and properties of cast binary Ti-Mo alloys, Biomaterials, 20 (1999), 2115-2122 .
75. Yao, C., J. Lu, and T. Webster, Titanium and cobalt–chromium alloys for hips and knees, in Biomaterials for artificial organs. 2011, Elsevier. p. 34-55.
76. Otawa N, Sumida T, Kitagaki H. et al. Custom-made titanium devices as membranes for bone augmentation in implant treatment: Modeling accuracy of titanium products constructed with selective laser melting. J Craniomaxillofac Surg 2015;43:1289–95. [PubMed] [Google Scholar]
77. Hothan A, Lewerenz K, Weiss C. et al. Vibration transfer in the ball–stem contact interface of artificial hips. Med Eng Phys 2013;35:1513–7. [PubMed] [Google Scholar]
78. Zaripova, F., A.Y. Eroshenko, and T. Petrashova. BIOMATERIALS:
79. APPLICATION OF METALS IN MEDICINE. in ВЫСОКИЕ ТЕХНОЛОГИИ В СОВРЕМЕННОЙ НАУКЕ И ТЕХНИКЕ. 2013.
80. Leonhardt Å, Bergström C, Lekholm U.. Microbiologic Diagnostics at Titanium Implants. Clin Implant Dentistry Relat Res 2003;5:226–32. [PubMed] [Google Scholar].
81. Savoldi F, Visconti L, Dalessandri D. et al. In vitro evaluation of the influence of velocity on sliding resistance of stainless steel arch wires

in a self-ligating orthodontic bracket. Orthodont Craniofac Res 2017;20:119–25. [PubMed] [Google Scholar].

82. Knee Replacement & HipReplacement Patient Advocacy & Online Communit.
83. Khorasani, A.M., Goldberg, M., Doeven, E.H. and Littlefair, G. (2015) 'Titanium in biomedical applications—properties and fabrication: a review', Journal of Biomaterials and Tissue Engineering, Vol. 5, No. 8, pp.593-619.
84. Sampaio M , Buciumeanu M, Henriques B , Silva F S , Souza J C.M. , Gomes J R , (2016) , Tribocorrosion behavior of veneering biomedical PEEK to Ti6Al4V structures , Elsevier
85. Vaithilingam J , Prina E , Goodridge R , Hague R J.M , Edmondson S , Rose F R.A.J , Christie S D.R. , (2016), Surface chemistry of Ti6Al4V components fabricated using selective laser melting for biomedical applications, elsevier.
86. Almanza E. , Perez M.J. Rodriguez N.A. , Murr L.E. (2017), Corrosion resistance of Ti-6Al-4V alloy processed by electron beam melting , Jmr&t (abm).
87. Dunstan M.K. , Paramore J. D., Fang Z.Z,(2018),The effects of microstructure and porosity on the competing fatigue failure T mechanisms in powder metallurgy Ti-6Al-4V, elsevier.
88. Liu S , Shin Y C. , (2018) , Additive manufacturing of Ti6Al4V alloy , elsevier.
89. Villa J. L. C. , Ruiz J.L. , Bouvard D. , Jimenez O. , Hernandez H. J. V. , Olmos L. , (2018) , Sintering study of Ti6Al4V powders with different particle sizes and their mechanical properties , elsevier.

90. Fazel M , Salimijazi H. , Shamanian M , Apachitei I , Zadpoor A, (2019), characteristics and electrochemical behavior of Ti-6Al-4V bio-functionalized through plasma electrolytic oxidation , elsevier.

91. Olmos L , Villa j.L.C, Bouvard D , Ruiz J L , Franco L.A.F , (2020), Synthesis and characterisation of Ti6Al4V/xTa alloy processed by solid state sintering , Taylor & Francis Group.

92. Cheung K. H. ,Pabbruwe M B , Chen W F , Koshy P , Sorrell C C , (2020), Effects of substrate preparation on TiO2 morphology and topography during anodization of biomedical Ti6Al4V, elsevier.

93. http://www.astm.org/cgi-bin/resolver.cgi?F136-13(2021) e1

94. T Odahara, H. Matsumoto and A. Chiba "Mechanical Properties of Biomedical Co-33Cr-5Mo-0.3N Alloy at Elevated Temperatures" Institute for Materials Research, Tohoku University, Sendai 980-8577, Japan 2008.

95. ASTM B-328" Standard Test Method for Density, Oil Content, and Interconnected Porosity of Sintered Metal Structural Part and Oil – Impregnated Bearing "ASTM international, 2003

96. S.M.Gawad" Effect of (Cu & Cr) Additives on Corrosion and Dry Sliding Wear of NiTi Shape Memory Alloy" , MS.C thesis , materials engineering college , university of Babylon / Iraq , 2015.

97. Kuroda, D., Kawasaki, H., Hiromoto, S., & HANAWA, T. (2005). Annual Book of ASTM Standards, Section 13, Medical Devices and Services Annual Book of ASTM Standards, Section 13, Medical Devices and Services, 2000. Materials transactions, 46(7), 1532-1539.

98. Jaber, H.H. (2014) 'The Effect of Addmixed Ti on Corrosion Resistance of High Copper Dental Amalgam', Journal of University of Babylon, Vol. 22, No. 2, pp.413-421.

99. N. M. Dawood, 'Preparation And Characterization Of Bio Nitinol With Addition Of Copper', PhD. thesis, materials engineering department , university of technology/ Iraq , 2014.
100. Hanawa, T. (2004) 'Metal ion release from metal implants', Materials Science and Engineering: C, Vol. 24, No. 6-8, pp.745-752.
101. Kolli, R. P., & Devaraj, A. (2018). A review of metastable beta titanium alloys. Metals, 8(7), 506.
102. Yamanoglu, R., Efendi, E. and Daoud, I. (2017) 'Sintering Properties of Mechanically Alloyed Ti-5Al-2.5 Fe', World Academy of Science, Engineering and Technology, International Journal of Chemical, Molecular, Nuclear, Materials and Metallurgical Engineering, Vol. 11, No. 5, pp.360-364.
103. E.W.Collings, The Physical Metallurgy of Titanium Alloys, American Society for Metals, 1984, P2.
104. E. Eisenbarth, D. Velten, M. Muller, R. Thull, J. Breme, Biocompatibility of β-stabilizing elements of titanium alloys, Biomaterials 25 (2004) 5705-5713.
105. Huber, D.E. (2016) 'Structure and Properties of Titanium Tantalum Alloys for Biocompatibility', PhD thesis, The Ohio State University.
106. gden, H.R. and Holden, F.C. (1958) 'Metallography of titanium alloys'(No. TML-103), Battelle Memorial Inst, Titanium Metallurgical Lab., Columbus, Ohio.
107. Jayaraman, M., Meyer, U., Bühner, M., Joos, U., & Wiesmann, H. P. (2004). Influence of titanium surfaces on attachment of osteoblastlike cells in vitro. Biomaterials, 25(4), 625-631.
108. Scimeca, M., Bischetti, S., Lamsira, H. K., Bonfiglio, R., & Bonanno, E. (2018). Energy Dispersive X-ray (EDX) microanalysis: A powerful

tool in biomedical research and diagnosis. European journal of histochemistry: EJH, 62(1).

109. Balog, M., Ibrahim, A. M. H., Krizik, P., Bajana, O., Klimova, A., Catic, A., & Schauperl, Z. (2019). Bioactive Ti+ Mg composites fabricated by powder metallurgy: The relation between the microstructure and mechanical properties. Journal of the mechanical behavior of biomedical materials, 90, 45-53.
110. Lide D. CRC handbook of chemistry and physics: a ready-reference book of chemical and physical data. 85th ed. Boca Raton, USA: CRC Press; 2004.
111. Erbil, H. Y. The Debate on the Dependence of Apparent Contact Angles on Drop Contact Area or Three-Phase Contact Line: A Review. Surf. Sci. Rep. 2014, 69, 325−365.
112. Fain, S. C., Jr.; McDavid, J. M. Work-Function Variation with Alloy Composition: Ag-Au. Phys. Rev. B 1974, 9, 5099.
113. M.C.L. Martins, B.D. Ratner, M.A. Barbosa, J. Biomed. Mater. Res. 67A (1) (2003) 158.
114. C.S. Zhao, X.D. Liu, M. Nomizu, N. Nishi, Biomaterials 24 (21) (2003) 3747.
115. D. Velten, V. Biehl, F. Aubertin, B. Valeske, W. Possart, J. Breme, J. Biomed. Mater. Res. 59 (1) (2002) 18.
116. Y.X. Leng, J.Y. Chen, J. Wang, G.J. Wan, H. Sun, P. Yang, N. Huang, Surf. Coat. Technol. 201 (2006) 157.
117. Z. Lin, I.S. Lee, Y.J. Choi, I.S. Noh, S.M. Chung, Biomed. Mater 4 (1) (2009) 011001.
118. M.B. Nasab, and M.R Hassan, "Metallic Biomaterials of Knee and Hip: A Review. Trends Biomaterial Artificial Organ", Vol: 24(1), P: 69-82, 2010.

119. S.M.Gawad" Effect of (Cu & Cr) Additives on Corrosion and Dry Sliding Wear of NiTi Shape Memory Alloy" , MS.C thesis , materials engineering college , university of Babylon / Iraq , 2015.
120. Hanawa, T. (2004) 'Metal ion release from metal implants', Materials Science and Engineering: C, Vol. 24, No. 6-8, pp.745-752.
121. I. Tripathy, "Effect of Microstructure on Sliding Wear Behaviour of Modified 9Cr-1Mo steel" , MS.C thesis , Metallurgical and Materials Engineering, National Institute of Technology, Rourkela, 2011.
122. Cvijović-Alagić, I., Cvijović, Z., Mitrović, S., Painć, V. and Rakin, M. (2011) 'Wear and corrosion behaviour of Ti–13Nb–13Zr and Ti–6Al–4V alloys in simulated physiological solution', Corrosion Science, Vol. 53, No. 2, pp.796-808.
123. S.M.Gawad" Effect of (Cu & Cr) Additives on Corrosion and Dry Sliding Wear of NiTi Shape Memory Alloy" , MS.C thesis , materials engineering college , university of Babylon / Iraq , 2015.
124. Singh. R.And N. B. Pahotre, (2007) 'Corrosion Degradation and Prevention by Surface Modification of Bio Metallic Materials', J Mat. Sci: Mater, Vol. 18 PP: 725 – 751
125. N. K. Sarkar and E. H. Greener, "Corrosion behavior of Tin-containing Silver-mercury phase of dental amalgam", J Det Res, Vol: 53, No: 4, P: 925-932, 1974.
126. Secchi, V., Franchi, S., Santi, M., Vladescu, A., Braic, M., Skála, T., Nováková, J., Dettin, M., Zamuner, A., Iucci, G. and Battocchio, C. (2018) 'Biocompatible Materials Based on Self-Assembling Peptides on Ti25Nb10Zr Alloy: Molecular Structure and Organization Investigated by Synchrotron Radiation Induced Techniques', Nanomaterials, Vol. 8, No. 3, p.148.

127. R. Singh And N. B. Pahotre , " Corrosion Degradation And Prevention By Surface Modification Of Bio Metallic Materials" , J Mat. Sci: Mater, Vol. 18, , P. 725 – 751, 2007.
128. Scully, J. R., Budiansky, N. D., Tiwary, Y., Mikhailov, A. S., & Hudson, J. L. (2008). An alternate explanation for the abrupt current increase at the pitting potential. Corrosion science, 50(2), 316-324.
129. Putz, B. The influence of high current densities on intact and cracked thin gold films on flexible polyimide substrate. Diploma Thesis, University of Leoben.2014.
130. Hansen, D. C. (2008). Metal corrosion in the human body: the ultimate bio-corrosion scenario. The Electrochemical Society Interface, 17(2), 31.
131. Ganesh, B. K. C., & Ramaniah, N. (2012) ' Effect of heat treatment on dry sliding wear of titanium-aluminum-vanadium (Ti-6Al-4V) implant alloy'. Journal of Mechanical Engineering Research, 4(2), 67-74.
132. Takayuki Yoneyama and Shuichi Miyazaki (2009)'Shape memory alloys for biomedical Applications 'Edited by,Boca Raton Boston New York Washington, DC.
133. Akagawa Y, Hosokawa R, Sato Y, Kamayama K. Comparison between freestanding and tooth-connected partially stabilized zir-conia implants after two years' function in monkeys: a clinical and histologic study. J Prosthet Dent 1998;80:551-8. [PMID: 9813805 DOI: 10.1016/s0022-3913(98)70031-9].
134. Okazaki Y, Gotoh E, Manabe T, Kobayashi K. Comparison of metal concentrations in rat tibia tissues with various metallic implants. Biomaterials 2004;25:5913-20.

135. Thirumalaikumarasamy, D., Shanmugam, K. and Balasubramanian, V. (2014) 'Comparison of the corrosion behaviour of AZ31B magnesium alloy under immersion test and potentiodynamic polarization test in NaCl solution', Journal of Magnesium and Alloys, Vol. 2, No. 1, pp.36-49.

الخلاصة

تتمتع سبيكة Ti6Al4V بإمكانيات واسعة في التطبيقات الطبية الحيوية نظرًا لدرجة عالية من التوافق الحيوي ، وخصائص ميكانيكية مواتية ، ومقاومة عالية للتآكل وإمكانية عالية للاندماج العظمي ، تحتوي سبيكة Ti6Al4V على العناصر (Al) و (V) التي تتميز بكونها عناصر سامة ضارة في جسم الإنسان ، ولكن مع وجود Ti تزيد من التوافق الحيوي للسبائك .

في هذه الدراسة ، تم تحضير جميع السبائك بواسطة تقنية ميتالورجيا المساحيق ، ثم تمت إضافة عناصر السبائك (التنتالوم ، الزركونيوم) بتركيبات مختلفة (0.5,1,1.5 & 2%wt) إلى السبيكة الرئيسية (90 wt %Ti-6 wt %Al-4 wt %V) من أجل دراسة تأثير هذه العناصر على توصيف البنية المجهرية (XRD ، SEM ، EDS والمجهر الضوئي) ، اختبارات الكهروكيميائية (اختبار الدائرة المفتوحة والاستقطاب) ، السمية (اختبار الغمر الساكن) والخصائص الميكانيكية والفيزيائية (الكثافة والمسامية ، زاوية التلامس ، الصلابة والجفاف اختبارات التآكل) لهذه السبيكة . تم تحديد الضغط المضغوط على أنه 600 Mpa وتم تلبيد السبائك الخضراء عند 550 درجة مئوية لمدة ساعة واحدة ثم عند 1000 درجة مئوية لمدة ساعتين في غاز خامل (أرجون) ، ثم تترك العينات في الفرن لتبرد الى درجه حراره الغرفه .

تظهر نتائج XRD أن جميع السبائك (مع وبدون إضافات) تتكون من طورين طور-α) (Ti وطور (β-Ti) ,عند درجة حرارة الغرفة وان إضافة Ta و Zr في هذه النسب المئوية لها تأثير في زياده طورβ.

الخواص الفيزيائيه , تنخفض نسبة المسامية تدريجياً مع زيادة اضافه (Ta) و (Zr) , قيم زاوية التلامس تشير إلى التناقص التدريجي في قيمه زاويه التلامس مع زيادة اضافه (Ta)، (Zr) مقارنة بقيمه زاوية التلامس لسبيكه الأساسية في محاليل Hank's وsaliva .

الخواص الميكانيكيه , قيم الصلابة تؤدي إضافة (Ta) ، (Zr) إلى قيم صلابة أعلى مقارنة بالسبيكة الرئيسية . تزداد مقاومة البلى الجاف مع إضافة عناصر (Ta و Zr) ، لكن مقاومة البلى الجاف للسبائك الرئيسية مع إضافات (Zr) أعلى مقارنة بالسبيكه الاساس والسبيكه الاساس مع إضافات (Ta) .

الخواص الكهروكيميائيه , أظهرت نتائج تآكل سبيكة Ti-6Al-4V تحسنًا ملحوظًا بعد إضافة كل من Ta و Zr في محاليل Hank's و saliva . وقد تبين أن اعلى تحسن عند إضافة 2 wt%Zr حيث كانت نسبة التحسن (91%) في محلول Hank's بينما كانت نسبة التحسن الأعلى في اللعاب الصناعي (77%) عند اضافه 2 wt%Zr كثافة و كثافه تيار التآكل للسبائك المستخدمة في محلول Hank's أقل من تلك المستخدمة في محلول saliva .

توضح اختبارات الغمر الساكن لجميع السبائك لمدة 21 يومًا في محلول saliva ومحلول Hank's أنه لوحظ وجود تركيزات منخفضة جدًا من إطلاق أيونات المعادن ,كمية الأيونات المحررة عندما تكون النسبه المضافة 2 wt%Zr أقل من سبيكة الاساس وسبيكه الاساس مع إضافة Ta في جميع المحاليل.

جمهورية العراق
وزارة التعليم العالي والبحث العلمي
جامعة بابل / كلية هندسة المواد
قسم هندسة المعادن

تحسين الخواص الميكانيكية والكهربائية لسبائك Ti6Al4V الحياتية بواسطه اضافة التنتالوم والزركونيوم

رسالة مقدمة
الى كلية هندسة المواد/جامعة بابل كجزء من متطلبات نيل درجة الماجستير في هندسة المواد / المعادن

من قبل
أُنس الوجود عامر محمود محمد

بإشراف
أ.د. حيدر حسن جابر أ.د. عبد الرحيم كاظم عبد علي

1442هـ 2021 م